EXPLORING ISOTOPIC SIGNATURES OF LAKE EL'GYGYTGYN SEDIMENTS FOR EVIDENCE OF ANOXIA AND METHANE CYCLING OVER THE PAST 50,000 YRS

A Thesis Presented

by

ADDIE ROSE HOLLAND

Submitted to the Graduate School of the
University of Massachusetts Amherst in partial fulfillment
of the requirements for the degree of

MASTER OF SCIENCE

September 2010

Geosciences

EXPLORING ISOTOPIC SIGNATURES OF LAKE EL'GYGYTGYN SEDIMENTS FOR EVIDENCE OF ANOXIA AND METHANE CYCLING OVER THE PAST 50,000 YRS

A Thesis Presented

by

ADDIE ROSE HOLLAND

Approved as to style and content by:

_____
Julie Brigham-Grette, Chair

_____
Steven T. Petsch, Member

_____
Stephen J. Burns, Member

_____
R. Mark Leckie, Department Head
Geosciences

ACKNOWLEDGMENTS

I would like to express gratitude toward all of the institutions and organizations that provide continuous funding and support to make research at Lake El'gygytgyn possible, including the International Continental Drilling Program, the U.S. National Science Foundation Earth Sciences Division and Office of Polar Programs, the German Federal Ministry for Education and Research, Alfred Wegener Institute, Geo Forschugs Zentrum-Potsdam, the Russian Academy of Sciences Far East Branch, Russian Foundation for Basic Research, and the Austrian Ministry for Science and Research.

I would like to extend my genuine appreciation and heartfelt thanks to my advisor, Julie Brigham-Grette, and thesis committee members, Steven Petsch and Stephen Burns, for their continuous attention, patience, and support. Thanks to Gerard Olack at the Yale University Stable Isotope Lab for GC-irMS measurements of compound-specific $\delta^{13}C$ and to Kenna Wilkie and Carrie Petrik at UMass for subsampling core LZ1029 and performing TOC and bulk $\delta^{13}C$ measurements. In addition, I want to thank members of the UMass Biogeochemistry Lab for their cheerful collaboration and assistance, as well as members of the Climate Center for inspirational conversation and fellowship. Thanks are especially due to the members of the Lake El'gygytgyn Drilling Project team, who have sincerely welcomed and patiently educated me during my short association with this project. I truly value the friendships and professional relationships I have developed during my time at UMass.

A special thank you to Dan Rosenberg for his continued love, support, and geologic enthusiasm.

ABSTRACT

EXPLORING ISOTOPIC SIGNATURES OF LAKE EL'GYGYTGYN SEDIMENTS FOR EVIDENCE OF ANOXIA AND METHANE CYCLING OVER THE PAST 50,000 YRS

SEPTEMBER 2010

ADDIE ROSE HOLLAND, B.S., TUFTS UNIVERSITY

M.S., UNIVERSITY OF MASSACHUSETTS AMHERST

Directed by: Professor Julie Brigham-Grette

Compound specific isotope analysis of lake sediments is a powerful tool in deciphering evidence of changing climatic and paleoenvironmental conditions through time. Isotopic analysis of Lake El'gygytgyn pilot sediment cores, PG1351 and LZ1029, have contributed increased insight into paleoenvironmental interpretations regarding conditions of permanent ice cover and water column anoxia at the lake over the past 250 kyr. Bulk sediment $\delta^{15}N$ was measured as a proxy for denitrification and a possible indicator for water column anoxia intensity. However, it appears that insufficient quantities of water column nitrate to fuel denitrification make its correlation with anoxia intensity ineffective. In pilot core LZ1029, compound-specific $\delta^{13}C$ of alkanes, fatty acids, and alcohols were analyzed to determine the changing sources of organic matter as well as the source of a strong negative isotopic shift in the bulk sediment $\delta^{13}C$ (-26‰ to -33‰) over the past 50 kyr. Results indicate that the majority of alkanes, fatty acids, and alcohols are long chain compounds consistent with a terrestrial plant origin, with increased aquatic contribution during the local last glacial maximum (LLGM). Among the compound classes examined, only the mid chain fatty acids display a strong LLGM

depletion ($\delta^{13}C$ = -43‰). Short chain fatty acids exhibit an LLGM depletion ($\delta^{13}C$ = -35‰) similar to bulk sediment $\delta^{13}C$, while the $\delta^{13}C$ trend of long chain alkanes, fatty acids, and alcohols differ from the bulk sediment $\delta^{13}C$ trend, suggesting an autochthonous source of bulk isotope depletion. Evidence of methane cycling exists only in the presence and isotopic value of diplopterol (LLGM $\delta^{13}C$ = -93.4‰), a biomarker for aerobic oxidation of methane. Two compounds indicative of archaeal lipids were present at considerable concentrations during the LLGM (394 and 668 μg/g TOC), but without the extreme negative $\delta^{13}C$ associated with methanogenesis and methanotrophy. These results suggest insufficient generation of methane in the lake to have derived from such a large anaerobic archaeal methanogen community suggesting that archaea are not acting entirely as methanogens. Furthermore, it appears unlikely that a significant anoxic layer existed in the water column of Lake El'gygytgyn during the past ~50kyr. The results of this work will be applied to ongoing investigations on the newest cores from Lake El'gygytgyn, which represent the past 3.5 Myr.

TABLE OF CONTENTS

LIST OF TABLES

Table Page

LIST OF FIGURES

CHAPTER 1

SEDIMENTARY BIOGEOCHEMISTRY OF LAKE EL'GYGYTGYN: IS THERE EVIDENCE FOR ANOXIA?

1.1 Introduction

Lakes provide a unique record of regional climate signals and environmental change, which adds substantially to the mixture of global and regional signals gained from ice core records and marine sediments. Arctic lakes in particular are important because they respond more dramatically to changes in the environment. Because summer temperatures in Arctic regions hover near freezing, small changes in warming can cause large changes in environmental response (Vincent et al., 2008). Impact Crater Lake El'gygytgyn is located in northeast Siberia approximately 100 km north of the Arctic Circle (see Figure 1.1). Lake El'gygytgyn is unique in that it contains a continuous sediment record since the time of impact, approximately 3.6 Myr BP (Brigham-Grette et al., 2007). This continuity has been validated through seismic surveys (Gebhardt et al., 2006). Studies of Beringian glaciation have revealed that the area around the lake has not been glaciated since impact, and thus has not experienced glacial erosion or interruption in sedimentation (Brigham-Grette et al., 2004). The long and continuous sedimentation record makes Lake El'gygytgyn unique because most high-latitude lakes experience ephemeral periods of existence, and therefore colonization and extinction of flora and fauna within their waters (Vincent et al., 2008). Thus, Lake El'gygytgyn holds promise to provide a long term, continuous record of climate and ecosystem change in the high Arctic from Pliocene to the present.

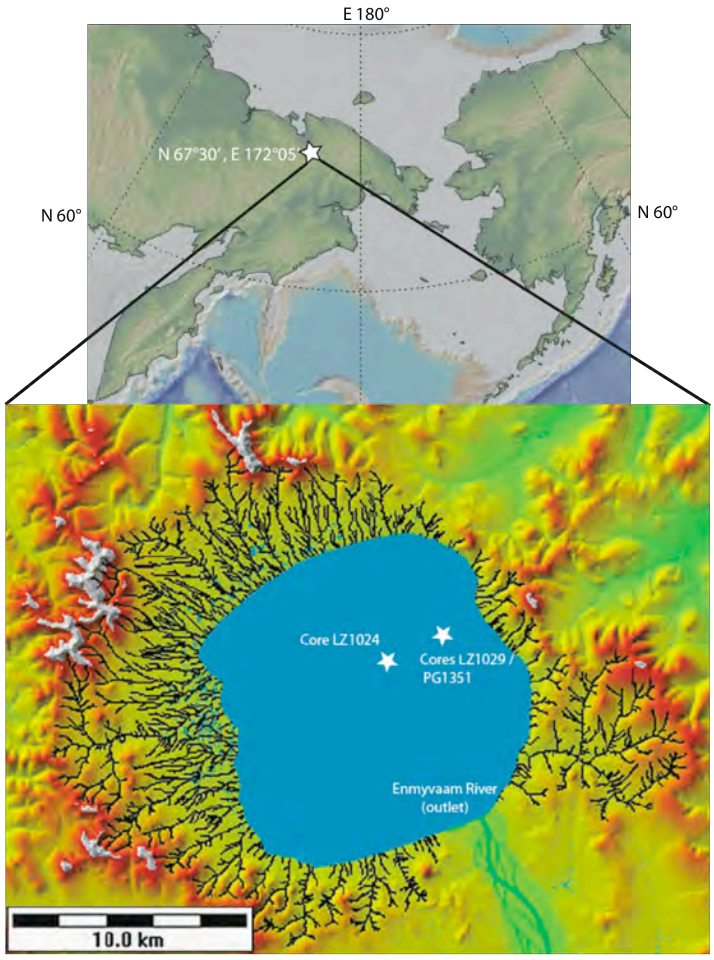

Figure 1.1: Location of Lake El'gygytgyn (from GeoMapApp.com and Nolan et al., 2003). The lake surface lies at approximately 400 meters a.s.l and the crater rim rises to a maximum of 850-950 m a.s.l. surrounding the lake. White stars indicate the locations of referenced cores.

Sedimentary geochemistry analyses, such as magnetic susceptibility (Nowaczyk et al., 2007), total organic carbon (TOC), total nitrogen (TN), total sulfur (TS), and carbon isotopes of bulk organic matter (δ^{13}TOC, herein bulk δ^{13}C) (Melles et al., 2007), as well as biogenic silica (opal) (Cherapanova et al., 2007), and titanium (TiO_2) (Minyuk et al., 2007) have been completed on three pilot cores obtained from Lake El'gygytgyn to determine the chronology and paleoenvironmental significance of sediments representing the last 300 kyr. Geochemical proxies show correlative patterns and trends, inferred to reflect oxygen content and biological production, but patterns of anoxia and associated

environmental change within the lake and its watershed have not been fully resolved. In particular, TOC and the organic carbon to nitrogen ratio (C/N) are intriguingly high during glacial periods, and accompanied by bulk $\delta^{13}C$ depletion. These high TOC, high C/N, low bulk $\delta^{13}C$ intervals are matched by low values of magnetic susceptibility suggesting a correlation with lake anoxia. This thesis seeks to gain a better understanding of the causes and responses of anoxia at Lake El'gygytgyn and the sources of organic matter through study of bulk sediment nitrogen isotopes and compound specific carbon isotopes.

1.2 Literature Review

1.2.1 Lake El'gygytgyn Previous Work

1.2.1.1 Core Collection

Sediments from Lake El'gygytgyn were sampled during two field seasons. In 1998, a 13-meter core (PG1351) was recovered from the central part of the lake and analyzed for a number of valuable paleoenvironment proxies (Melles et al., 2007). In 2003, a 15-meter core (LZ1024) was recovered from nearby and a 3-meter core (LZ1029) was recovered from almost the same location as core PG1351 (Melles et al., 2005). The cores were collected using gravity and percussion piston corers and have been stored in plastic (PG1351) and glass (LZ1024 and LZ1029) containers at both the University of Cologne, Germany and the University of Massachusetts, Amherst.

1.2.1.2 Age Model & Chronology

Data from PG1351 were used to establish an age model for correlating depth and age of the sediments (Nowaczyk et al., 2007). Cores LZ1024 and LZ1029 correlate well with the age model developed for PG1351 (Juschus et al., 2007). Geochemistry proxies have been studied to determine paleoenvironmental conditions in the lake, which assist in interpreting the paleoclimatic conditions of the region. Nowaczyk et al. (2002) constructed the first age model based on measurements of magnetic susceptibility, pollen, radiocarbon and IRSL dating. These records were compared with records interpreted as proxies for global climate variations, such as oxygen isotope records at the Greenland GRIP ice core and a marine record from Ocean Drilling Program (ODP) 677 site in the equatorial Pacific (Nowaczyk et al., 2002). The radiocarbon age estimates from PG1351 were consistently older than the IRSL ages, interpreted as slow turnover of soil carbon pools and storage of terrestrial carbon on the landscape before deposition (Melles et al., 2005). Tuning to the GRIP ice core provides a high-resolution correlation for the most recent 100 ka, but resolution in the ice core declines beyond this point. The older section of the core was tuned to the oxygen isotope record from marine record ODP-677, resulting in a core basal age estimate of 300 kyr BP (Nowaczyk et al., 2002). However, as other proxy data became available and proved to be informative, a different age model was developed.

The current age model for PG1351 is based on the IRSL dating of the core sediments and the magnetic susceptibility record tuned to July insolation at 70˚N (Forman et al., 2007; Nowaczyk et al., 2007). During the tuning of the magnetic susceptibility, geochemical, pollen, and diatom data were found to support this tuned

record, resulting in a revised age of 250 kyr BP for the bottom of the core. Core LZ1024 is slightly longer than PG1351, and extends to approximately 340 kyr BP (updated from Juschus et al., 2009). The sedimentology and magnetic susceptibility records in cores PG1351 and LZ1024 are very similar (Melles et al., 2005; Juschus et al., 2007).

1.2.1.3 Sedimentary Geochemistry Proxies

The study of paleoclimatology at Lake El'gygytgyn requires understanding of lake dynamics and how each proxy record responds to changing lake conditions. This information can be used to extrapolate a relative climate scheme at the lake, answering questions regarding possible relative temperatures (warm/cold) and humidity (moist/dry). Each of the geochemical and sedimentary proxies carries a signal of rapid transitions and relatively high amplitude changes, which corresponds with similar trends in other proxies. The record from these cores is useful because of the matching trends of several proxies, but the challenge remains in accurately interpreting the meaning of each geochemical transition.

The magnetic susceptibility record in core PG1351 has been used as a chronological tool but also reveals information regarding past lake conditions. In many other lake systems, magnetic susceptibility is used as a tool for measuring lithogenic input to the lake. This application holds that variations in magnetic material reaching the lake bottom would be directly proportional to input of allocthonous clastic material from the lake basin (which includes magnetic minerals). However, at Lake El'gygytgyn, magnetic susceptibility varies by two orders of magnitude, which is a much greater amplitude than can be accounted for simply by lithogenic input. In this case, magnetic susceptibility is interpreted as a proxy for preservation/dissolution of magnetite

(Nowaczyk et al., 2002). High values of magnetic susceptibility (magnetite preservation) are interpreted as periods of relative warmth with ice-free summers and oxic lake waters, while low values (increased dissolution of magnetite) are interpreted as cold periods with significant annual or multi-year ice cover, producing intense anoxic conditions in the bottom waters of the lake (Nowaczyk et al., 2007).

In addition to magnetic susceptibility, sediments in core PG1351 were analyzed for geochemical parameters that include TOC, TN, TS, opal, bulk sediment $\delta^{13}C$, (Melles et al., 2007) and titanium content (Minyuk et al., 2007). Each characteristic reveals information about the conditions of the lake at the time of deposition with implications for paleoclimatic change. TOC and TN are often interpreted as proxies for relative production and preservation of organic matter, depending on the rate of production versus the rate of decomposition. C/N ratios, on the other hand, are frequently used to infer the source of organic matter in the sediment. Vascular land plants tend to have higher C/N ratios due to the abundance of cellulose. Algal material tends to be rich in proteins and lacking in cellulose, resulting in a low C/N value (Meyers, 1998). Bulk sediment $\delta^{13}C$ is also frequently used to determine organic matter source. Organic matter derived from terrestrial sources tends to display a more depleted isotopic signal than that derived from aquatic sources (Meyers, 1998). TS can be used as an indicator for ventilation and oxygenation in the bottom waters. If the lower water column is well mixed, then sulfide formation is inhibited, and TS values in the sediment will be low (Melles et al., 2007). The organic sedimentary geochemistry proxies in Lake El'gygytgyn correspond with the magnetic susceptibility record in that they display cyclic variations at similar timing throughout the cores. This suggests that changing regional environmental conditions

have an impact on the general geochemistry of the lake and this is reflected in the geochemistry of the accumulated sediment.

Inorganic geochemistry of lake sediment is also used to interpret environmental conditions in and surrounding the lake. Specifically, titanium (weight %) is often used as a proxy for lithogenic (clastic) input and is usually anti-correlated with biogenic input, as fluctuations in organic matter burial dilute or concentrate the inorganic fraction in the sediment. Frequently, titanium directly corresponds with magnetic susceptibility. However at Lake El'gygytgyn, titanium and magnetic susceptibility are almost anti-correlated, further contributing to the theory that magnetic susceptibility is not a proxy for lithogenic input but rather indicates dissolution of magnetite under anoxic conditions (Nowaczyk et al., 2007).

1.2.1.4 Paleoenvironmental Lake Modes

The sedimentary geochemistry data have been interpreted to reflect four paleoenvironmental modes (units) at the lake, deposited as four specific sedimentary units (Figure 1.2). Units 1 and 2 reflect relatively warm conditions and units 3 and 4 reflect relatively cold conditions. The behavior of each proxy correlates with particular lake environment conditions and dominant climate patterns (wet/dry, warm/cold) at the lake during deposition (Melles et al., 2007).

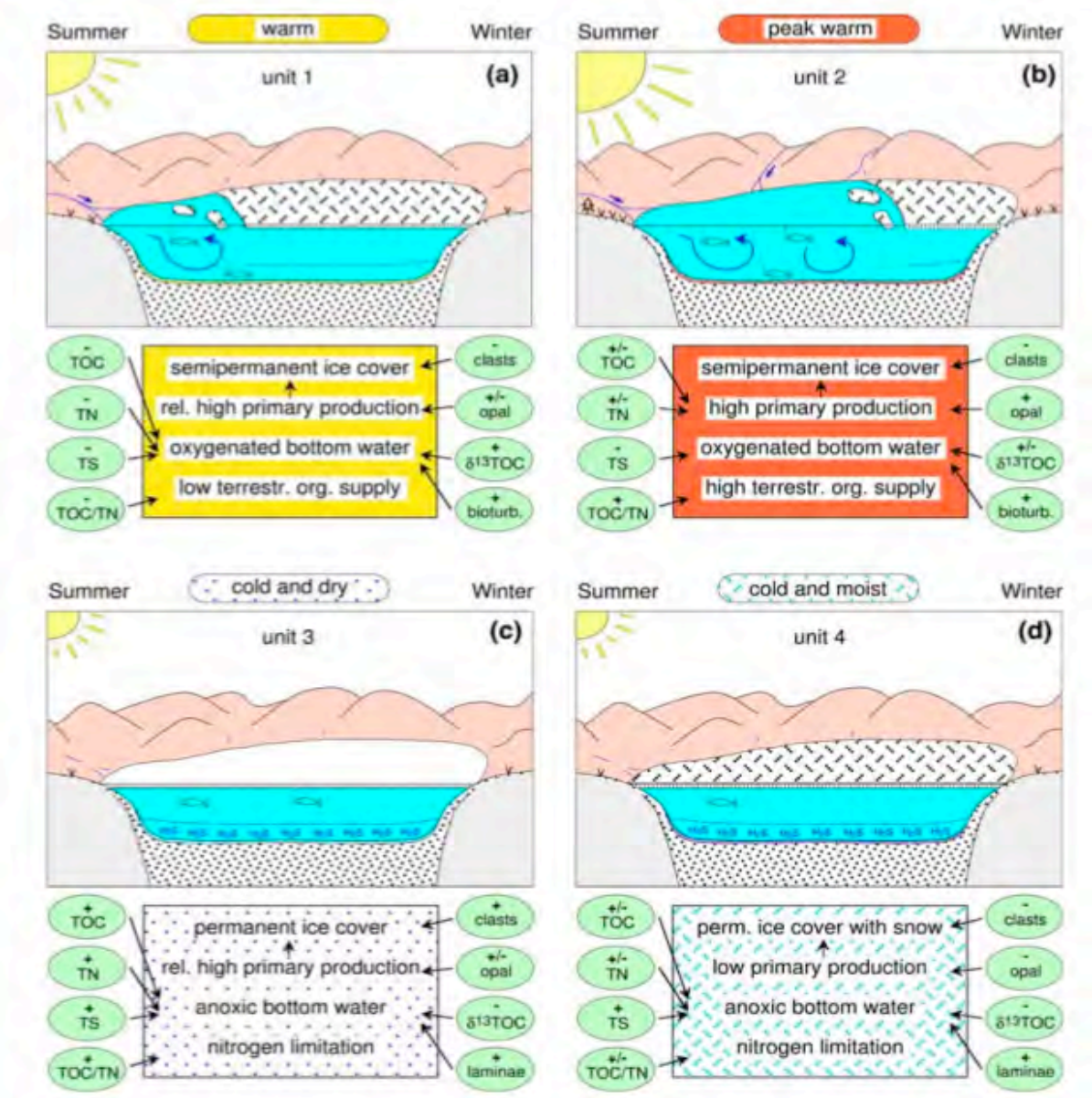

Figure 1.2: Paleoenvironmental modes of Lake El'gygytgyn. Four environmental modes: warm (a), peak warm (b), cold and dry (c), and cold and moist (d) (Melles et al., 2007). See text for further explanation.

Unit 1 is interpreted to represent a relative warm period with semi-permanent ice cover, relatively high primary production and oxygenation, and relatively low terrestrial influx. According to data from core PG1351, Unit 1 sediments exhibit low TOC, TN, TS, TiO_2 and sediments are weakly stratified and bioturbated (Melles et al., 2007; Minyuk et al., 2007). These data are interpreted to reflect highly efficient organic matter

degradation in the water column and/or sediments. Because there is open water for part of the year during this mode, mixing of lake water may assist in circulating nutrients and promoting decomposition of organic matter. Light penetration through the ice cover also may be high which is essential for primary production of organic matter. Perhaps due to semi permanent ice cover or dilution from biogenic production, the lithogenic terrestrial input (TiO_2) is relatively low and sedimentation is largely autochthonous. This environmental mode corresponds with the current environment at Lake El'gygytgyn. Therefore, scientific observation of this mode has been possible during various expeditions (1998, 2000, 2003) to study current environmental conditions regarding ice cover duration, sedimentation source, wind direction and intensity, and biogeochemistry of the lake (Melles et al., 2005).

Unit 2 occurs once in core PG1351 between approximately 130 and 120 kyr BP and is associated with peak warm conditions at the lake (Nowaczyk et al., 2007, Melles et al., 2007). Biogenic silica content is high as well as TOC, TN, and magnetic susceptibility. Bioturbation is more intense during this unit and TiO_2 is relatively low. High oxygen levels and continuous mixing could contribute to a higher rate of organic matter degradation, magnetite preservation, and increased presence of bioturbating organisms. Terrestrial sources include a wider variety of sediment and palynological sources, which are interpreted to indicate a warmer growing season and increased weathering (Melles et al., 2007). However, relatively low TiO_2 values could indicate dilution of lithogenic input by biogenic material and/or increased terrestrial vegetation, which would inhibit land surface erosion into the lake. The interpreted lake environment

includes open water more than six months annually, high production, well oxygenated and well mixed lake water, as well as high terrestrial sediment and organic matter influx.

Unit 3 sediments are interpreted to represent cold and dry environmental conditions at Lake El'gygytgyn. The magnetic susceptibility in Unit 3 is low and correlates with high TOC, TN, and TS values, as well as laminated sediment. These conditions indicate bottom water anoxia, since anoxic conditions would increase the preservation of organic matter, enhance the formation of sulfides, as well as inhibit bottom-dwelling organisms that would bioturbate the sediment. An additional proxy introduced during unit 3 conditions is the appearance of relatively coarse-grained clasts in the sediment (cryocanites), interpreted as eolian influx and suggesting extremely dry terrestrial conditions (Melles et al., 2007). Ice cover may be permanent during this mode. However, without heavy snow cover there is still some light transmitted below the surface, a condition essential for primary production.

Finally, unit 4 conditions are interpreted to represent a cold and moist environment. Under these conditions, magnetic susceptibility is very low, suggesting more pronounced anoxia, laminae are more defined, and aquatic biogenic silica production decreases significantly. TOC, TN, and TS values remain high as in unit 3 and bulk $\delta^{13}C$ values are again depleted. No clasts are found in these sediments because the surrounding environment is likely snow-covered and moist, conditions unfavorable to weathering and erosion. The lake is portrayed as permanently covered by ice and snow which would block transmission of sunlight to the waters below, thus reducing primary production in the surface waters (Melles et al., 2007).

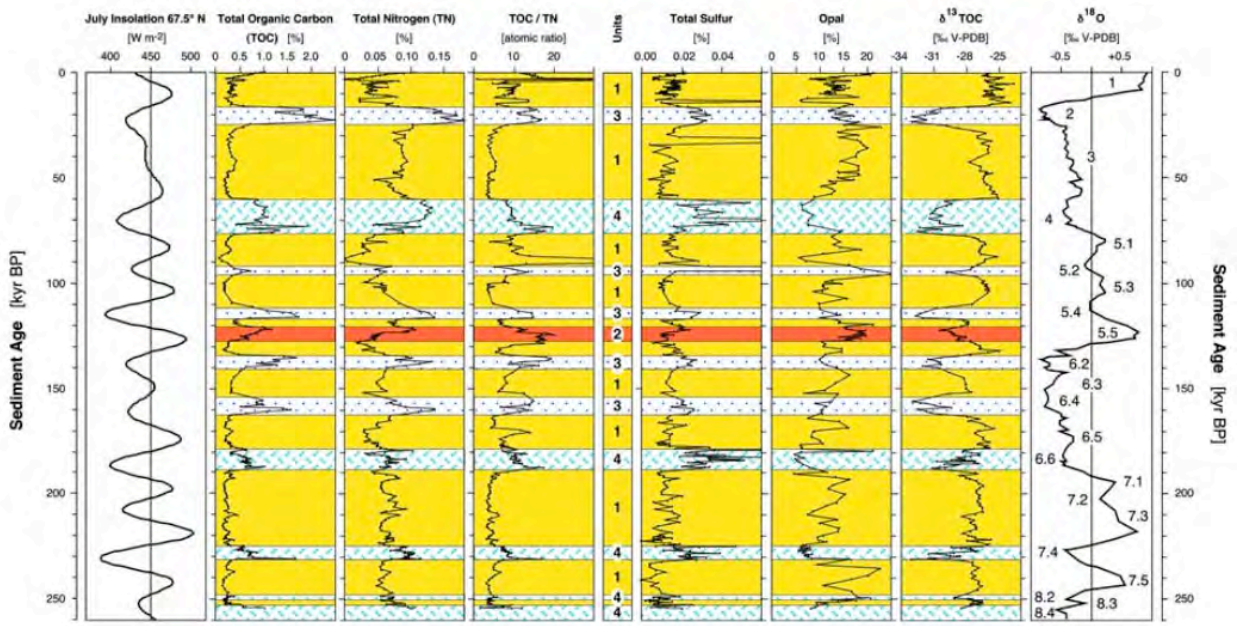

Figure 1.3: Core PG1351 sedimentary geochemistry proxies. Paleoenvironmental units are indicated by horizontal bands and compared with July insolation at 67.5° and a benthic $\delta^{18}O$ record (Melles et al., 2007).

During the last 250 kyr, the predominant paleoenvironmental mode at Lake El'gygytgyn is unit 1 (Figure 1.3). Unit 2 appears only once from about 130-120 kyr at a high insolation peak. Melles et al., (2007) suggest that regional warmth was significantly stronger during the Eemian (MIS 5e, approximately 125-140 kyr BP), as demonstrated by high TOC and TN values signifying increased production of organic matter. Units 3 and 4 appear in the sediments at semi-regular intervals, generally matching summer insolation lows. The paleoenvironmental units appear to correspond with the stacked marine isotope record and isotopic stages, suggesting a correlation with global paleoclimate indicators (Melles et al., 2007).

1.2.2 Lake El'gygytgyn Current Work in Biogeochemistry

The biogeochemical record of lake sediments makes the connection between lakes, terrestrial environments, and therefore the regional paleoclimatic signal (Vincent et al., 2008). In the case of Lake El'gygytgyn, paleoclimatic interpretations are constructed based on general understanding of biogeochemical cycles in lakes under various climate schemes. More detailed biogeochemical analyses, such as those outlined in this proposal, are needed to supplement ongoing analyses and interpretations.

Currently, work is ongoing on core LZ1024 to study the isotopic signature of hydrogen in specific compounds in the lake sediment. This work contributes to understanding the source of organic matter to lake sediments as well as sources of regional precipitation. Additional biogeochemical analyses are needed to clarify the interpretation of existing data from the core. The work outlined in this thesis intends to confront two important questions regarding the cycle of oxic/anoxic conditions in the lake and the source of organic matter in the lake sediments.

1.2.2 Leading Science Questions

1.2.2.1 Is Magnetic Susceptibility a Proxy for Anoxia?

One of the primary assumptions guiding the interpretation of data from Lake El'gygytgyn is that the magnetic susceptibility record is a signal of magnetite preservation under oxic conditions and dissolution under anoxic conditions (Nowaczyk, 2007). The high-amplitude swings of magnetic susceptibility are currently understood to represent the presence or absence of oxygen at the bottom of the lake. However, this hypothesis has not been fully examined. Through analysis of lake sediments for bulk

sediment nitrogen isotopes and compound-specific carbon isotopes, this proposed research seeks to gain a better understanding of how the biogeochemical cycles in the lake are driven by regional climatic conditions. The current running hypothesis is that anoxia occurs in or at the lake bottom due to regional cooling trends that cause permanent ice cover over the lake. Anoxic conditions caused by the lack of water column mixing lead to specific biogeochemical processes and reactions, which may be traced in the isotope record. At present, evidence for syndepositional anoxia includes extremely low magnetic susceptibility values, microscopic examination of etched magnetite grains (Brigham-Grette, unpublished), as well as the post depositional diagenesis growth of vivianite in the sediments (Asikainen, 2007). If anoxic conditions exist, there should also be evidence for impacts on organic matter preservation, nutrient cycling, and productivity. Proxies TOC, TN, and TOC/TN generally support magnetic susceptibility as evidence for anoxia. This thesis seeks to investigate other geochemical analyses (bulk sediment $\delta^{15}N$ and compound specific $\delta^{13}C$) that might offer more definitive indications of anoxic cycles in the lake.

1.2.2.2 What Drives the Extreme Negative Shifts in Bulk Sediment $\delta^{13}C$?

Bulk sediment $\delta^{13}C$ is frequently used as a proxy for organic matter source, based on the assumption that terrestrial organic matter exhibits a more depleted isotopic signature than aquatic organic matter. However, Units 3 and 4 sediments at Lake El'gygytgyn record an isotopic signature even more depleted than a typical terrestrial signal ($\delta^{13}C$ of C3 land plants = -23‰ to -30‰) (Meyers, 1994). Bulk $\delta^{13}C$ at Lake El'gygytgyn ranges from approximately -24‰ to -33‰, with depleted values corresponding with cold and postulated anoxic conditions. It is difficult to imagine that

the depleting bulk $\delta^{13}C$ trend indicates increased contribution of terrestrial organic matter during conditions of near permanent ice cover when the surrounding landscape is frozen. Bulk $\delta^{13}C$ is used to determine whether organic matter is largely terrestrial or aquatic but is not sufficient to identify the specific source of organic matter. Compound-specific biogeochemistry will help to identify which compounds make up the bulk of the organic matter, as well as determine which compounds (and therefore which organic matter sources) carry the most depleted $\delta^{13}C$ signature. One hypothesis contends that bacteria involved in methane cycling within the lake system are processing some of the organic matter during periods of anoxia and contributing a much more isotopically depleted signal. By examining the isotopic signature of specific compounds derived from such bacteria, the source of the very negative isotopic shift in bulk sediment $\delta^{13}C$ may be determined.

1.2.3 Anoxia

In a water body, anoxia is used to describe the absence of dissolved oxygen in the water column. During periods of low circulation or when the lake water has a limited oxygen supply (e.g. during ice cover), an oxycline develops within the water column, below which very little oxygen exists (Talbot, 2001). Biogeochemical processes that take place under anoxic conditions require anaerobic bacteria or facultative anaerobes, which prefer oxic conditions but are able to operate as anaerobes when no oxygen is available. Degradation of organic matter is much less efficient under anoxic conditions due to depleted numbers of electron acceptors (Killops and Killops, 2005). However, a debate exists over the specific controls on organic matter preservation. Scientists agree that factors such as primary production rate, sedimentation rate, and oxygen content in the

water column all play important roles in the preservation and burial efficiency of organic carbon, but there is no consensus regarding the largest contributing factor. Canfield (1994) summarizes the debate by contending that organic carbon preservation rates depend on many factors and tend to have a higher burial efficiency in anoxic bottom waters. However, he also suggests that even in oxic bottom waters, organic carbon degrades by anaerobic pathways. Hartnett et al. (1998) suggest that organic carbon burial efficiency is considerably controlled by the oxygen exposure time that sediments experience from the pore waters. In another study, Hartnett et al. (2003) explored organic carbon oxidation rates under conditions of varying oxygen concentrations and found that conditions of lower oxygen favored increased carbon preservation (low rate of oxidation). According to Van Mooy et al. (2002), anoxic conditions lead to higher preservation of certain fractions of organic material. For example, proteins degrade very efficiently under both oxic and anoxic conditions. Other types of organic matter degrade at very different rates, depending on the processes at work. Some anoxic processes may lead to a recognizable isotopic fractionation pattern in the preserved organic matter, which can be traced to a particular process, function, or species within the anaerobic microbial community. In the case of Lake El'gygytgyn, conditions of anoxia may be linked to periods of near permanent ice cover, which leads to interpretations regarding climate variations. This work examines two types of possible anoxic signatures, bulk sediment $\delta^{15}N$ and compound-specific $\delta^{13}C$ in order to gain more understanding about the conditions that cause anoxia in Lake El'gygytgyn.

1.2.4 Bulk Sediment Nitrogen Isotope Signatures

1.2.4.1 In Marine Systems

Bulk sediment $\delta^{15}N$ has been used in marine systems to study a wide variety of mechanisms, including marine nitrogen cycling and general nutrient cycling as well as marine currents and interpretations of climate variations. Altabet et al., (1999) used compound-specific $\delta^{15}N$ to interpret marine currents in the Eastern North Pacific at various depths, using the understanding that sediments in marine environments may carry an average denitrification signal for the water column above; or that sediments may be influenced by dominant water currents, which may be carrying particles from other areas of the ocean with varying bulk sediment $\delta^{15}N$ values. In the Arabian Sea, bulk sediment $\delta^{15}N$ of sinking particles is related to denitrification intensity, which Altabet et al. (1995) associate with changing sea level and ice volume. The bulk sediment $\delta^{15}N$ values are found to correspond with the 100-kyr periodicity of Milankovitch cycles, thus presenting a strong linkage to, and perhaps indicative of, climate cycles. In a very different study, Cloern et al., (2002) perform a statistical analysis and comparison of bulk sediment $\delta^{15}N$ and $\delta^{13}C$ in order to determine organic matter origin as well as the food source of primary consumers in the system. In both marine and lacustrine systems, bulk sediment $\delta^{15}N$ indicates the intensity of denitrification, and exhibits a strongly enriched signal under anoxic conditions.

1.2.4.2 In Lake Systems

Lake systems do not experience the dramatic currents or extreme depths that are present in marine systems, thus study of lake bulk sediment $\delta^{15}N$ spans a different set of

questions. Bulk sediment $\delta^{15}N$ is used to determine a variety of environmental conditions within a lake as well as within the immediate region surrounding the lake. This analysis can be used to determine changes in parameters such as productivity, organic matter source, and lake circulation. Filippi and Talbot (2004) even used bulk $\delta^{15}N$ at Lake Malawi to interpret changing lake levels as well as wind direction and intensity. Depending on the conditions at the lake, bulk $\delta^{15}N$ in combination with other geochemical proxies may prove valuable in interpreting the changing geochemistry within the stratigraphic record.

In a nutrient-poor system such as Lake El'gygytgyn, nitrogen cycles very efficiently in the surface waters. The main forms of nitrogen available as nutrients are nitrate (NO_3^-) and ammonia (NH_3). Nitrate is immediately consumed by phytoplankton, released through degradation (mainly heterotroph grazing and bacteria in the surface waters), and very quickly consumed again. The nitrogen that is not released during degradation accompanies sinking particulate organic matter to the bottom of the lake and is buried in the sediment. When dissolved inorganic nitrogen supplies are low, nitrogen fixing bacteria convert nitrogen gas (N_2) into forms that biota can metabolize (Schlesinger, 1997). Phytoplankton consume nutrient nitrogen in the surface waters of the lake by ammonia or nitrate assimilation. Some bacteria fix nitrogen, thus increasing the N_2 supply. However, these bacteria expend more energy than those that process combined forms of nitrogen and will be outcompeted if ammonia and nitrate are available. When available, dissolved ammonia and nitrate are consumed quickly, encouraging the nitrogen fixers to bring nitrogen gas into the biological cycle. During oxic conditions, aerobic heterotrophic bacteria use oxygen to metabolize. As shown in

Figure 1.4, aerobic processes involving nitrogen include remineralization of nitrogen in organic mater to nitrate as well as aerobic oxidation of ammonium to nitrate or nitrite (nitrification) under low nutrient conditions. Anaerobic microbial processes include ammonification, which decomposes organic matter and produces ammonia, and denitrification, which reduces nitrate to nitrogen gas (Talbot, 2001). Denitrification is concentrated in the upper part of the anoxic bottom water but occurs throughout the anoxic water column as well as in the sediments. Denitrification is the most important mode of respiration for organic matter in suboxic environments and is responsible for much of the net nitrogen loss from the water column (Van Mooy et al., 2002).

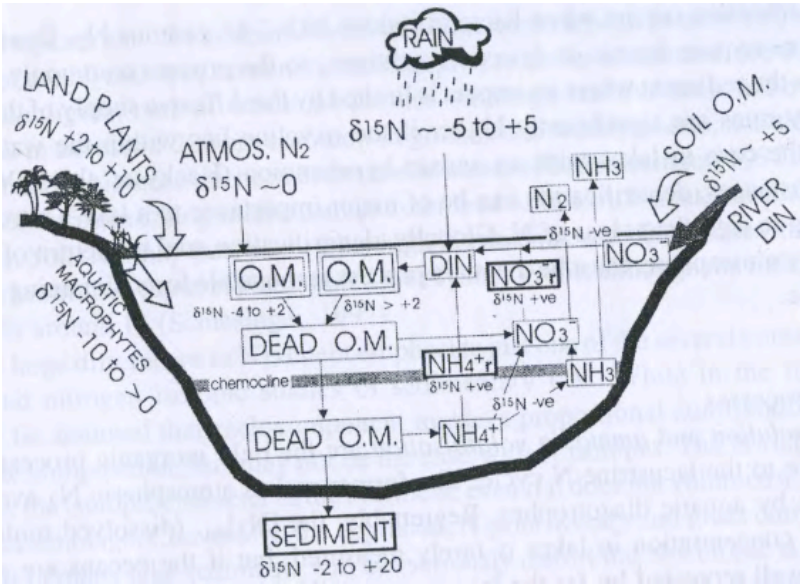

Figure 1.4: Nitrogen cycle in an anoxic lake (Talbot, 2001).

Analyses of $\delta^{15}N$ may be used to determine what types of microbial processes are occurring in the lake. Under conditions of low oxygen, inefficient microbial processes do not reach completion and lack of circulation prevents nutrients from being recirculated back into surface waters, resulting in net storage of organic matter and nitrogen in the sediments (Schlesinger, 1997). Denitrification has a very large fractionation effect,

releasing isotopically depleted nitrogen gas and enriching the nitrate pool in the photic zone where it is used by phytoplankton. The unreacted nitrate in the water column becomes increasingly isotopically enriched because the reaction preferentially uses the lighter isotope and releases it from the lake system as nitrogen gas. Denitrification has a much larger fractionation effect than other reactions involving nitrogen, and since it only occurs in the water column during anoxic conditions, evidence of denitrification may be used as a signal of anoxia. As anoxic conditions increase in intensity, the rate of denitrification increases, and the bulk nitrogen in the settling organic matter becomes increasingly isotopically enriched. Thus, $\delta^{15}N$ measurements may be used as a possible indicator for anoxia intensity in the lake bottom.

1.2.5 Lipid Biomarkers in Lake Sediments

1.2.5.1 Carbon Sources and Carbon Cycling

The cycling and availability of nutrients within the lake depends on primary production, lake water mixing, and bottom water and sediment reducing conditions. Mixing of lake waters and reducing conditions are controlled by oxygen availability or, in the case of Lake El'gygytgyn, the duration of ice cover. In general, primary production in lake surface waters is controlled by total irradiance, phosphorus and nitrogen availability, the rate of CO_2 dissolution, and changes in trace micronutrient concentrations (Schlesinger, 1997). During production in oxygenated waters, nutrients in surface waters are used rapidly by phytoplankton. Under oxic conditions, degradation of dead organic matter is also rapid and efficient in the water column, almost completely degrading before reaching the lake bottom. Thus, most nutrients remain in the water

column. During conditions of low oxygen and reduced light, such as periods of ice cover, some algae concentrate in the surface waters to use the available light penetration (Pienitz et al., 2004). However, without additional oxygen input during ice cover, organic matter degradation depletes the available oxygen reservoir quickly, limiting degradation in the water column and increasing preservation in the sediments. Stratification of the water column decreases resupply of nutrients to surface waters, and increases nutrient content in bottom waters. Enhanced storage of nutrients and organic carbon in the lake sediments represent inefficient microbial metabolic function.

Though much of the organic matter produced in lakes degrades within the water column, the remaining organic matter preserved in the sediment retains valuable information in the form of elemental and isotopic composition. In particular, TOC, carbon to nitrogen ratios, and bulk sediment $\delta^{13}C$ are useful for interpretations of organic matter source and preservation (Meyers, 1994). TOC indicates the amount of organic matter that has escaped degradation in the water column and has been buried in the sediments. The C/N ratio represents the type of organic matter accumulated in the sediment. For example, high C/N ratios correspond with material derived from vascular land plants. Low C/N ratios, on the other hand, correspond with algal sources due to the high protein content and absence of cellulose in aquatic organic matter. Bulk sediment $\delta^{13}C$ reflects the original isotopic effect of primary production (aquatic and terrestrial) as well as the effect of diagenesis and other bacterial input. Bulk $\delta^{13}C$ has also been used to estimate sources of organic carbon derived from autochthonous phytoplankton production and allochthonous inputs from land vegetation (Schlesinger, 1997). In oligotrophic lakes, more contribution from land vegetation (or less contribution from

aquatic primary producers) leads to a more depleted bulk $\delta^{13}C$. At Lake El'gygytgyn, high amplitude shifts in bulk $\delta^{13}C$ values have been measured in pilot core PG1351, ranging from -24‰ to -33‰, with very negative values corresponding with interpreted cold conditions (Melles et al., 2007). These negative values could reflect largely terrestrial sources of organic matter. However, this is difficult to reconcile with cold climatic conditions and permanent ice cover. Instead, the strong isotopic depletion may reflect production under ice-covered conditions with low nutrient availability and anoxic bottom water. Moreover, methanogenesis and methanotrophy may further contribute to this depletion. Bacterial processes associated with methane cycling can contribute to increased isotopic fractionation. Further carbon isotopic investigation of various organic matter sources is required to determine the sources of organic matter in the sediment as well as diagenetic processes occurring in the lake, which are important for reconstructing the patterns of carbon cycling.

1.2.5.2 Compound-Specific Carbon Isotopes

Bulk sediment $\delta^{13}C$ values are useful for study of the overall isotopic composition of organic matter preserved in sediment. However, bulk isotopic values are limited in their use for identifying specific sources of organic matter. Identification of specific compounds allows tracking of specific organic matter sources. Isotopic analysis of specific compounds reveals the isotopic composition of individual compounds and provides more accurate and precise information regarding the source of the organic matter, the CO_2 source for the compounds' biosynthesis, as well as the conditions of the lake during decomposition of the organic matter. Compounds that make up organic

matter decompose at different rates depending on conditions within the lake. Those that are most resistant to decay and ultimately preserved in sediments are termed biomarkers.

All the lipid biomarkers described here preserve an isotopic signature, which reflects the biosynthetic processes undergone by the organic matter as well as its original source. There are three possible sources of organic carbon accumulation in sediment, in which an isotopic signature is preserved: 1) Terrestrial sources such as leaf waxes, 2) aquatic sources such as phytoplankton or other primary producers, and 3) bacterial and archaeal sources associated with methane cycling. Terrestrially sourced organic carbon is slightly more isotopically depleted (approximately -30‰) than carbon from aquatic sources (approximately -20‰). However, organic carbon associated with methane cycling is much more depleted (approximately -60‰) than both terrestrial and aquatic sources (Whiticar, 1999). At Lake El'gygytgyn, there are two possible factors contributing to carbon isotopic depletion in the lake sediment. First, ice cover in the lake might cut off the link to atmospheric CO_2, thus leading to a continually depleted reservoir of CO_2 in the lake as it is processed by primary producers. This depleted signature would be picked up by aquatic organic matter and deposited in the sediments. Second, it may be that the highly depleted bulk $\delta^{13}C$ (-33‰) may be at least partially driven by bacterial sources. The bacterial processes involved in methane cycling, which requires anoxia, may play an important role in the depleted carbon isotopic signature in the sediments. Compound-specific isotope analysis will be useful in determining whether the depleted signature derives from aquatic primary producers or bacterial sources. For the purpose of this proposal, three groups of biomarker compounds, fatty acids, alkanes, and alcohols are examined for carbon isotopic signatures.

1.2.5.2.1 Fatty Acids

Fatty acids occur in all organisms and are preserved in recent sediments. They are produced by all eukaryotes, including terrestrial plants, aquatic phytoplankton, and bacteria. Typically, long chain (C_{20}-C_{30}) and predominantly even-numbered fatty acids are produced from terrestrial sources and short, even-numbered chains (C_{14}-C_{20}) derive from aquatic sources. Bacterial sources produce short chain (C_{13}-C_{20}) straight and methyl-branched fatty acids with both odd and even carbon number (Volkman et al., 1998). Fatty acids are produced primarily in the cell membrane and are often further metabolized by microbial processes in the sediment (Meyers and Ishiwatari, 1993). In terrestrial plants, fatty acids function as waxes on the vegetative surface of the plants (Volkman et al., 1998). Fatty acids from bacterial sources fall into two biosynthetic groups: Straight-chain fatty acids and branched-chain fatty acids. Bacterial fatty acids are unique in including iso- or anteiso- branched-chain compounds, which can be distinguished from fatty acids of aquatic and terrestrially sourced compounds (Kaneda, 1991). Microbial biomarkers of fatty acids are useful in quantifying microbial biomass as well as gaining information regarding the microbial community structure, such as possible identification of aerobic and anaerobic bacterial populations (Rajendran et al., 1993). Specific fatty acids may be analyzed for $\delta^{13}C$ in order to determine the contributing isotopic signature from different organic matter sources. The long chain saturated compounds tend to be slightly more resistant to degradation than short chain compounds (Volkman et al., 1998). Like lipids in general, fatty acids are commonly preserved in modern and recent sediments. Fatty acids have a greater sensitivity to degradation than other lipid compounds and their rate of degradation depends on many

factors including the lake environment, rate of burial, and oxygen content. It is important to measure fatty acids along with other compounds in order to separate degradation and modification from a change in organic matter source (Meyers and Ishiwatari, 1995).

1.2.5.2.2 Alkanes

Alkanes also occur in most organisms and, unlike fatty acids, are very resistant to degradation and often preserved in a greater age range of lake sediments (Meyers, 1998). Alkanes derive from degradation of fatty acids produced by both terrestrial and aquatic plants as well as bacteria, and the chain lengths of alkanes can be used to determine the source of organic matter. Like fatty acids, longer odd carbon number chain alkanes (C_{27}, C_{29}, and C_{31}) indicate the presence of leaf waxes from terrestrial sources, while shorter chains (C_{17} and C_{19}) indicate algal sources (Meyers, 1998; Pancost et al., 2007). Similar to fatty acids, compound-specific $\delta^{13}C$ of alkanes can be used to determine the source of organic compounds in the lake system (Meyers and Ishiwatari, 1993). Alkanes are particularly useful because of their stability and resistance to post-depositional degradation. In older sediments, where fatty acids are no longer available due to decomposition, alkanes derived from fatty acids are preserved and retain the same isotopic signature.

Additionally, other compounds from the hydrocarbon fraction, such as 2,6,10,15,19-pentamenthylicosane (PMI) and crocetane, indicate evidence of methanogenic archaeal sources (Pancost et al., 2000; Bouloubassi et al., 2009; Hinrichs et al., 1999).

1.2.5.2.3 Alcohols

Alcohols occur in all organisms as membrane lipids. For this study, the most useful alcohols are biomarkers of archaeal methanogens and bacterial methanotrophs. In particular, archaeol and hydroxyarchaeol are diagnostic biomarkers of archaeal sources. Hydroxyarchaeol is most often found in methanogenic archaea (Pancost et al., 2001; Bouloubassi et al., 2009). In addition, alcohols occasionally diagnostic of methanotrophic bacteria include C_{30} hopanes, such as diplopterol (Elvert et al., 2000; Pancost et al., 2000; Werne et al., 2002; Hinrichs et al., 2003), as well as sterol 4 α-methyl-5α-cholest-8(14)-n-3β-ol (Birgel and Peckmann, 2008; Elvert et al., 2008; Bouloubassi et al., 2009).

1.2.5.3 Methane Cycling

The most likely factor in considering the very negative shift in bulk $\delta^{13}C$ at Lake El'gygytgyn is the presence of bacteria associated with methane cycling. Evidence of these bacterial processes indicates the diagenetic state of the depositional environment as well as a distinctive isotopic signature in the sediments (Whiticar, 1999). Methanogens are anaerobic archaea that process simple carbon compounds and produce methane. As detailed in Summons et al. (1998) and Whiticar (1999), there are three types of methanogenic fermentation which produce an isotopically depleted signal: CO_2 reduction has a fractionation effect of -60 to -90‰, acetate fermentation has a fractionation effect of -50 to -70‰ (Whiticar, 1999), and the fractionation effect from methylotrophic methanogens is -80.6 to -86.4‰ (Summons et al., 1998). This last group can exist in oxic water conditions by producing methane in anaerobic microenvironments, such as inside other organisms or within particles. The dominant

fermentation in freshwater environments is acetate (methyl-type) fermentation, which generates methane with a highly isotopically depleted signature ($\delta^{13}C$ of -50‰ to -70‰) relative to terrestrial or aquatic sources. However, as other substrates become limited, CO_2 reduction fermentation ($\delta^{13}C$ of -50‰ to -70‰) becomes more important (Whiticar, 1999). Biomarkers of methanogenic archaea may reflect the highly isotopically depleted methane signature, or other organisms might metabolize the depleted carbon, thus producing a greater variety of compounds with the diagnostic highly depleted $\delta^{13}C$. Bacterial methanotrophs aerobically oxidize the isotopically depleted methane generated by methanogens and assimilate some of the carbon into their cellular biomass, thus forming lipid biomarkers that preserve the depleted isotopic signature of the methane (Schouten et al., 2001). Due to the very negative isotopic shift in $\delta^{13}C$ during interpreted cold conditions at Lake El'gygytgyn, there is likely some contribution of isotopically depleted organic matter derived from microorganisms associated with methane cycling, resulting in a signal more depleted than typical of terrestrial vegetation.

Sedimentary geochemistry of Lake El'gygytgyn up until this work has provided clues of episodic anoxia, which have encouraged interpretations of glacial periods with permanent ice cover, anoxic dissolution of magnetite, and increased preservation of organic matter due to anoxia. However, none of the work provides evidence for the presence of anoxia. The work from this thesis seeks to provide more concrete evidence for anoxia by disentangling the sources of organic matter and determining which contribute the most depleted bulk $\delta^{13}C$ through analysis of specific biomarkers.

CHAPTER 2

USING BULK AND COMPOUND SPECIFIC ISOTOPE ANALYSIS TO EXPLORE CONNECTIONS BETWEEN EPISODIC ISOTOPE DEPLETION AND ANOXIA AT LAKE EL'GYGYTGYN

2.1 Introduction

As we embark on a new age of future climate uncertainty and the body of evidence grows for current and recent global changes in climate (Kaufman et al., 2009), it becomes increasingly important to expand our understanding of how climate change impacted the natural landscape in the past. Currently, Polar Regions are gaining both scientific and public interest because of their vulnerability to changing climate as well as the potential global impacts resulting from polar change if rapid warming continues unabated. The particular sensitivity of Arctic regions presents them as unique recorders of past climate because summer temperatures in these regions hover near freezing, thus small changes in warming may cause large changes in environmental response (Vincent et al., 2008). Arctic lakes provide evidence of changes in the terrestrial environment through accumulated sediment, which partially documents conditions of life and erosion within the lake basin. Impact Crater Lake El'gygytgyn (Figure 2.1) is unique in that it contains a continuous sediment record since the time of impact approximately 3.6 Myr BP (Brigham-Grette et al., 2007). This continuity has been validated through seismic surveys (Gebhardt et al., 2006). Studies of Beringian glaciation have revealed that the area around the lake has not been glaciated since impact, and thus has not experienced glacial erosion or interruption in sedimentation (Brigham-Grette et al., 2004). The long and continuous sedimentation record makes Lake El'gygytgyn unique because most high-latitude lakes experience ephemeral periods of existence and therefore colonization and

extinction of flora and fauna within their waters (Vincent et al., 2008). Thus, Lake El'gygytgyn holds promise to provide a long term, continuous record of climate and ecosystem change in the high Arctic from Pliocene to the present.

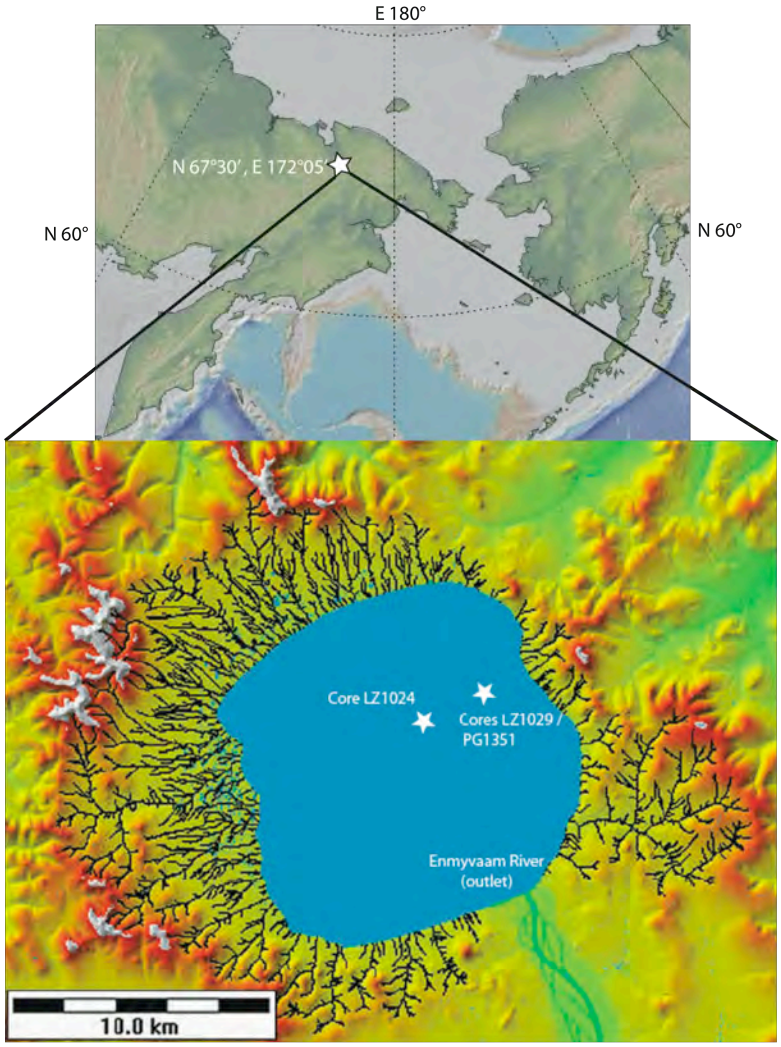

Figure 2.1: Lake El'gygytgyn site location (N 67°30', E 172°05'). The lake surface elevation is approximately 400 meters a.s.l. surrounded by a crater rim at 850-950 meters a.s.l. The lake lies off-center within the basin.

Current studies of sediments collected at Lake El'gygytgyn provide information relating to paleoenvironmental conditions at the site throughout the past 250 kyr. Specifically, conditions of permanent ice cover and anoxia have been interpreted through

proxy data including organic and inorganic geochemistry and magnetic susceptibility, leading to interpretations of past climate modes (Melles et al., 2007). Further analysis of pilot cores PG1351 and LZ1029 seeks to gain increased insight into the climatically driven isotopic information preserved in the sediments. Currently, extreme shifts in magnetic susceptibility are interpreted to represent dissolution of magnetite grains during intense anoxic glacial intervals (Nowaczyk et al., 2007). This interpretation is supported by the co-occurrence of laminated sediments, suggesting minimal bioturbation due to suboxic conditions, and inspection of microscopic magnetite grains that show etching and dissolution (Melles et al., 2007; Brigham-Grette, unpublished data). However, there is no explicit evidence for anoxia occurring within the water column at the lake. In this work, bulk sediment $\delta^{15}N$ was measured as a possible proxy for denitrification and thus anoxic intensity. In addition, compound-specific $\delta^{13}C$ of alkanes, fatty acids, and alcohols was analyzed to determine the source of organic matter, the extent of methane cycling in the lake, as well as the source of a strong negative isotopic shift in the bulk sediment $\delta^{13}C$ during glacial intervals (Figure 2.4(a)). Specifically, two questions are posed: What organic matter source(s) drive the highly depleted bulk $\delta^{13}C$ (Kenna Wilkie, unpublished) signature during the interpreted glacial intervals? And, is there specific evidence for anoxia in the water column during glacial intervals at Lake El'gygytgyn? The hypothesis guiding this study suggests that these questions may be linked through processes involved in methane cycling because the methane production in the lake would require anoxia. This work will assist in a greater understanding of the biogeochemical cycles occurring within Lake El'gygytgyn throughout various climate modes and will further constrain a working paleoenvironmental interpretation of conditions within and surrounding Lake

El'gygytgyn for use in analysis of the newest cores that cover the last 3.6 Myr of regional environmental change.

2.2 Background

Impact Crater Lake El'gygytgyn is located in northeast Siberia approximately 100 km north of the Arctic Circle (Figure 2.1). The lake lies toward the eastern edge of an 18 km basin surrounded by the crater rim, which rises approximately 350-450 meters above the surface of the lake. The majority of input to the lake comes from the western portion of the basin. The lake itself is 170 meters deep and 12 km in diameter (Brigham-Grette et al., 2007). Lake El'gygytgyn is surrounded by dry arctic tundra, and today experiences mean July temperatures from +4 to +8°C and January temperatures from -32 to -36°C (Brigham-Grette et al., 2007).

Prior to 2009, three pilot cores were collected at Lake El'gygytgyn: Core PG1351 (1998), core LZ1024 (2003), and core LZ1029 (2003). The bulk of this work involves sediment from cores PG1351 and LZ1029 but reference is made to previously published data from core LZ1024 because of its proximity. Core LZ1029 represents approximately the past 50 kyr of sedimentation at Lake El'gygytgyn. There exists no precise age model for this core, though age models have been constructed for both cores PG1351 (Nowaczyk et al., 2007) and LZ1024 (Juschus et al., 2007; 2009). The age model for core PG1351 is based on the IRSL dating of the core sediments (Forman et al., 2007) and the magnetic susceptibility record tuned to July insolation at 70˚N (Nowaczyk et al., 2007). Other geochemical, pollen, and diatom data were found to support this tuned record, resulting in an age of 250 kyr BP for the bottom of the core. Core LZ1024 is slightly longer than core PG1351 and extends to approximately 340 kyr BP based on

close correlation with core PG1351 (updated from Juschus et al., 2007; 2009). Core LZ1029 has been roughly correlated to cores PG1351 and LZ1024 through turbidite layers, but no detailed age correlation exists (Juschus et al., 2009)

2.3 Methods and Materials

2.3.1 Core LZ1029 Chronology

In order to assign a coarse chronology to core LZ1029, six tie points were chosen between the LZ1029 total organic carbon (% TOC; herein, TOC) curve (Kenna Wilkie, unpublished) and that of core LZ1024 (ages updated from Juschus et al., 2007; 2009). These ages are indicated on figures within this text, but a constant sedimentation rate cannot be assumed between the age correlations. A detailed correlation has not been performed between core LZ1029 and other cores from Lake El'gygytgyn. Figures 2.2-2.4 also refer to Intervals A (0-94 cm), B (95-215 cm), and C (216-290 cm), which reflect distinct trends in concentration and isotopic data. Within Interval B, figures 2.2-2.4 further delineate the period referred herein as the LLGM (110-154 cm), an interval previously identified as "Unit 3 – cold and dry", and inferred to have experienced relatively colder temperatures and drier humidity in the region of Lake El'gygytgyn (Melles et al., 2007). In this study, the LLGM will refer to the period of most extreme changes in concentration and isotopic data, including extreme shifts in magnetic susceptibility, TOC, and bulk $\delta^{13}C$. Interval B refers to a more extended period of molecular variability within this study, which is not reflected in TOC, bulk $\delta^{13}C$, or magnetic susceptibility.

2.3.2 Sampling

Sediment cores were recovered from 175 m water depth using a gravity corer and a 3 m long percussion piston corer (UWITEC Ltd., Austria) through holes drilled in the lake ice in 1998 (core PG1351) and 2003 (core LZ1029). Composite cores measured 12.91 m (PG1351) and 2.78 m (LZ1029) in length. Previous sampling of core PG1351 at 2 cm resolution yielded paleomagnetic properties (Nowaczyk et al., 2007), sedimentary organic geochemistry (Melles et al., 2007), particle size (Asikainen et al., 2007), palynology (Lozkhin et al., 2007), and inorganic geochemistry analysis (Minyuk et al., 2007). For this work, 68 samples (30-100 μg) from core PG1351 were obtained for $\delta^{15}N$ analysis from archived core material stored at UMass and previously used for grain size analysis. Core LZ1029 was shipped to UMass in 2003 and subsequently subsampled (2 cm resolution), freeze-dried, crushed, and stored at UMass (Kenna Wilkie and Brigham-Grette, pers. comm.). For this work, 14 samples (4.7-11.8 g) were obtained for biomarker analysis and 29 samples (26-66 μg) were obtained for $\delta^{15}N$ analysis from the archive half.

2.3.3 Bulk Sediment $\delta^{15}N$ Analysis

Nitrogen isotopes of bulk sediment were analyzed using a Costech elemental combustion system coupled to a Thermo Delta V Advantage isotope ratio mass spectrometer (EA-irMS). Results are expressed as δ values, where: $\delta^{15}N = [(R_{sample}/R_{standard}) - 1] \times 1000$; $R = {}^{15}N/{}^{14}N$, and the standard is atmospheric nitrogen ($\delta^{15}N = 0‰$). Instrument precision was evaluated with replicate analyses of standard reference materials (ammonium sulfate: USGS25 and IAEA-N1). Throughout sample analysis, 17 replicates of USGS25 ($\delta^{15}N = -30.4‰$) yielded an average of -30.3‰ and

one standard deviation of 0.3‰; 20 replicates of IAEA-N1 ($\delta^{15}N$ = 0.4‰) yielded an average of 0.45‰ and one standard deviation of 0.24‰. Laboratory methods are explained in further detail in Appendix A.

2.3.4 Lipid Analysis

Freeze dried and homogenized sediment from core LZ1029 (with 21.26 µg C_{36} alkane internal standard injected per sample) was extracted with a 9:1 dichloromethane: methanol (DCM:MeOH) solvent mixture in an accelerated solvent extractor (Dionex ASE 200) to generate total lipid extract (TLE), which was then evaporated to near dryness under N_2 gas. The TLE was then separated by column chromatography into neutral (4 mL DCM:isopropyl alcohol (IPA)) and acid (8 mL 2% formic acid in DCM) fractions, using amino-propyl columns (Supelco, Supelclean LC-NH_2). The neutral fraction was further separated using a silica gel (Fischer Scientific, silica gel sorbent 170-400 mesh) column to elute four fractions: hydrocarbons (4 ml hexane), aldehydes / ketones (4 mL DCM), alcohols and sterols (4 mL 3:1 hexane:ethyl acetate (EtOAc) solution), and other more polar compounds (4 mL MeOH). The acid fraction and an external isotope mass balance standard (heniocosanoic acid C_{21}), were derivatized with BF_3-Methanol to convert fatty acids to fatty acid methyl esters (FAMES), which were purified on a silica gel column with 4 mL hexane and 4 mL DCM to elute waste and purified FAMEs, respectively. The alcohol fraction (F3), along with two external isotope mass balance standards (nonadecanol C_{19} and octacosanol C_{28}) was derivatized with N,O-bis(trimethylsilyl)trifluoracetamide (BSTFA) to convert alcohols to trimethylsilyl ethers. Additional internal standard (21.26 µg C_{36} alkane per sample) was added as a

quantification standard to each sample from the FAME and TMS-alcohol fractions before instrumental analysis. Laboratory methods are explained in further detail in Appendix A.

2.3.5 Gas Chromatography – Mass Spectrometry (GC-MS)

Identification analyses were conducted on a Hewlett Packard 6890 series gas chromatograph – mass selective detector (GC-MSD) equipped with a 5% phenyl methyl siloxane column (HP-5MS, 30m x 0.25mm i.d., film thickness 0.25 μm). Helium was the carrier gas and the inlet temperature was 300°C. The oven program for alkanes was 40°C (2 min), 20°C/min to 130°C, 4°C/min to 320°C (15 min). The oven program for FAMEs was 40°C (2 min), 6°C/min to 320°C (2 min). The oven program for alcohols was 60°C (2 min), 20°C/min to 160°C, 4°C/min to 320°C (15 min). Positive identification was achieved by comparing mass spectral fragmentation patterns and relative retention times with those from published literature.

2.3.6 Gas Chromatography – Flame Ionization Detector (GC-FID)

Quantification analyses were conducted on a Hewlett Packard 6890 series gas chromatograph – flame ionization detector (GC-FID) equipped with a 5% phenyl methyl siloxane capillary column (30m x 0.25mm i.d., film thickness 0.25 μm). Helium was the carrier gas and the inlet temperature was 320°C. The oven program for alkanes was 60°C (1 min), 15°C/min to 315°C (15 min). The oven program for FAMEs was 60°C (2 min), 15°C/min to 315°C (10 min). The oven program for alcohols was 60°C (2 min), 20°C/min to 160°C, 4°C/min to 320°C (15 min). Quantification was achieved using the mass of a known internal quantification standard (C_{36} alkane). A bacterial fatty acid

methyl ester (BAME) standard (Supelco, 47080-U) was run in comparison with the FAME samples to assist in identification of bacterial fatty acids.

2.3.7 Gas Chromatography – Isotope Ratio Mass Spectrometry (GC-irMS)

The samples were then run on a Thermo Scientific (Trace GC Ultra 2000)-combustion interface gas chromatograph coupled to a Thermo Scientific Finnigan MAT 253 stable-isotope ratio mass spectrometer (GC-irMS) and equipped with a DB-1 column (SOLGEL-IMS / SGE manufacturer, 60 m x 250 μm i.d., 0.25 μm film thickness) for the purpose of obtaining compound-specific $\delta^{13}C$ values. The oven program for alkanes was 115°C (2 min), 16°C/min to 145°C, 12°C/min to 200°C, 8°C/min to 290°C, 3°C/min to 325°C (13.62 min) with the inlet temp at 260°C. The oven program for fatty acids was 80°C (2 min), 12°C/min to 145°C, 12°C/min to 200°C, 8°C/min to 290°C, 3°C/min to 325°C (11 min) with the inlet temp at 260°C. The oven program for alcohols was 80°C (2 min), 20°C/min to 200°C, 4°C/min to 325°C (15 min) with the inlet temp at 300°C. Results are expressed as δ values, where: $\delta^{13}C = [(R_{sample}/R_{standard}) - 1] \times 1000$; $R = {}^{13}C/{}^{12}C$, and the standard is Vienna Pee Dee belemnite ($\delta^{13}C$ = 0‰ VPDB). Instrument precision was determined with replicate analysis of a known isotope standard (C_{36} alkane), measured relative to VPDB. For the alkane fraction (13 replicates) and alcohol fractions (15 replicates), the average values were within one standard deviation (<0.66‰) of the known $\delta^{13}C_{C36}$ value (-29.88‰). Fatty acid fraction replicates (14) consistently displayed values outside one standard deviation (average $\delta^{13}C_{C36}$ = -30.54‰, Std. dev. = 0.25‰). Therefore, fatty acid values were reevaluated by correcting the IS to the known $\delta^{13}C_{C36}$ value and adjusting other values in each sample accordingly, an average adjustment of +0.658‰. Isotope analyses were conducted at Yale University's Earth

System Center for Stable Isotopic Studies. The fractionation associated with the methyl ester (ME) is calculated by the expression: $\delta^{13}C_{ME} = 22(\delta^{13}C_{C21:FAME}) - 21(\delta^{13}C_{C21:FA})$, where C21:FAME = the derivitized C_{21} fatty acid standard and C21:FA = the solid form of the underivitized C_{21} fatty acid standard. Using the calculated value for $\delta^{13}C_{ME}$, subsequent conversions for all $\delta^{13}C_{FAMEs}$ to $\delta^{13}C_{FAs}$ were found using the equation: $\delta^{13}C_{FA} = \delta^{13}C_{FAME}$ $(\#C_{FAME}/\#C_{FA}) - (\delta^{13}C_{ME}/\#C_{FA})$, where #C is the number of carbons in each compound. The fractionation associated with the TMS group was calculated with the expression: $\delta^{13}C_{TMS} = [22(\delta^{13}C_{Cn:OTMS}) - 29(\delta^{13}C_{Cn:OH})]/3$, where Cn:OTMS and Cn:OH are the derivitized and underivitized alcohol standards (C_{19} and C_{28} alcohols), respectively. Conversions for all $\delta^{13}C_{OTMS}$ to $\delta^{13}C_{OH}$ values were found using the equation: $\delta^{13}C_{OH} = [\delta^{13}C_{OTMS}(\#C_{OTMS}) - \delta^{13}C_{TMS}(\#C_{TMS})]/ \#C_{OH}$, where #C is the number of carbons in compound or TMS group. Both $\delta^{13}C_{Cn:OH}$ values were measured three times and standard deviations were within 0.15‰.

2.4 Results

2.4.1 Bulk Nitrogen Isotopes

Data collected from cores LZ1029 and PG1351 show different trends in bulk nitrogen isotopes (Appendix B). Values measured from core LZ1029 indicate a trend of slight $\delta^{15}N$ enrichment before the LLGM, which quickly becomes depleted, corresponding with increased TOC and decreased magnetic susceptibility (Figure 2.2). The correlation coefficients between $\delta^{15}N$ and TOC and bulk $\delta^{13}C$ are $R^2 = 0.30$ and 0.13, respectively (Figures B.15 and B.16). A more comprehensive record from core PG1351, which is compared with magnetic susceptibility, indicates an almost random scatter of

$\delta^{15}N$ values, ranging from -5.8‰ to 4.4‰, over the 12 m core (Figure B.17). There appears to be no correlation between $\delta^{15}N$ and the large changes in magnetic susceptibility values ($R^2 = 0.045$) or opal, TN, TOC, TS, C/N, bulk $\delta^{13}C$ ($R^2 < 0.019$) (Figures B.18-B.24).

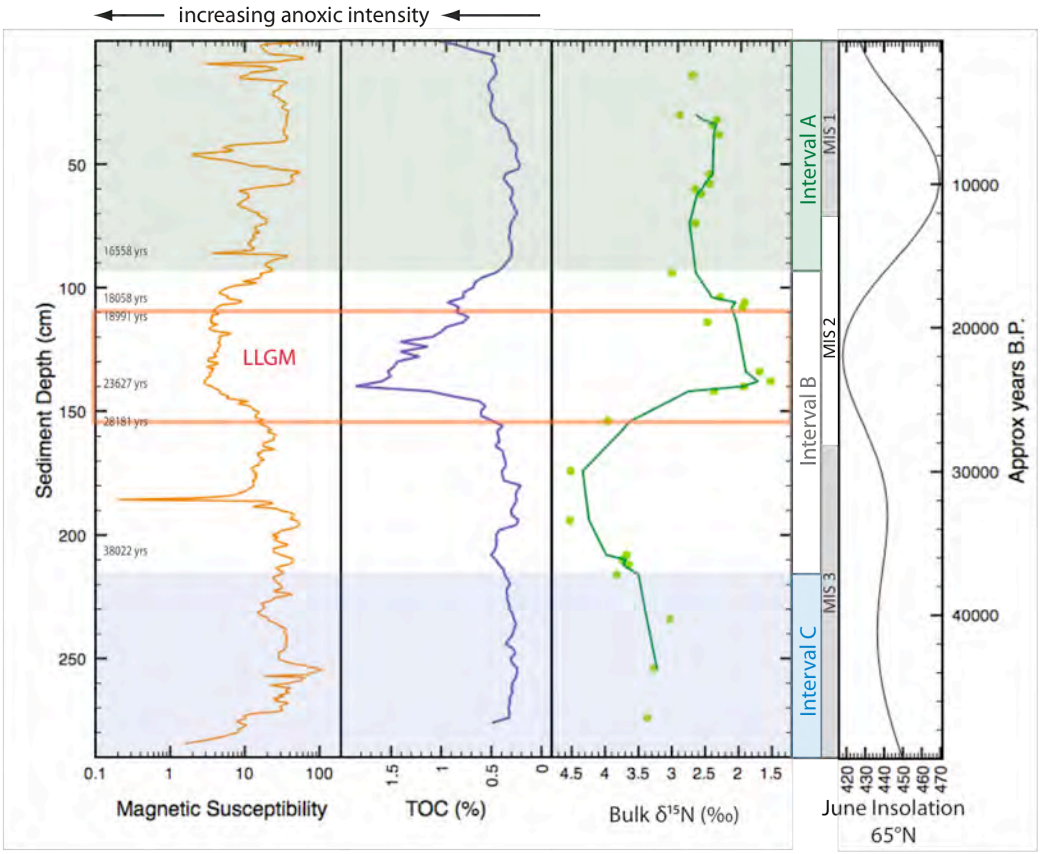

Figure 2.2: Bulk $\delta^{15}N$ relative to TOC and magnetic susceptibility. According to previous interpretations, increased TOC (Kenna Wilkie, unpublished) and decreased magnetic susceptibility (Majocka, 2007) are suggested to indicate increased anoxic intensity (Melles et al., 2007; Nowaczyk et al., 2007). An enriching signal of bulk $\delta^{15}N$ is expected with increasing anoxic intensity due to increased denitrification. Bulk $\delta^{15}N$ values show some enrichment at the beginning of Interval B, but do not follow the expected trend of continued enrichment during the LLGM. Green, white, and blue bands represent Intervals A, B, and C, respectively. The orange box represents the LLGM. MIS 1-3 and 65°N summer insolation provide a coarse chronology.

2.4.2 Isotopic Composition and Distribution of Lipid Biomarkers

Three fractions of the total lipid extract, alkanes, fatty acids, and alcohols, were separated, quantified, and measured for compound-specific carbon isotopes (data tables in Appendix B). For simplicity of presentation, results are organized below according to compound class rather than analytical method. Based on abundance and isotopic characteristics, data from the core is separated into Intervals A, B, and C, and references will be made to these designations throughout the text.

2.4.2.1 Alkanes

The most abundant alkanes in samples from core LZ1029 include odd-chain *n*-alkanes from C_{21} through C_{33}. Long chain compounds, especially C_{29} and C_{31}, dominate concentrations of *n*-alkanes. Alkane C_{31} demonstrates consistently high concentrations ranging from 217 to 461 μg/g TOC (except for the most recent value, which extends to 626 μg/g TOC). During the LLGM, however, C_{21} dominates at 628 μg/g TOC. Total *n*-alkane concentrations range from 593 μg/g TOC during Interval C to 2976 μg/g TOC during the LLGM (Figure 2.3(f)). Alkane concentrations are displayed relative to the maximum concentration (identified as 1.0) for each compound in order to create a visual representation of the abundance trend of each compound throughout the core. Abundance of alkanes C_{23} through C_{29} generally follow the trend of TOC during the LLGM, while C_{31} and C_{33} display a distinctly different trend, displaying initial peaks in concentration before the LLGM in the early part of Interval B (Figure 2.3(b)). Alkane C_{33}, though it reflects the long chain initial peak in concentration, displays a relatively unchanging concentration in comparison to the other long chain *n*-alkanes. As shown in

Figure 2.3(f), the total *n*-alkane concentration increases gradually during the beginning of Interval B before a sharp increase at the onset of the LLGM.

Isotopic values of *n*-alkanes show relatively constant values throughout core LZ1029. The mass weighted average (MWA) was calculated for each sample and varies less than 3‰ over the entire core. As shown in Figure 2.4(b), $\delta^{13}C$ MWA values of *n*-alkanes do not follow the trend of bulk $\delta^{13}C$ (Figure 2.4(a)) from core LZ1029.

2.4.2.2 Fatty Acids

Consistent with *n*-alkane concentrations in core LZ1029, fatty acids also display more abundant saturated long chain compounds. Fatty acid C_{26} concentrations largely dominate, ranging from 159 to 1324 μg/g TOC. Total fatty acid concentrations range from 861 μg/g TOC during Interval C to 6054 μg/g TOC during the LLGM (Figure 2.3(f)). Figure 2.5 shows two chromatograms from an LLGM sample and an Interval C sample, indicating the range of intensities within the core. All fatty acid concentrations generally follow the TOC peak during the interpreted LLGM. However, short and long chain lengths display distinctly different trends of abundance. Short (C_{14}-C_{18}) and mid chain (C_{19}-C_{23}) compounds display relatively low and constant concentrations throughout the core and form one synchronous peak with the TOC (Figure 2.3(d)). Long chain compounds (C_{24}-C_{30}) all display a preliminary peak before the LLGM. The absolute concentrations (Figure 2.3(f)) clearly show a trend of increasing concentration starting at the beginning of Interval B. Fatty acids diagnostic of bacterial sources, such as the iso- and anteiso-C_{15} compounds, are present in samples with the highest TOC, though at low concentrations relative to the saturated fatty acids. No other BAMEs were identified in

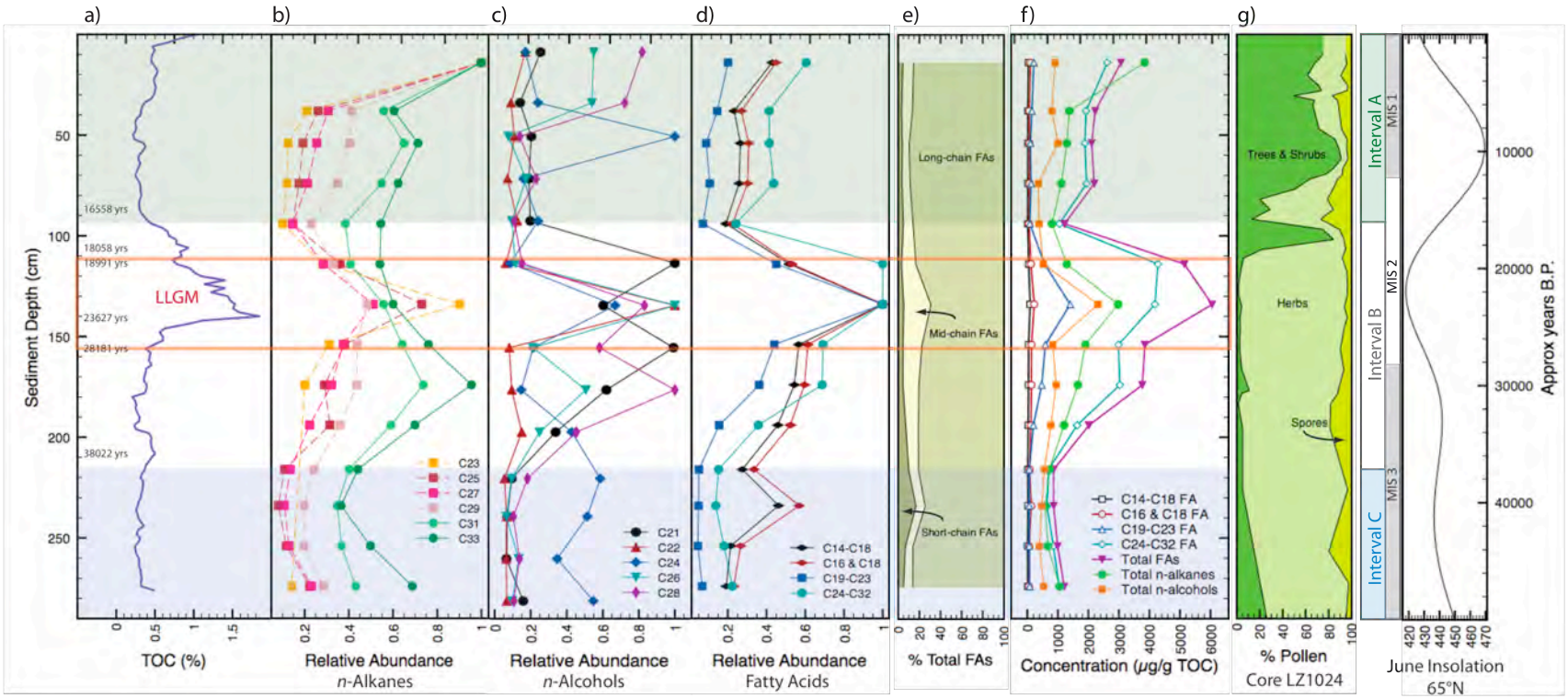

Figure 2.3: Concentrations of alkanes, fatty acids and alcohols relative to TOC and pollen (core LZ1024). TOC (Kenna Wilkie, unpublished) with six age tie points correlating to core LZ1024 (a), abundance of *n*-alkanes relative to the maximum value of each compound (b), abundance of *n*-alcohols relative to the maximum value of each compound (c), abundance of grouped fatty acids relative to the maximum value of each group (d), contribution (%) of short, mid, and long chain fatty acids (e), absolute concentrations of grouped fatty acids and total *n*-alcohols, *n*-alkanes, and fatty acids (f), pollen from core LZ1024 (Lozhkin et al., 2007b) (g). Green, white, and blue bands represent Intervals A, B, and C, respectively. The orange box represents the LLGM. MIS 1-3 and 65°N summer insolation provide a coarse chronology.

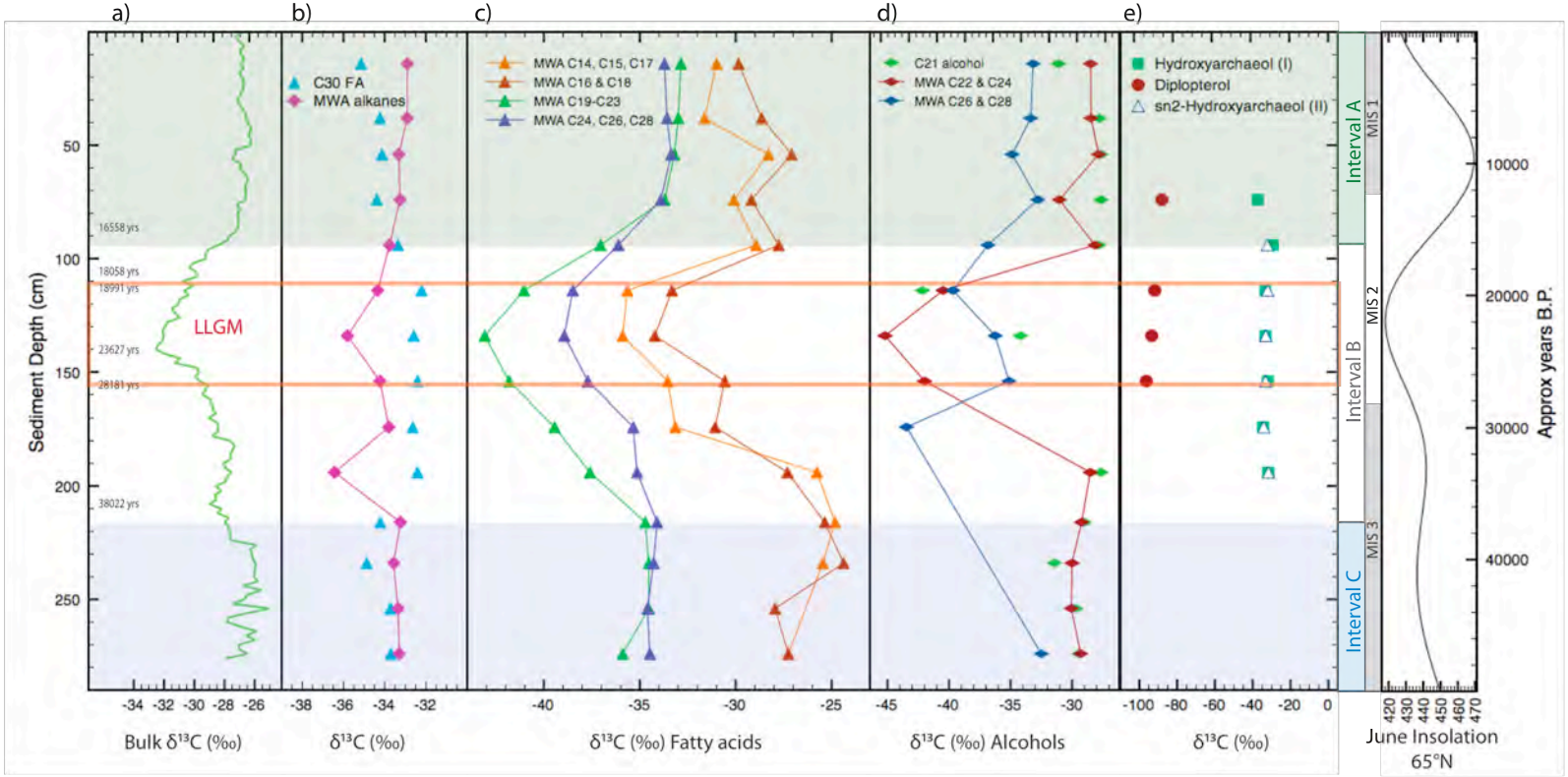

Figure 2.4: Bulk and compound-specific $\delta^{13}C$ values of alkanes, fatty acids, and alcohols. Bulk $\delta^{13}C$ (Kenna Wilkie, unpublished) with six age tie points correlating to core LZ1024 (a), inferred terrestrial long chain *n*-alkanes (MWA) and C_{30} fatty acid grouped to emphasize the relatively constant $\delta^{13}C$ (b), fatty acids grouped by long chain (C_{24}, C_{26}, C_{28}), mid chain (C_{19}-C_{23}), and short chain (C_{14}-C_{18}) MWA (c), *n*-alcohols grouped by $\delta^{13}C$ trend (d), archaeal hydroxyarchaeols and bacterial diplopterol (e). Green, white, and blue bands represent Intervals A, B, and C, respectively. The orange box represents the LLGM. MIS 1-3 and 65°N summer insolation provide a coarse chronology.

the fatty acid fraction. Figure 2.3(e) displays fatty acid chain length group concentrations proportionate to total fatty acids, showing that during the LLGM, the mid chain fatty acid contribution increases, while the long chain contribution decreases. A similar pattern is reflected at 234 cm where both the mid and short chain fatty acid contributions increase. This event is not reflected in the TOC.

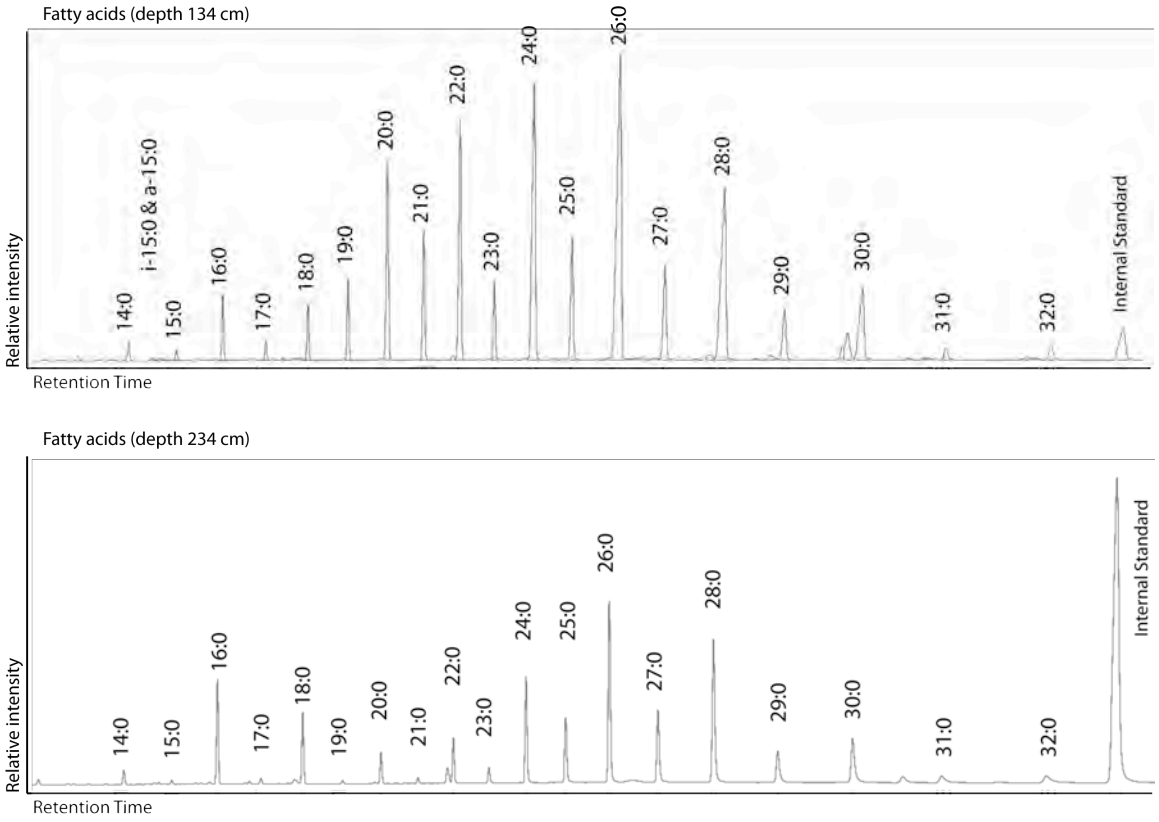

Figure 2.5: Representative LLGM (134 cm) and Interval C (234 cm) FAME chromatograms. Note that identical amounts of internal standard were injected into each sample, thus peak intensities for each sample are relative to the intensity of the internal standard. Nomenclature used here (x:y) represents the number of carbons in each compound (x) relative to the number of double bonds (y).

The calculated MWA isotopic values of fatty acid chain length groups are shown in comparison to the bulk $\delta^{13}C$ (Figure 2.4(c)). Fatty acids show three distinct isotopic trends corresponding with short, mid, and long chain carbon compounds. Short chain compound mass weighted averages trend similarly to bulk $\delta^{13}C$ values. Mid chain

compounds display the most depleted excursion between Interval C and Interval B (~10‰), while long chain compounds reflect a less pronounced excursion (~5‰). Both excursions are greatest during the LLGM but increase steadily throughout the beginning of Interval B. Fatty acid C_{30} (Figure 2.4(b)) departs from the trend of the other long chain fatty acids and remains constant throughout the LLGM and Interval B. Fatty acids C_{15} iso- and anteiso- exhibit isotope values consistent with bulk $\delta^{13}C$ values.

2.4.2.3 Alcohols

Alcohol concentrations are dominated by straight chain even numbered *n*-alcohols (C_{22} to C_{28}), as well as C_{21}. Alcohol C_{24} concentrations largely dominate, ranging from 58 to 675 μg/g TOC. During the LLGM, however, C_{22} dominates at 701 μg/g TOC. Total alcohol concentrations range from 393 μg/g TOC during Interval C to 2314 μg/g TOC during the LLGM (Figure 2.3(f)). Similar to total fatty acid concentrations, total *n*-alcohols begin to increase during Interval B with a sharp increase in abundance during the LLGM. As shown in Figure 2.3(c), abundance trends of individual *n*-alcohols display peaks throughout Interval B. Sterols (Figure 2.6) occur at low abundance (<150 ug/g TOC) in only one sample (depth 134 cm) during the LLGM and are represented by cholesterol, cholestanol, stigmasterol, β-sitosterol, sigmastanol, and possibly campesterol (Henderson et al., 1972), and dinosterol (Piretti et al., 1997), as identified by relative retention times and published mass spectra. Isoarborinal, which has been used as a marker for both angiosperms and phytoplankton (in different settings), is also identified in sediments from the LLGM (mass spectra from Hanisch et al., 2003). Two diether analogs of hydroxyarchaeol (I and II) are present at relatively high concentrations during the LLGM (394 μg/g TOC and 668 μg/g TOC, respectively), eluting before and after the

C_{36}-alkane internal standard, and persist throughout Interval B and into the beginning of Interval A (mass spectra from Hinrichs et al., 1999, 2000a, 2000b; Stadnitskaia et al., 2008; Elvert and Niemann, 2008). At first evaluation, these compounds were identified as archaeol (I), tentatively identified by relative retention time (Bouloubassi et al., 2009) as well as information that it is the most common of the archaeal diethers (Koga et al., 1998; Pancost et al., 2001, 2003), and sn2-hydroxyarchaeol (II), identified by reasonable correspondence to published mass spectra (Hinrichs et al., 1999, 2000; Stadnitskaia et al., 2008). However, further investigation demonstrates that compound I cannot be archaeol, due to abundant m/z 341 in the mass spectra, which correlates to a hydroxyphytanyl group specific to hydroxyarchaeol, but not occurring in archaeol (Teixidor and Grimalt, 1992; Gill et al., 2010). It is not clear how to identify compound I, but it is likely an analog of hydroxyarchaeol, which derives from archaeal lipids (Koga et al., 1993; Koga and Morii, 2005). A coeluting peak just before compound II could possibly represent sn3-hydroxyarchaeol (Pancost et al., 2001; Pancost and Damste, 2003). Diplopterol, a biomarker of aerobic methanotrophy, occurs at relatively low concentrations during the LLGM (63 μg/g TOC) and the beginning of Interval A, as identified by relative retention time and published mass spectra (Elvert and Niemann, 2008; Hinrichs, 2001). Mass spectra for representative compounds are provided in Appendix C.

Isotopic values of *n*-alcohols trend similarly to mid and long chain fatty acids, with alcohols C_{21}, C_{22}, and C_{24} displaying an excursion of ~15‰ (similar to mid chain fatty acids) and alcohols C_{26} and C_{28} depleting by ~7‰ (similar to long chain fatty acids) (Figure 2.4(d)). Compounds I and II (herein, archaeal lipids) are isotopically similar to bulk $\delta^{13}C$ values (Figure 2.4(e)), remaining relatively constant through the LLGM (-29‰

to -37‰). Compound I was also identified in the deepest Interval C sample (274 cm), but at insufficient concentration to obtain an isotope value. In future work, the isotopic value of this compound should not be used precisely as more positive identification could impact the TMS-derivative mass balance correction, based on the number of TMS groups on the molecule (one TMS group is assumed for this thesis). Diplopterol is highly depleted with respect to bulk $\delta^{13}C$ values, ranging from -88‰ to -96‰.

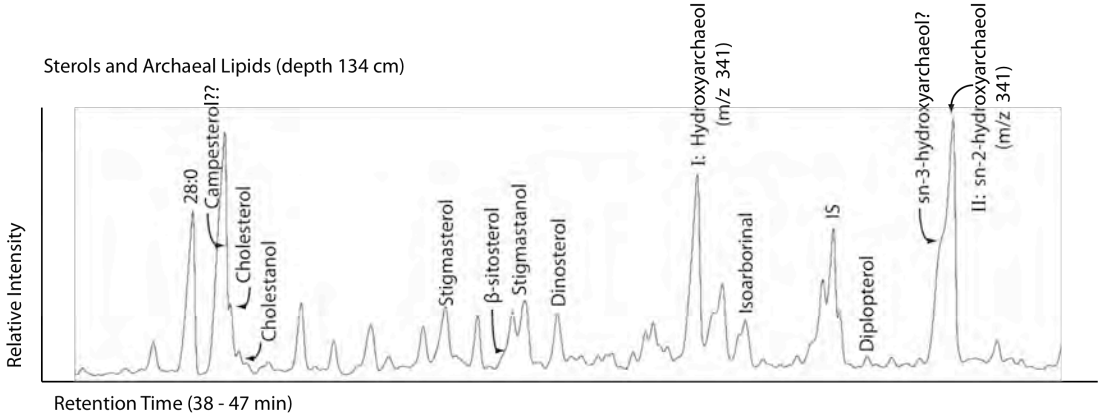

Figure 2.6: Sterols, archaeal, and bacterial lipid chromatogram (LLGM). Illustrates elution times and relative intensities of identified sterols as well as archaeal lipids (I and II) and bacterial diplopterol from the LLGM. Sterols occur in highest abundance during the LLGM, though still well below *n*-alcohols, and too low to obtain $\delta^{13}C$ values. Archaeal lipids are abundant during the LLGM, while diplopterol quantities remain extremely low.

2.5 Discussion

2.5.1 Sources of Organic Matter

Organic matter in sediments at Lake El'gygytgyn fall into four source categories: Terrestrial, aquatic, bacterial, and archaeal. In the alkane and fatty acid fractions, these sources are loosely identified by chain length: short chain compounds (~C_{14} to C_{18}) are interpreted to represent a mixture of aquatic and bacterial sources, mid chain (~C_{19} to C_{23}) compounds are largely representative of aquatic sources, and long chain (~C_{24} to

C_{33}) compounds are thought to derive primarily from terrestrial sources. Evidence for all four sources of organic matter is found in the combination of the alkane, fatty acid, and alcohol fractions, both in concentration and isotopic data. Both the fatty acid and alkane fractions display dominantly terrestrial organic matter. In the alkane fraction, aquatic and bacterial compounds are almost undetectable. In the fatty acid fraction, both aquatic and bacterial compounds exist but are considerably exceeded by the long chain compounds. The alcohol fraction represents all sources, including evidence of methane cycling.

2.5.1.1 Terrestrial Sources

Results indicate that terrestrial organic matter is a critical input source to Lake El'gygytgyn throughout the past ~50 kyr, which is consistent with findings from other Siberian lakes (Ouellette, 2003; Rodgers, 2005). Pollen data from core LZ1024 indicate that terrestrial vegetation is dominated by herbaceous plants in Intervals C and B with a large spike in tree and shrub contribution toward the end of Interval B before quickly transitioning into a tree and shrub dominated vegetation system (Lozhkin et al., 2007b) (Figure 2.3(g)). Normal alkane $\delta^{13}C$ values demonstrate an expected level trend for terrestrial carbon, thus supporting the supposed terrestrial source of the dominant long chain *n*-alkanes (C_{21} to C_{33}). Total *n*-alkane abundance reaches peak concentration during the LLGM. However, the increase in abundance starts considerably earlier than the TOC peak, suggesting that increased organic matter input began much earlier than is reflected in the TOC peak (Figure 2.3(f)). In addition, steadily increasing concentrations in the longest chain alkane compounds during Interval B with a peak before the LLGM reflects a rolling contribution to the TOC peak, suggesting that the expressed peak in TOC is derived from multiple sources contributing increased organic carbon at different

times (Figure 2.3(b)). These terrestrially sourced compounds also display relatively constant isotopic values throughout the entire glacial-interglacial cycle, supporting the hypothesis that the compounds are derived from an atmospheric carbon source, which isn't likely to change substantially over this timescale. According to pollen data, terrestrial contributions during Intervals C and B are largely herbaceous vegetation and quickly transition after the LLGM to a tree- and shrub-dominated setting.

A similar trend was expected in the long chain fatty acids (C_{23} to C_{30}). In fact, concentrations of these long chain fatty acids trend similar to the progression of TOC, except that all compounds display a steady increase in concentration throughout Interval B (Figures 4(f)), suggesting both a common source between the long chain fatty acids as well as supporting the notion that the TOC peak is not an increase in abundance of only one source of organic matter but a result of multiple sources with various stages of increased abundance. Similar to long chain *n*-alkanes, the isotopic values of fatty acid C_{30} remain relatively constant throughout the LLGM, suggesting an entirely terrestrial source (Figure 2.3(b)). However, the isotopic values of other fatty acids tell a different story. Even numbered long chain fatty acids (C_{24}, C_{26}, C_{28}) display a ~5‰ depletion between Interval C and Interval B. This suggests that there may be some contribution to these compounds from non-terrestrial sources during this time period. Further, it suggests that long chain fatty acids (except C_{30}) cannot be interpreted as entirely terrestrial. This is consistent with other literature confirming numerous (if infrequent) microalgal and bacterial sources of long chain fatty acids (Volkman et al., 1980; 1998; Bobbie and White, 1980; Fulco, 1983; Schouten et al., 1998; Logan & Eglinton, 1994).

Contributions of organic matter from terrestrial sources during the LLGM may also be supported by the presence of sterols. However, Volkman (1986) holds that sterols are more widely distributed than originally thought and similar compounds can be found in both terrigenous and aquatic organic matter. This review of sterol markers also suggests that terrestrially derived sterols are more resistant to degradation than aquatic sterols, which may indicate increased preservation of terrestrial sterols during the LLGM (Volkman, 1986).

2.5.1.2 Aquatic Sources

Aquatic sources are identified primarily in the fatty acid fraction. Short and mid chain saturated fatty acids are usually interpreted to derive from aquatic organisms (Meyers and Ishiwatari, 1993). These fatty acids occur in relatively low concentrations during the Late Pleistocene (when compared with long chain fatty acids) but increase to moderate concentrations during the LLGM. The short to mid chain fatty acids (C_{14} to C_{22}) all display a similar concentration trend with TOC, displaying one predominant peak during the glacial period (Figures 2.3(d-f)). The divergence between this trend and the long chain fatty acid concentration trend supports the interpretation that the different chain lengths are derived from diverse sources of organic matter. The simultaneous excursions in mid chain (~10‰) and long chain (~5‰) fatty acid isotopic values during the LLGM suggests either a difference in carbon source between mid chain and long chain compounds, or some degree of C_{24}, C_{26}, C_{28} fatty acid mixing between a constant $\delta^{13}C$ terrestrial carbon source (confirmed by the C_{30} fatty acid) and the mid chain fatty acid carbon source (which shows a 10‰ depletion between Interval C and Interval B). The alcohol fraction displays a few diagnostic aquatic sterols during the LLGM, such as

dinosterol (a marker for dinoflagellates) and isoarborinal (a marker for both angiosperms and phytoplankton, in this case it is more likely a marker for the latter). Values for the carbon to nitrogen ratio (C/N) from other adjacent cores (PG1351) indicate that C/N increases during the LLGM, suggesting either an increase in terrestrial input or severe nitrogen limitation due to ice cover and stratification (Melles et al., 2007). Results indicate that there cannot be an increase in terrestrial contribution (Figure 2.3(e)), as concentration data suggest that the fraction of aquatic organic matter contribution to the total fatty acids during the LLGM increases while the fraction of terrestrial organic matter decreases. This is consistent with a condition of permanent ice cover over the lake during the LLGM, as well as with lipid biomarker results from nearby Lake Elikchan (Ouellette, 2003).

2.5.1.3 Bacterial Sources

Bacteria produce many of the same fatty acids as aquatic organisms, thus making it difficult to distinguish between the two sources. However, there are a few fatty acids diagnostic of bacteria, such as methyl-branched iso- and ante-iso fatty acids, which can be used to determine a portion of the bacterial contribution. Only two bacterial biomarkers were identified at relatively low concentrations in the fatty acid fraction (C_{15} iso- and C_{15} ante iso-) during the LLGM (depth 154 cm), suggesting slightly increased bacterial input relative to the rest of the core. Another bacterial biomarker, diplopterol, was identified in the alcohol fraction and also occurrs largely during the LLGM and beginning of Interval A. Diplopterol occurs in many organisms including cyanobacteria, ferns, lichen, and methanotrophic bacteria (Bechtel and Schubert, 2009). Due to its extreme $\delta^{13}C$ depletion in this case, diplopterol is indicative of methane cycling and

specifically aerobic oxidation of methane (Hinrichs, 2001). The bacterial contribution to the lake during the LLGM appears to be small relative to other organic matter sources.

2.5.1.4 Archaeal Sources

Two biomarkers diagnostic of archaea (I and II) were identified in sediments from the LLGM. These compounds are present in quantities similar to *n*-alcohols throughout Interval B and the beginning of Interval A, suggesting significant archaeal production. Hydroxyarchaeol has been identified almost exclusively in methanogenic archaea (Pancost et al., 2001; Bouloubassi et al., 2009). However, due to the relatively enriched $\delta^{13}C$ signature of both archaeal lipids (hydroxyarchaeol analogs), it is likely that archaea were not entirely acting as methanogens during Interval B.

2.5.2 Production vs. Preservation of Organic Matter

Periods of high TOC in Lake El'gygytgyn sediment cores have been interpreted to represent increased preservation of organic matter due to a lack of oxygen during times of interannual lake ice cover (Melles et al., 2007). This interpretation is supported by an increase in total fatty acid concentrations (normalized to TOC) and especially long chain fatty acids during Interval B. All identified organic compounds display an increasing trend in concentration well before the LLGM, which corresponds with the largest peak in TOC, suggesting that oxygen in the water column did not suddenly disappear, as is evoked by the sudden and sharp TOC transition, but gradually weakens over the course of Interval B. The TOC peak must largely reflect preservation of organic compound classes other than those evaluated in this study because the TOC trend is not reflected in the fatty acids, alkanes, or alcohols.

2.5.3 What Source(s) Drive the Negative Shifts in Bulk Sediment $\delta^{13}C$? (Or, Is There Evidence for Methanogenesis?)

The original hypothesis driving this study proposed that compounds diagnostic of methanogenic archaea and methanotrophic bacteria existing during periods of near permanent ice cover would display extremely depleted $\delta^{13}C$ values, suggesting methane cycling associated with water column anoxia. In order to demonstrate that biomarkers from sources other than bacteria behave as expected at Lake El'gygytgyn, the concentrations and isotopic values of terrestrial *n*-alkanes were used to confirm that an atmospheric carbon source is reflected. Long chain fatty acid isotopic values were expected to show a similar trend to the terrestrial alkanes (as exhibited by fatty acid C_{30}), but most of the long chain fatty acids appear to derive from somewhat mixed source material, as displayed by a ~5‰ excursion during the LLGM. This "terrestrial" fatty acid excursion might be explained by an approximately equal mix of organic matter with a constant carbon source, such as terrestrial fatty acid C_{30}, and aquatic or bacterial organic matter with a carbon source depleted by ~10‰ over the course of Interval B (same source as mid chain fatty acids). An equal mix between these two sources would produce an excursion of approximately 5‰.

2.5.3.1 Isotopic Depletion in Aquatic Lipids

The considerable glacial depletion of bulk $\delta^{13}C$ at Lake El'gygytgyn differs from the trend of bulk $\delta^{13}C$ at nearby Lake Elikchan which experiences glacial enrichment; interpreted to result from stressed pCO_2 conditions (Rodgers, 2005). However, the latitude difference, duration of ice cover, and thus access to atmospheric CO_2 between these two lakes could provide the solution to this discrepancy. The most isotopically

depleted fatty acids were found within the mid chain group (C_{19} to C_{23}), which are usually associated with aquatic organisms. The mid chain fatty acid MWA ~10‰ carbon isotope excursion during Interval B suggests that aquatic organic matter is utilizing depleted carbon in the water column that is not fully mixed with atmospheric CO_2. This depleted carbon is likely recycled by aquatic primary producers as organic matter in the water column degrades to CO_2 and is used to produce new biomass, some of which degrades and releases CO_2, thus repeating the process. As shown in Figure 2.7, aquatic organic matter could be using carbon from a number of possible sources (estimated isotopic values): dissolved atmospheric CO_2 (0‰), sinking degraded organic matter (-25 to -45‰), dissolved inorganic carbon (DIC) from stream input (-10‰), dissolved or particulate organic carbon (DOC/POC) from stream input (-30‰), or methane/CO2 from methanogenesis/methanotrophy (-90‰). During the LLGM, the depletion of aquatic lipids to -44.5‰ (C_{21} LLGM) suggests that these compounds are certainly deriving from autochthonous sources because the only carbon sources with the potential to drive these negative $\delta^{13}C$ signatures are degraded organic matter and carbon from methanogenesis and methanotrophy. Extremely depleted $\delta^{13}C$ values attributed to methane cycling (diplopterol $\delta^{13}C$= -96‰) suggest that only a little over 10% of bacterial lipids with a $\delta^{13}C$ reflecting methane cycling (~ -90‰) would be required to impact the $\delta^{13}C$ of aquatic organic matter (from -27‰ during Interval C to -35‰ during LLGM). Alternatively, the depleted aquatic lipid $\delta^{13}C$ signature could also be achieved if aquatic primary producers were in large part using recycled CO_2 from depleted sinking organic matter rather than atmospheric CO_2. In a situation where there is little atmospheric carbon input (semi-permanent ice cover), $\delta^{13}C$ of sinking organic matter using a

combination of 1/3 recycled CO_2 and 2/3 atmospheric CO_2 could become progressively more $\delta^{13}C$ depleted (by ~ -10‰) until a carbon source with an enriched $\delta^{13}C$ is made available.

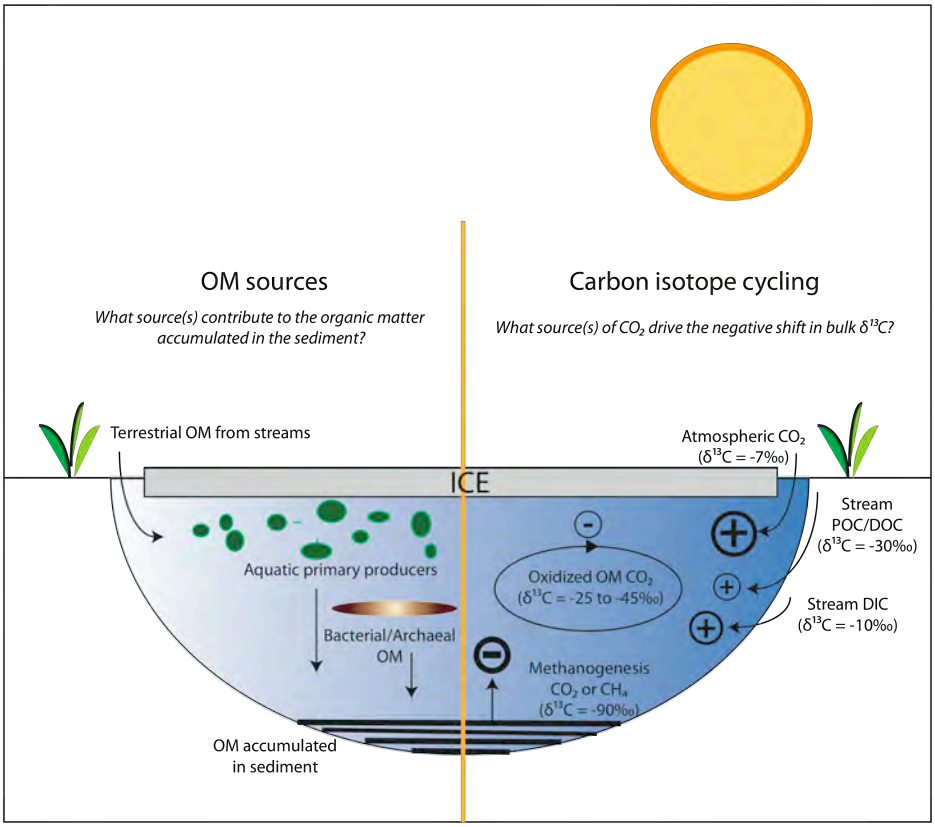

Figure 2.7: Organic matter sources and carbon isotope cycling schematic. During the LLGM, when the lake experiences nearly permanent ice cover conditions, there is still evidence of input from terrestrial, aquatic, and bacterial/archaeal sources (left). The most influential CO_2 drivers of $\delta^{13}C$ are indicated by the size of the +/- signs (right). The largest positive driver of bulk $\delta^{13}C$ is atmospheric CO_2, while the largest negative driver is methanogenesis.

There may be some bacterial contribution to this depletion, but because mid chain fatty acids are normally considered a mixture of mostly algal and some bacterial sources, and there are no diagnostic bacterial biomarkers identified within the mid chain fraction, it is impossible to separate the algal and bacterial contributions within this group. There

may be a small contribution of bacteria associated with methane cycling, which causes the mass weighted short chain fatty acid $\delta^{13}C$ value to display greater isotopic depletion (~3‰) than the bulk $\delta^{13}C$. However, we must look to other fractions besides fatty acids to find biomarkers associated with methane cycling that display a highly depleted isotopic signature.

2.5.3.2 Bacterial Fatty Acids Associated with Methane Cycling

The largest contribution of depleted $\delta^{13}C$ was expected to derive from extreme depletion in fatty acids diagnostic of bacterial sources within the short chain fatty acids (C_{14} to C_{18}). These compounds were expected to display $\delta^{13}C$ values of near -60‰ (Whiticar, 1999). Contrary to expectation, these compounds were largely not present in high enough concentrations to measure $\delta^{13}C$. Methyl-branched fatty acids (C_{15} iso- and C_{15} ante iso-) were identified at sufficient concentrations in one glacial sample (depth 134 cm), but displayed isotopic values near bulk $\delta^{13}C$ (-33.0‰ to -33.7‰). Other saturated short chain fatty acids may have derived from bacterial sources, but none displayed highly depleted $\delta^{13}C$ values. These results suggest the existence of bacterial fatty acids associated with processes other than methane cycling.

2.5.3.4 Bacterial Biomarker of Aerobic Oxidation of Methane

Diplopterol, a bacterial biomarker demonstrating aerobic oxidation of methane (as indicated by its extreme $\delta^{13}C$ depletion), was identified in three sediment samples deposited during the LLGM (depths 114 cm to 154 cm), as well as during Interval A (74 cm). As expected for a biomarker of methanotrophy, $\delta^{13}C$ values for diplopterol range as low as -96‰, signifying bacterial oxidation of methane either in the water column or at

the sediment/water interface. The isotopic values indicate the simultaneous production of methane by CO_2-reduction methanogenesis because only this type produces sufficiently depleted $\delta^{13}C$ values (Whiticar, 1999). Any amount of acetate fermentation, which is more often associated with freshwater systems, would likely dilute the isotopic signal with more enriched values. Diplopterol does not occur in large abundance but the associated isotopic values are depleted enough to influence the bulk $\delta^{13}C$ signature even at low concentrations.

2.5.3.3 Archaeal Biomarkers

Archaeal lipids were identified in large abundance in sediment from the LLGM, Interval B, and the beginning of Interval A. Hydroxyarchaeol has been used as an indicator for both methanogenesis and reverse methanogenesis (anaerobic oxidation of methane) (Hoehler et al., 1994; Pancost et al., 2000; Hinrichs and Boetius, 2002). Reverse methanogenesis involves sulfate-reducing bacteria, thus requiring a minimum concentration of sulfate, which is scarce at Lake El'gygytgyn. These compounds must be partly derived from methanogens due to the existence and extremely depleted isotopic values of methanotrophic bacteria, which require a certain amount of CO_2-reduction methanogenesis. However, archaeal lipid $\delta^{13}C$ values trend only slightly lower than bulk $\delta^{13}C$ values and appear considerably sooner than diplopterol, indicating that the large community of archaea during the LLGM mostly employs another type of metabolism besides methanogenesis. Similarly, the constant isotopic values of both archaeal lipids throughout Interval B and including the LLGM suggest that the archaeal community remains constant in diversity of species (largely not methanogens) and in carbon source throughout its existence.

Examination of the lipid biomarkers reveals only one conclusive piece of evidence for methane cycling: small quantities of bacterial diplopterol with highly depleted $\delta^{13}C$ occurring during the LLGM and demonstrating aerobic oxidation of methane. Consequently, evidence of methanotrophy with extremely depleted $\delta^{13}C$ demonstrates that there is simultaneous CO_2-reduction methanogenesis occurring in the archaeal fraction as well. The abundant archaeal lipids must be partly producing methane in order for the bacterial methanotrophs to exist. However, due to the relatively enriched archaeal $\delta^{13}C$ signatures, they cannot derive entirely from methanogens. In fact, it is likely that an extremely small fraction of the archaea during the LLGM were methanogens else the $\delta^{13}C$ signature would show a greater depletion in reflection of the extreme fractionation effect of CO_2-reduction methanogenesis. However, it cannot be determined whether these methane cycling processes are occurring in the water column or strictly in the sediments. Previous studies (Melles et al., 2007; Nowaczyk et al., 2007) have posited that extremely low magnetic susceptibility values as well as finely laminated sediments supports evidence for extreme water column anoxia during periods of interpreted glacial conditions. Perhaps there was a very thin anoxic layer at the sediment-water interface, which could provide conditions suitable for depositing laminated sediments and production of small amounts of methane. Small quantities of methane could support a small community of methanotrophic bacteria (as evidenced by low concentrations of diplopterol), produced by methanogens from a small fraction of the archaeal community. The results of this compound-specific $\delta^{13}C$ work require minimal methane cycling, and therefore anoxia, within the lake.

It is also possible that the diplopterol and archaeal lipids derive from allocthonous sources, such as terrestrial soils or permafrost, which could be supported by the constant trend of $\delta^{13}C$ signatures similar to terrestrial alkanes and the C_{30} fatty acid. However, the timing of the occurrence supports a connection with increasing anoxic conditions in the lake sediments and possibly the water column. Furthermore, it would be expected that these terrestrially sourced compounds would exist throughout the entire core and not exclusively at a time when sediments exhibit increasing contributions of aquatic (not terrestrial) organic matter.

2.5.4 Is Magnetic Susceptibility a Proxy for Anoxia?

As another possible indicator for anoxia, this study attempted to link the magnetic susceptibility record to the nitrogen cycle through bulk $\delta^{15}N$ to show evidence of anoxia through denitrification. However, the original interpretation that magnetic susceptibility is a proxy for lake ice cover, due to dissolution of magnetite grains under highly anoxic conditions, is not supported by the results of this work. Bulk $\delta^{15}N$ was expected to show enrichment during periods of low magnetic susceptibility and high TOC (LLGM), due to intensified denitrification under anoxic conditions. Neither core (PG1351 or LZ1029) displays a clear enrichment signal during the LLGM. Furthermore, in core LZ1029, bulk $\delta^{15}N$ actually appears to be anti-correlated with TOC during the LLGM (Figure 2.2). However, there appears to be some enrichment during the beginning of Interval B, suggesting some level of denitrification in response to anoxia, but this trend deteriorates resulting in relative $\delta^{15}N$ depletion during the LLGM. In another more extended record from core PG1351 (compared with magnetic susceptibility) there is no correlation at all. The $\delta^{15}N$ values are within a reasonable range for lakes (Meyers and Eadie, 1993; Pang

and Nriagu, 1976; 1977) and other high-latitude soils and terrestrial water bodies (Wolfe et al., 1999; Gaye et al., 2007; Routh et al., 2007; Zech and Glaser, 2007). Vitousek et al. (1991) suggest that, under certain circumstances, nitrogen fixation is limited by the source of nitrogen. For example, in environments where decomposition is slow, such as the frozen landscape surrounding Lake El'gygytgyn during glacial periods, carbon-bonded detrital nitrogen might prove limited in supply to nitrogen fixers, thus limiting the supply of un-bonded nitrogen in the water column. This situation might limit the amount of nitrate produced in the water column, which would in turn limit the process of denitrification by causing it to react to completion, thus producing no isotope effect and reflecting the original $\delta^{15}N$ of nitrogen input to the lake. This condition may explain the initial $\delta^{15}N$ enrichment during Interval B, associated with decreasing oxygen, as well as the transition to $\delta^{15}N$ depletion resulting from nitrate limitation.

2.6 Conclusions

This study set out to test hypotheses (Melles et al., 2007; Nowaczyk et al., 2007) that Lake El'gygytgyn experiences severe anoxia during cold intervals when the lake is under permanent ice cover. In addition, this study sought to determine the source(s) of organic matter contributing to the depleted bulk $\delta^{13}C$ during the same cold intervals. The original hypothesis suggested that the answers to these two questions might be related through evidence of methane cycling. For example, if the depleted bulk $\delta^{13}C$ could be traced to increasing LLGM contributions from methane, whose generation requires anoxic conditions, then a story of increasing anoxic severity could be built. However, through analysis of compound-specific $\delta^{13}C$ and bulk $\delta^{15}N$, there is limited evidence to show that anoxia is present at any time in the water column at Lake El'gygytgyn. The

presence and isotopic composition of bacterial lipid diplopterol demonstrate that methanotrophy, and consequently methanogenesis and anoxia, existed during Interval B in at least the sediment and perhaps a portion of the water column. Conversely, the identification of diplopterol associated with methane cycling also indicates aerobic oxidation of methane throughout the LLGM, demonstrating that the water column does not become completely anoxic. Likewise, the isotopic composition of bacterial fatty acids follow the values of bulk $\delta^{13}C$ as well as the trend of aquatic lipid $\delta^{13}C$ but not those indicating preferential incorporation of methane or CO_2 from oxidized organic matter (i.e., more than aquatic lipids experience), suggesting that much of the bacterial community exists under oxic conditions. In addition, evaluation of the possible contributions to the depleted bulk $\delta^{13}C$ indicate that methanogenesis may be a small part of the driving force toward bulk $\delta^{13}C$ depletion, though evidence is only found in one compound (diplopterol) at low concentrations. However, there is substantial depletion in aquatic lipids, which demonstrates either methane cycling or considerable recycling of CO_2 from degraded organic matter back to aquatic primary producers with limited atmospheric CO_2 exchange. The latter scenario influences bulk $\delta^{13}C$ depletion, yet does not necessitate methanogenesis. The isotopic data presented here do not require anoxic conditions in the water column, though neither is anoxia necessarily precluded. Observations of extreme magnetic susceptibility shifts, laminated sediments, and even images from grain mounts providing hints of magnetite dissolution during the local LGM all suggest that anoxia cannot be confined only to the sediments. However, the questions remain: How intense is water column anoxia? And, where is the oxycline? The results presented here could be compatible with a thin anoxic layer just above the sediment water

interface. The presence of archaeal lipids throughout Interval B and the appearance of bacterial diplopterol (with its highly depleted $\delta^{13}C$) during the LLGM demonstrate that there may be a gradational increase in the intensity of anoxia throughout Interval B. Anoxia may not be an "on/off" switch, as the sudden shifts of magnetic susceptibility and TOC suggest, but a slow process that impedes degradation of organic matter (as shown by increased concentrations of fatty acids, alkanes, and alcohols relative to TOC) even before the sharp spike in TOC is apparent. It is clear that bulk $\delta^{15}N$ alone cannot disprove anoxia in the water column. Furthermore it appears, through all of the data provided in this study, that a severe and significant anoxic layer throughout the water column is unlikely to have persisted at Lake El'gygytgyn during the LLGM.

CHAPTER 3

FUTURE WORK

3.1 Introduction

This chapter focuses on ongoing and future work from Lake El'gygytgyn sediments and specifically how results from this thesis might guide future projects. Details include remaining unresolved questions relating to this work as well as recommendations toward research that might help to further constrain the research questions posed as part of this thesis.

In Spring 2009, a major field campaign was conducted to collect core material spanning the entire depositional history of Lake El'gygytgyn Crater. My work on the pilot cores PG1351 and LZ1029 determines the scientific significance of the analyses proposed here and will be used to determine whether the same analyses will be conducted on the newest (longer time scale) cores.

3.2 Remaining Questions / Future Work

3.2.1 Bulk Nitrogen Isotopes

Bulk sediment $\delta^{15}N$ does not exhibit a strong anoxia intensity signal during the LLGM, possibly due to nitrogen limitation, and thus may not be a useful analysis for the entire core. However, results do indicate that under less severe conditions, such as the beginning of Interval B (Figure 2.2), there may be evidence for increased denitrification. Perhaps there are intervals elsewhere in the longer cores where there are indications for less severe nitrogen limitation and where bulk nitrogen isotopes may serve as an indicator for anoxia intensity after all. Examination of such intervals may reveal a threshold of

total nitrogen concentration, under which there is insufficient nitrogen to support denitrification. Such a threshold might provide valuable information about patterns of change in the lake system.

3.2.2 Anoxia

Results presented in this thesis partially contradict a theory presented by Nowaczyk et al. (2007), suggesting that the extreme shifts in magnetic susceptibility represent dissolution of magnetite grains under conditions of extreme water column anoxia. Though cycles of anoxia are maintained in this work as a possible conclusion, there is no evidence in the $\delta^{15}N$ to suggest the severe intensity of anoxic cycling or full water column anoxia that might be required to cause dissolution of magnetite grains. Are there other solutions besides dissolution of magnetite grains to explain the extreme shifts in magnetic susceptibility? Are there other conditions besides intensely severe anoxia that could explain etched magnetite grains, as seen in previous research (Brigham-Grette, unpublished data)? These are important questions to consider in evaluating the existing data as well as moving forward to interpretation of the newest cores.

3.2.3 Compound-Specific Carbon Isotopes

Compound-specific $\delta^{13}C$ has proven to be a useful tool in determining the contribution and isotopic composition of the various sources of organic matter at Lake El'gygytgyn. The combination of concentration trends, absolute concentrations, and isotopic values provides valuable information concerning the changes in production, preservation, organic matter sources, and carbon sources throughout time. These combined analyses should be performed covering specific intervals of the core, such as

significant marine isotope stage transitions when major transitions between organic matter sources and carbon sources might be observed. A comparison of concentrations and isotope values during similar paleoenvironmental intervals, perhaps comparing intervals of different intensities, would be useful in further constraining the conclusions presented in this work. In particular, identifying intervals that display a less intense environmental change toward colder conditions might reveal that there are certain thresholds over which biomarkers associated with methane cycling appear. Conversely, intervals that display more intense signals of increasing cold and more permanent ice cover may also show that methane cycling becomes much more severe, thus depleting the bulk $\delta^{13}C$ further and yielding higher concentrations of compounds diagnostic of methane cycling. Are there any glacial intervals in the cores that hold evidence for highly $\delta^{13}C$ depleted archaeal lipids? If so, this would indicate a significant change in the archaeal community in the lake.

Additionally, more positive identification of compounds identified as archaeal lipids (compounds I and II) may provide insight into specific sources for these compounds. Hydroxyarchaeol (m/z 341) almost exclusively derives from archaeal methanogens (Pancost et al, 2001). However, from this work it is likely that these compounds are deriving from source(s) other than methanogens, given the $\delta^{13}C$ signatures of archaeal lipids (Figure 2.4(e)). Is this an example of hydroxyarchaeol occurring in non-methanogen biomass? Or, can these compounds be specifically traced to another type of archaeal organism? Future work might endeavor to use the mass spectra to provide a more detailed identification of these compounds.

3.2.4 Methane Cycling

Conclusions presented in Chapter 2 provide for an oxycline that exists just above the sediment-water interface during the LLGM. This explanation allows for sediment that remains undisturbed by bioturbation during this interval as well as etched grains of magnetite thought to have resulted from anoxia (Melles et al., 2007; Brigham-Grette, unpublished). However, from these data it cannot be established how far the oxycline extends up into the water column. Compounds indicative of methane cycling suggest there is minimal methanogenesis occurring in either the water column or the sediments. Future work may attempt to disentangle indicators of sediment anoxia from indicators of water column anoxia in order to assess the contribution of each anoxic environment to the evidence in the form of biomarkers and isotopic signatures. Perhaps down-core compound-specific isotopic work will assist in determining environmental conditions under which more intense anoxia prevails. Starting with the assumption that the LLGM provides minimal water column anoxia to maintain both undisturbed sediments yet negligible concentrations of biomarkers of methanotrophy, perhaps an interval with greater concentrations and a variety of biomarkers indicative of methane cycling will serve to demonstrate increased water column anoxia. If there is evidence to show that the sediments are already fully anoxic during the LLGM, then any further evidence for anoxia may be indicative of water column anoxia. For example, archaeal lipids with depleted $\delta^{13}C$ might demonstrate increased methanogen activity in the water column.

One of the guiding questions of this work has focused on the depleted bulk $\delta^{13}C$ and the contributing source(s) of organic matter. A part of this question that was not fully addressed involves the fate of the unused ^{13}C atoms. If aquatic primary producers

are continually recycling depleted CO_2 during Interval B, then relatively enriched CO_2 must remain. However, a continually increasing depletion is seen throughout this interval, suggesting that the enriched CO_2 is being incorporated somewhere else or is released from the lake. Further evaluation of the carbon isotope cycle within Lake El'gygytgyn would be useful toward a better understanding of how carbon is metabolized, recycled, and buried within the lake system.

3.2.5 Other Potential Efforts

There are perhaps other conditions which impact the lake system and produce the effects seen in this and previous data, but for which the source has not yet been discovered. For example, could variations in pH associated with glacial cycles have an impact on magnetite? If carbon is not able to escape from the lake due to permanent ice cover, yet organic matter in the water column and sediment continues to degrade and force increased concentrations of dissolved CO_2 into the water, thus acidifying the water column, what impact might this have on biogeochemical as well as physical processes within the lake? In order to resolve this question, additional data may be required to estimate alkalinity in the water column throughout time.

In addition to continuing the work conducted in this thesis down core, future work may incorporate other analyses that would help interpret changing environments at Lake El'gygytgyn throughout time. For example, might analysis of iron isotopes potentially help to indicate environments of reduction and oxidation? Current bulk geochemical analysis of the longer cores is revealing evidence for inorganic carbon at certain intervals (V. Wennrich, pers. comm.). The addition of carbonate might facilitate the precipitation of Fe(III), which produces a large equilibrium isotope fractionation (Johnson et al.,

2002). Perhaps this analysis, in combination with other parameters, could aid in determining intervals of bottom water oxidation and reduction.

3.3 Conclusion

The sediments from Lake El'gygytgyn are a vast repository of unlimited information regarding past climate and environmental change in Northeast Siberia. Even the scales to which implications and connections can be drawn (local, regional, polar, global) seem infinitely intricate. The work on the pilot cores reveals literally the surface of this immense database and even this information promises further interpretation and implications. Each analysis holds the opportunity to refine an interpretation, identify a pattern, or build a new story. The challenge lies in choosing the analyses wisely. The down-core record from Lake El'gygytgyn seems infinite in its potential to be measured, but consideration for previous work on the pilot cores will help to guide the next steps. Specifically, continued work to resolve the complexity of Lake El'gygytgyn's carbon and oxygen cycles through time will require reference to detailed investigations such as this thesis, but assisted (or confounded) by vastly more information. The questions posed in this thesis and the attempts to answer them will serve the continued efforts to unravel the mysteries contained in the sediment of Lake El'gygytgyn.

APPENDICES

APPENDIX A

LABORATORY METHODS

A.1 Bulk $\delta^{15}N$

1. Pack sediment in Costech tin capsules (5 x 9 mm), weigh on microbalance, and fold into a short cylinder.
2. Range of masses determined by amount of total nitrogen (TN %) per sample. Each sample needs between 30 and 60 μg of nitrogen in the capsule.
3. Load sediment cylinders into the elemental analyzer, coupled with an isotope ratio mass spectrometer (EAirMS).
4. Due to the large volume of sediment needed per sample, only 20 samples can be run at a time. In between runs, the EA column must be changed.
5. QA/QC: Include alternating standards (8547 & 8550) at most within 10 samples to confirm consistent values from the EAirMS. Every 10 samples shall include a triplicate.

A.2 Compound-specific $\delta^{13}C$

In addition to samples chosen from core LZ1029 for lipid biomarker analysis, samples from cores PG1351 and LZ1024 were simultaneously prepared through only a portion of the process. Three samples from core PG1351 (depths 139-141(PG141), 199-201(PG201), 241-243(PG243)) were ASE extracted, the TLE was dried under N_2, and stored under refrigeration. Fifteen samples from core LZ1024 (listed below) were ASE extracted, the TLE was separated on an amino acid column into acids and neutrals, and the neutral fraction was further separated on a silica gel column into hydrocarbons, ketones, alcohols, and a polar fraction. The hydrocarbon fractions were identified on the

GC-MSD, quantified on the GC-FID, and measured for isotopic composition on the GC-irMS, along with fractions from core LZ1029. All fractions are stored under refrigeration in the UMass Biogeochemistry Lab.

Samples from core LZ1024 (Figure A.1):

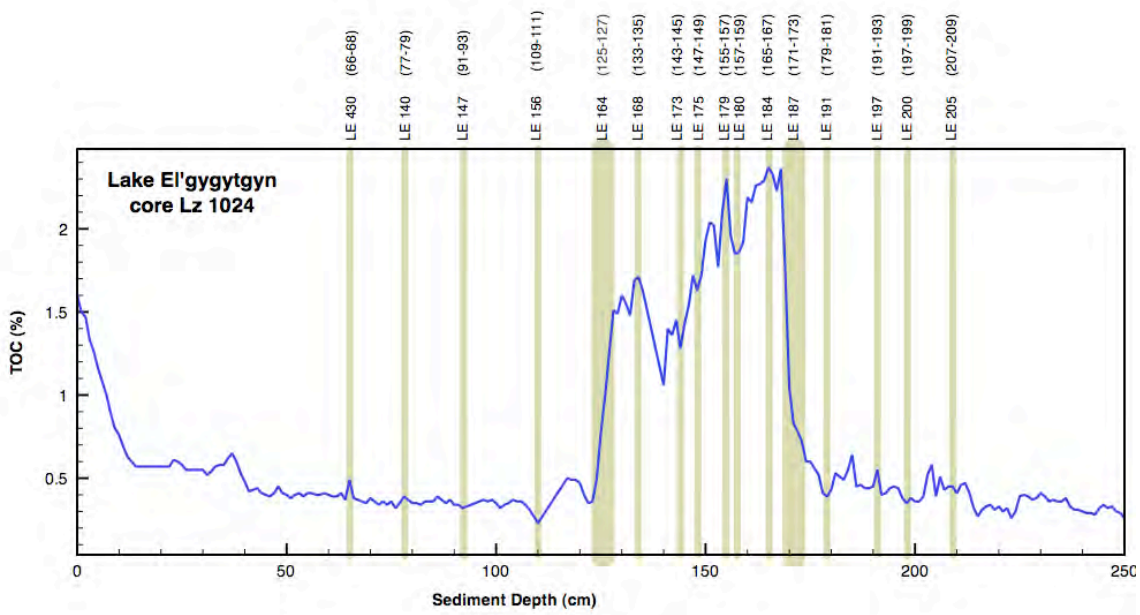

Figure A.1: Samples chosen and prepared for alkane $\delta^{13}C$ analysis from core LZ1024.

A.2.1 ASE Extraction (Accelerated Solvent Extractor)

1. Crush and weigh sediment.
2. When mass > 6.0 g, separate sediment into 2 ASE cells (A & B).
3. Mix sand into sediment (approximately 1:1).
4. Pack ASE cells in the following order (bottom to top): 2 G6 filters, sand/sample, 10 µL C_{36} alkane (20 µL per sample), 1 G6 filter, sand to top, 1 G6 filter.
5. Cap ASE cells, load ASE with packed cells and empty 60 mL vials, and perform run.

6. After run, dry total lipid extract (TLE) down and transfer to 4 mL vials, combining parts A & B of each sample.

A.2.2 Amino-propyl Column Chromatography

1. Pack amino-propyl columns with NH_2-propyl gel into Pasteur pipettes, leaving ½ inch of space below indent in pipette, and plugging the tip of the pipette with a small amount of glass wool.
2. Store packed columns in 80°C oven until use.
3. Begin by rinsing the column with 8 mL of dichloromethane and isopropyl alcohol (DCM:IPA, 2:1 solution). Aim solvent to the side of the pipette to avoid disturbing the top of the gel. Once wet, do not let the column dry out.
4. Transfer TLE onto column with ~ 250 µL of DCM:IPA (3 times). With each transfer, aim TLE increasingly toward the top of the pipette to rinse compounds down to the top of the gel. Wait for previous transfer to settle into column before adding the next transfer.
5. Elute fraction F1 with 4 mL of DCM:IPA into 4 mL vial ("Neutrals").
6. Transfer TLE with 200 µL of 2% Formic Acid in DCM (1 time).
7. Elute fraction F2 with 8 mL of 2% Formic Acid in DCM into two 4 mL vials ("Acid A" and "Acid B").
8. Elute fraction F3 with 4 mL of methanol (MeOH) into 4 mL vial ("MeOH" archive).
9. Dry down vials of neutrals, acids, and MeOH. Transfer Acid B into Acid A with 2% Formic Acid in DCM (3 times).

10. Store dried fractions under refrigeration.

A.2.3 Silica Gel Column Chromatography

1. Pack silica gel columns into Pasteur pipettes, leaving ½ inch of space below indent in pipette, and plugging the tip of the pipette with a small amount of glass wool.
2. Store packed columns in 80°C oven until use.
3. Begin by rinsing the column with 8 mL of hexane. Aim solvent to the side of the pipette to avoid disturbing the top of the gel. Once wet, do not let the column dry out.
4. Transfer neutral fraction onto column with ~ 250 µL of hexane (3 times). With each transfer, aim increasingly toward the top of the pipette to rinse compounds down to the top of the gel. Wait for previous transfer to settle into column before adding the next transfer.
5. Elute fraction F1 with 4 mL of hexane into 4 mL vial ("Hydrocarbons").
6. Transfer neutral fraction with 200 µL of DCM (1 time).
7. Elute fraction F2 with 4 mL of DCM into 4 mL vial ("Ketones").
8. Elute fraction F3 with 4 mL of hexane and ethyl acetate (hex:EtOAc, 3:1 solution) into 4 mL vial ("Alcohols").
9. Elute fraction F4 with 4 mL of Methanol (MeOH) into 4 mL vial ("MeOH" archive).
10. Dry down vials of hydrocarbons, ketones, alcohols, and MeOH.
11. Store dried fractions under refrigeration.

A.2.4 FAME Derivitization

1. Heneicosanoic acid (C_{21} FA) was derivitized, along with other fatty acid samples, and used as an isotope mass balance standard to correct for the fractionation associated with addition of a methyl ester during derivitization. Mix solutions at 1.0 µg/µL and pull out 20 µL (20 µg) for derivitization. Store stock solutions in freezer.
2. Pack Na_2SO_4 into Pasteur pipettes, leaving ½ inch of space below indent in pipette, and plugging the tip of the pipette with a small amount of glass wool.
3. Prepare solvent extracted water:
   - Add DCM to deionized water in a glass funnel with a Teflon valve.
   - Mix vigorously, releasing pressure every few seconds. Let DCM settle to bottom and drain, leaving a small amount of DCM in funnel.
   - Add DCM and repeat 3 times, letting funnel sit between mixing and draining. The 3rd time, the funnel should sit for 30 minutes before draining all of the DCM, plus a small amount of the water.
   - Let water sit in covered funnel overnight in the hood to allow any remaining DCM to evaporate. Drain water into storage vessel.
4. Add ~ 500 µL Bf_3MeOH (from Supelco) to each acid fraction (Danger! Very Toxic!!)
5. Cap and heat at 70°C for 15-20 minutes.
6. Prerinse Na2SO4 columns with:
   - 1 volume MeOH

- 1 volume DCM
- 1 volume Hexane

7. Add ~ 1 mL solvent extracted water to each acid fraction
8. Add 1 mL hexane to each acid fraction.
9. Sonicate, vortex, and draw off top layer (hexane) with dedicated pipette.
10. Transfer hexane layer to Na2SO4 column, collecting "Dirty FAMEs" into a 4 mL vial.
11. Repeat steps 7-9 as many times as needed until the hexane is clear and there is a clear boundary between the water and the hexane.

A.2.5 Silica Gel Clean-up (FAMEs)

1. Pack silica gel columns into Pasteur pipettes, leaving ½ inch of space below indent in pipette, and plugging the tip of the pipette with a small amount of glass wool.
2. Store packed columns in 80°C oven until use.
3. Begin by rinsing the column with 4 mL of DCM, then 4 mL of hexane. Aim solvent to the side of the pipette to avoid disturbing the top of the gel. Once wet, do not let the column dry out.
4. Transfer dirty FAMEs onto column with 250 µL of hexane (3 times).
5. Elute fraction F1 with 4 mL of hexane into 4 mL vial ("Junk").
6. Transfer dirty FAMEs onto column with 250 µL of DCM (1-3 times, depending on visual inspection of dirty FAMEs vial).
7. Elute fraction F2 with 4 mL of DCM into 4 mL vial ("Clean FAMEs").

8. Add C_{36} alkane standard (20 µL @ 1.063 µg/µL) to each vial for quantification with GC-FID.
9. Dry down under N_2 gas.
10. Transfer to 2 mL vials with conical insert with ~ 200 µL of hexane.

A.2.6 Alcohol Derivitization

1. Two isotope mass balance standards, Nonadecanol (C_{19} alcohol) and Octacosanol (C_{28} alcohol), were derivitized with the same method as other alcohol samples in order to determine the fractionation associated with addition of a trimethylsilyl (TMS) group. Mix solutions at 1.02 µg/µL and pull out 200 µL (200µg) for derivitization. Store stock solutions in freezer.
2. Add 100 µL pyridine (from Supelco) to each alcohol fraction.
3. Add 100 µL BSTFA (from Supelco) to each alcohol fraction.
4. Cap quickly and tightly, heat at 70°C for 20-30 minutes.
5. Let cool to room temperature.
6. Add C_{36} alkane standard (20 µL @ 1.063 µg/µL) to each vial for quantification with GC-FID.
7. Dry down vials under N_2 gas.
8. Transfer to 2 mL vials with conical insert using ~ 200 µL of toluene (preferred) or DCM.
9. BSTFA is not stable for long term storage. 60 days after derivitizing, a run on the GC-irMS showed that TMS-alcohols had considerably

degraded in the interim. Alcohols were then re-derivitized and run on the GC-irMS within a few days, with significantly better results.

A.2.7 Gas Chromatograph – Mass Selection Detector (GC-MSD)

1. Details: Hewlett-Packard 6890 series. Column is an HP-5MS #HP19091S-433 (325°C max), with a 5% phenyl methyl siloxane capillary, dimensions 30 m x 250 μm inner diameter x 0.25 μm film thickness.
2. Oven program:
   - Alkane method (MPW_NALK.M): 40°C hold for 2 min, ramp to 130°C at 20°C/min, ramp to 320°C at 4°C/min, hold at 320°C for 15 min. Inlet temp 300°C.
   - Fatty acid method (AHFAME.M): 40°C hold for 2 min, ramp to 320°C at 6°C/min, hold at 320°C for 2 min. Inlet temp 300°C.
   - Alcohol method (AHALCOHL.M): 60°C hold for 2 min, ramp to 160°C at 20°C/min, ramp to 320°C at 4°C/min, hold at 320°C for 15 min. Inlet temp 300°C.
3. Representative mass spectra for selected identified compounds are included in Appendix C.

A.2.8 Gas Chromatograph – Flame Ionization Detector (GC-FID)

1. Details: Hewlett-Packard 6890 series. Column is an HP-5 Agilent (manuf.) #19091J-433 (325°C max), with a 5% phenyl methyl siloxane

capillary, dimensions 30 m x 250 μm inner diameter x 0.25 μm film thickness.

2. Oven program:
   - Alkane method (AHALKANE.M): 60°C hold for 1 min, ramp to 315°C at 15°C/min, hold at 315°C for 15 min. Inlet temp 320°C
   - Fatty acid method (KWACID.M): 60°C hold for 1 min, ramp to 315°C at 15°C/min, hold at 315°C for 15 min. Inlet temp 320°C
   - Alcohol method (AHALCOHL.M): 60°C hold for 2 min, ramp to 160°C at 20°C/min, ramp to 320°C at 4°C/min, hold at 320°C for 15 min. Inlet temp 320°C.
3. Identify compounds using retention time as compared with GC-MSD traces.
4. Calculate the mass of each compound using a quantification standard (C_{36} alkane)

   For compound "Y":

$$\text{Mass of Y in vial} = \frac{(\text{Mass of standard in vial}) \times (\text{Area Y})}{(\text{Area under standard peak})}$$

5. Calculate concentrations normalized to the mass of TOC in the original dry sediment.

   For compound "Y":

$$\text{Concentration Y } (\mu g/g \text{ TOC}) = \frac{(\text{Mass of Y in vial } (\mu g)) \times 100}{(\text{TOC\%}) \times (\text{Mass dry sediment } (g))}$$

A.2.9 Gas Chromatograph – isotope Ratio Mass Spectrometer (GC-irMS)

1. Samples were run at Yale University's Earth System Center for Stable Isotopic Studies. The technician who ran the samples and served as a contact for my work was Gerard Olack.
2. Details: Thermo Scientific Finnigan MAT 253 stable-isotope mass spectrometer equipped with a dual inlet and a Thermo Scientific gas chromatograph (Trace GC Ultra 2000)-combustion interface. DB-1 Column (SOLGEL-IMS / SGE manufacturer part # 054793) is 60 m x 250 μm inner diamter x 0.25 μm film thickness.
3. Oven program:
   - Alkane method: 115°C hold for 2 min, ramp to 145°C at 16°C/min, ramp to 200°C at 12°C/min, ramp to 290°C at 8°C/min, ramp to 325°C at 3°C/min, hold at 325°C for 13.62 min. Inlet temp 260°C.
   - Fatty acid method: 80°C hold for 2 min, ramp to 145°C at 12°C/min, ramp to 200°C at 12°C/min, ramp to 290°C at 8°C/min, ramp to 325°C at 3°C/min, hold at 325°C for 11 min. Inlet temp 260°C.
   - Alcohol method: 80°C hold for 2 min, ramp to 200°C at 20°C/min, ramp to 325°C at 4°C/min, hold at 325°C for 15 min. Inlet temp 300°C.
4. Check ISODAT peaks to be sure that baseline and peaks were automatically chosen correctly. Peaks can be deleted and redefined in the ISODAT software. Especially if there are problems with coelution or noisy background, this step is very important before using the data. For

the most part, and for the compounds that were important to this study, ISODAT chose the peaks relatively well. Only a few peaks in the alcohol fraction needed to be redefined.

5. VPDB Correction
    - Alkane $\delta^{13}C$ values were corrected to the reference gas (VPDB) used during the GC-irMS run. These values were confirmed by measuring the average and standard deviation of the C_{36} alkane internal standard (IS) in all samples and comparing these to a $\delta^{13}C$ value of the IS solid form, which was measured on the EA-irMS ($\delta^{13}C$ = -29.88‰). The average $\delta^{13}C_{IS}$ in the alkane fraction was -29.85‰ and the standard deviation was 0.32‰, demonstrating a consistent $\delta^{13}C_{IS}$ value throughout the run, with the average value falling within one standard deviation from the EA-irMS $\delta^{13}C$ value. No further corrections were made.
    - Alcohol $\delta^{13}C$ values were also corrected to the reference gas (VPDB), similar to the alkane fraction, and confirmed by the use of the IS. The average $\delta^{13}C_{IS}$ value was -29.79‰, with a standard deviation of 0.70. When compared to the $\delta^{13}C$ of the IS solid form, measured on the EA-irMS (-29.88‰), the average $\delta^{13}C_{IS}$ value falls within one standard deviation from the EA-irMS $\delta^{13}C$ value. Further corrections include isotope mass balance calculation for each compound.
    - Fatty acid average $\delta^{13}C_{IS}$ values (-30.54‰) did not fall within the standard deviation (0.25‰) from the EA-irMS $\delta^{13}C$ value of the IS

solid form (-29.88‰). Therefore, the reference gas corrected values were not trusted, and all $\delta^{13}C$ values were reprocessed in ISODAT by setting the IS value at -29.88‰ (VPDB), and correcting the $\delta^{13}C$ values in each sample accordingly. The isotope mass balance standard (C_{21} FA) did not include the IS, and needed to be adjusted manually. In order to correct the $\delta^{13}C_{C21\text{-}FAME}$ value (-27.213‰) to VPDB, the offset from the EA-irMS $\delta^{13}C$ value to the average $\delta^{13}C_{IS}$ value (-29.88‰ – (-30.54‰) = + 0.6584‰) was added to the measured value. The final $\delta^{13}C_{C21\text{-}FAME}$ value, corrected to VPDB, was calculated as -26.56‰ (-27.213‰ + 0.6584‰). This value was used in the isotope mass balance correction calculations (see below).

A.2.10 Isotope Mass Balance Corrections

1. Fatty Acids:
   - Heneicosanoic acid (C_{21} FA) was used to correct for the fractionation effect associated with the addition of the methyl ester to fatty acids during derivitization, producing FAMEs. The solid form $\delta^{13}C_{C21:FA}$ value from the EA-irMS was measured at -27.33‰. The $\delta^{13}C_{C21:FAME}$ value from the GC-irMS was measured at -26.56‰.
   - Therefore, the fractionation associated with the methyl ester (ME) is calculated as follows:

$$\delta^{13}C_{ME} = 22(\delta^{13}C_{C21:FAME}) - 21(\delta^{13}C_{C21:FA}) = -10.17‰$$

   - Using this value for $\delta^{13}C_{ME}$, isotopic values were corrected for all other fatty acids with the following equation:

$$\delta^{13}C_{FA} = \delta^{13}C_{FAME}(\#Carbons_{FAME}/\#Carbons_{FA}) - (\delta^{13}C_{ME}/\#Carbons_{FA})$$

2. Alcohols:

- Two isotope mass balance standards, Nonadecanol (C_{19} alcohol) and Octacosanol (C_{28} alcohol), were used to determine the fractionation associated with adding TMS groups during derivitization, producing TMS-alcohols. Nonadecanol was derivitized with the same BSTFA lot #s as samples LE067 – LE137. Octacosanol was derivitized with the same BSTFA lot #s as samples LE007 – LE057.
- Nonadecanol: The solid form $\delta^{13}C_{C19:OH}$ value from the EA-irMS was measured (average of 3 values) at -29.312‰. The $\delta^{13}C_{C19:OTMS}$ value from the GC-irMS was measured at -28.392‰. Therefore, the fractionation associated with the TMS group is calculated as follows:

$$\delta^{13}C_{TMS} = [22(\delta^{13}C_{C19:OTMS}) - 29(\delta^{13}C_{C19:OH})]/3 = -22.57‰$$

- Octacosanol: The solid form $\delta^{13}C_{C28:OH}$ value from the EA-irMS was measured (average of 3 values) at -27.529‰. The $\delta^{13}C_{C28:OTMS}$ value from the GC-irMS was measured at -28.258‰. Therefore, the fractionation associated with the TMS group is calculated as follows:

$$\delta^{13}C_{TMS} = [22(\delta^{13}C_{C28:OTMS}) - 29(\delta^{13}C_{C28:OH})]/3 = -35.062‰$$

- Using this value for $\delta^{13}C_{TMS}$, isotopic values were corrected for alcohol samples with the following equation:

$$\delta^{13}C_{OH} = [\delta^{13}C_{OTMS}(\#Carbons_{OTMS}) - \delta^{13}C_{TMS}(\#Carbons_{TMS})]/ \#Carbons_{OH}$$

APPENDIX B

DATA TABLES AND ADDITIONAL FIGURES

B.1 Concentration Data

Table B.1: Core LZ1029 Normal alkane concentrations (µg /g TOC)

Sample ID	Sample depth (cm)	C21 Alkane	C23 Alkane	C25 Alkane	C27 Alkane	C29 Alkane	C31 Alkane	C33 Alkane
LE 007	14		568.27	679.41	992.51	846.25	626.20	129.75
LE 019	38		119.20	177.24	303.60	348.63	348.89	78.60
LE 027	54		70.84	130.69	252.41	342.60	406.75	92.70
LE 037	74		68.54	118.53	210.78	293.91	343.04	80.99
LE 047	94		56.81	98.59	145.38	194.75	240.32	70.83
LE 057	114		160.21	245.01	282.80	277.94	255.42	70.29
LE 067	134	628.01	512.13	495.64	505.61	408.63	348.72	78.07
LE 077	154	221.34	176.62	258.89	371.44	370.76	401.82	98.89
LE 087	174	72.36	114.06	196.85	318.91	368.73	461.10	124.12
LE 097	194			213.34	220.98	304.94	369.89	90.87
LE 108	216			74.11	134.52	203.71	251.39	57.37
LE 117	234			54.64	107.05	167.11	217.44	47.48
LE 127	254			79.19	127.68	167.16	229.53	64.65
LE 137	274		80.26	151.17	229.25	240.56	269.92	89.39

Table B.2: Core LZ1029 Short chain fatty acid concentrations (µg /g TOC)

Sample ID	Sample depth (cm)	C14 FA	C15 FA	C16 FA	C17 FA	C18 FA
LE 007	14	17.50	5.76	55.84	11.20	44.02
LE 019	38	4.15	2.45	30.33	6.07	29.80
LE 027	54	7.36	3.15	37.86	3.94	30.63
LE 037	74	6.84	2.69	37.08	4.04	30.14
LE 047	94	5.11	1.77	27.51	2.92	22.30
LE 057	114	16.74	9.24	66.52	17.72	51.52
LE 067	134	36.48	18.77	120.74	35.40	101.84
LE 077	154	17.21	7.78	75.14	15.88	61.31
LE 087	174	16.48	7.10	69.79	13.93	62.83
LE 097	194	16.38	4.46	68.16	6.38	48.17
LE 108	216	6.45	2.06	42.33	3.05	32.19
LE 117	234	10.64	3.01	74.59	4.16	52.04
LE 127	254	4.20	1.60	33.92	2.30	25.22
LE 137	274	3.43	1.83	27.32	3.51	23.98

Table B.3: Core LZ1029 Mid chain fatty acid concentrations (µg /g TOC)

Sample ID	Sample depth (cm)	C19 FA	C20 FA	C21 FA	C22 FA	C23 FA
LE 007	14	7.39	46.66	19.83	137.42	102.66
LE 019	38	5.11	34.80	14.47	95.03	77.47
LE 027	54	3.02	26.68	6.84	62.44	39.04
LE 037	74	4.35	35.32	9.42	73.64	43.91
LE 047	94	4.48	22.51	7.30	46.38	31.37
LE 057	114	44.89	159.23	79.34	279.00	140.32
LE 067	134	148.60	431.27	257.53	566.65	156.86
LE 077	154	57.45	177.24	97.46	258.66	96.60
LE 087	174	39.25	147.49	64.84	220.23	93.37
LE 097	194	12.40	62.86	22.28	100.56	44.68
LE 108	216	2.84	20.92	4.96	34.32	16.52
LE 117	234	2.43	22.20	4.39	34.23	12.03
LE 127	254	2.50	18.41	4.50	31.72	13.51
LE 137	274	4.70	21.75	8.05	40.15	30.59

Table B.4: Core LZ1029 Long chain fatty acid concentrations (µg /g TOC)

Sample ID	Sample depth (cm)	C24 FA	C25 FA	C26 FA	C27 FA	C28 FA	C29 FA	C30 FA	C31 FA	C32 FA
LE 007	14	516.63	251.51	721.79	214.26	610.81	83.06	171.41	19.99	29.79
LE 019	38	341.70	217.51	505.04	194.10	414.48	84.49	141.32	24.26	
LE 027	54	232.26	158.92	453.22	184.94	491.47	103.71	176.40	32.99	52.71
LE 037	74	276.32	159.29	514.53	176.48	459.85	94.77	182.39	29.83	48.88
LE 047	94	171.64	78.48	294.41	85.98	240.11	53.05	88.17	14.90	22.51
LE 057	114	776.15	311.07	1279.49	300.85	876.90	227.59	398.56	47.28	60.97
LE 067	134	872.06	305.10	1324.39	276.48	803.53	166.74	325.05	41.71	65.43
LE 077	154	616.76	238.70	797.69	224.71	648.27	136.92	227.46	40.24	55.18
LE 087	174	566.11	242.87	767.04	257.07	680.64	153.11	243.27	47.82	73.01
LE 097	194	274.58	144.15	410.67	152.83	359.36	92.37	130.43	28.90	37.81
LE 108	216	101.10	55.30	169.45	68.56	161.30	41.48	64.66	14.61	19.64
LE 117	234	82.80	53.54	159.24	68.58	148.83	39.09	59.79	13.41	16.19
LE 127	254	103.27	71.65	194.53	90.76	195.93	58.44	87.16	22.51	30.02
LE 137	274	169.12	88.82	230.77	102.12	219.38	66.83	101.65	26.37	36.96

Table B.5: Core LZ1029 Normal alcohol concentrations (µg/g TOC)

Sample ID	Sample depth (cm)	C21 alcohol	C22 alcohol	C23 alcohol	C24 alcohol	C25 alcohol	C26 alcohol	C27 alcohol	C28 alcohol
LE 007	14	84.33	119.17	0.00	115.48	52.24	199.17	71.73	263.09
LE 019	38	46.63	63.36	0.00	161.87	49.71	195.76	54.44	232.14
LE 027	54	67.26	76.41	28.60	675.31	46.39	27.45	41.36	44.84
LE 037	74	63.16	50.21	0.00	107.76	0.00	63.16	0.00	74.18
LE 047	94	65.44	88.12	0.00	162.45	0.00	34.62	0.00	34.90
LE 057	114	331.63	43.33	0.00	58.82	0.00	41.28	0.00	48.68
LE 067	134	199.72	701.14	95.88	451.91	131.85	362.65	104.17	267.23
LE 077	154	329.03	56.82	0.00	144.27	18.16	77.06	21.09	186.84
LE 087	174	205.58	66.43	0.00	99.29	0.00	183.46	67.30	321.39
LE 097	194	112.13	105.22	0.00	288.98	0.00	90.43	28.70	145.57
LE 108	216	31.30	38.06	0.00	395.54	0.00	34.07	0.00	58.47
LE 117	234	23.17	46.54	0.00	346.83	0.00	23.64	0.00	33.36
LE 127	254	21.53	45.17	0.00	234.19	0.00	48.07	0.00	44.23
LE 137	274	52.40	46.75	0.00	369.99	0.00	35.63	0.00	34.28

Table B.6: Core LZ1029 Other alcohol concentrations (µg/g TOC)

Sample ID	Sample depth (cm)	Hydroxyarchaeol? (Compound I)	diplopterol	Hydroxyarchaeol (Compound II)
LE 007	14	0.00	0.00	0.00
LE 019	38	0.00	0.00	0.00
LE 027	54	0.00	0.00	0.00
LE 037	74	16.84	0.00	0.00
LE 047	94	0.00	0.00	0.00
LE 057	114	38.21	42.43	38.15
LE 067	134	394.31	64.89	668.78
LE 077	154	44.79	19.77	18.11
LE 087	174	51.66	0.00	112.45
LE 097	194	0.00	0.00	0.00
LE 108	216	0.00	0.00	0.00
LE 117	234	0.00	0.00	0.00
LE 127	254	0.00	0.00	0.00
LE 137	274	29.03	0.00	0.00

B.2 Isotopic Data

Table B.7: Core LZ1029 Alkane $\delta^{13}C$ values (‰)

Sample ID	Sample depth (cm)	C21	C23	C25	C27	C29	C31	C33	Mass weighted average (MWA) C23-C33 odd
LE 007	14	-30.871	-32.925	-33.274	-32.836	-32.593	-32.987		-32.90
LE 019	38	-32.171	-32.353	-32.928	-32.671	-32.72	-33.246	-33.96	-32.91
LE 027	54		-31.666	-33.044	-33.039	-33.239	-33.757	-34.067	-33.32
LE 037	74		-32.219	-32.856	-32.992	-33.216	-33.57	-34.276	-33.26
LE 047	94			-34.122	-33.54	-33.452	-33.778	-34.576	-33.77
LE 057	114	-38.114	-35.418	-35.856	-34.268	-33.194	-33.539	-34.358	-34.34
LE 067	134	-40.244	-35.352	-35.857	-34.458	-33.198	-33.633	-34.797	-35.80
LE 077	154	-36.355	-34.475	-34.794	-33.995	-33.171	-33.777		-34.23
LE 087	174	-38.253	-33.982	-33.966	-33.589	-33.073	-33.53	-34.507	-33.80
LE 097	194				-34.57	-35.161	-37.684	-40.14	-36.43
LE 108	216				-33.232	-32.827	-33.467	-33.71	-33.24
LE 117	234				-33.182	-33.452	-33.702	-34.249	-33.57
LE 127	254			-32.758	-33.116	-33.225	-33.498	-34.387	-33.36
LE 137	274			-32.434	-32.951	-33.3	-33.678	-34.476	-33.30

Table B.8: Core LZ1029 Short chain Fatty Acid $\delta^{13}C$ values (‰)

Sample ID	Sample depth (cm)	C14	C15	C15 iso	C15 ante iso	C17	MWA C14, C15, C17	C16	C18	MWA C16 & C18
LE 007	14	-29.174	-32.389			-33.114	-30.99	-29.565	-30.209	-29.85
LE 019	38	-28.501				-33.754	-31.62	-27.542	-29.775	-28.65
LE 027	54	-25.931				-32.710	-28.30	-26.375	-27.956	-27.08
LE 037	74	-28.318				-33.091	-30.09	-28.514	-30.003	-29.18
LE 047	94	-28.931					-28.93	-26.825	-28.912	-27.76
LE 057	114	-32.585	-36.399			-38.145	-35.65	-31.718	-35.388	-33.32
LE 067	134	-32.457	-36.417	-33.034	-33.712	-39.172	-35.90	-31.874	-36.993	-34.22
LE 077	154	-27.859	-37.185			-37.925	-33.54	-28.612	-32.968	-30.57
LE 087	174	-28.677	-34.837			-37.559	-33.14	-29.530	-32.780	-31.07
LE 097	194	-25.768					-25.77	-26.387	-28.582	-27.30
LE 108	216	-24.818					-24.82	-25.405	-25.294	-25.36
LE 117	234	-24.089				-28.951	-25.46	-24.396	-24.332	-24.37
LE 127	254							-27.885	-28.017	-27.94
LE 137	274					-27.249	-27.25	-27.256		-27.26

Table B.9: Core LZ1029 Mid chain Fatty Acid $\delta^{13}C$ values (‰)

Sample ID	Sample depth (cm)	C19	C20	C21	C22	C23	MWA C19-C23
LE 007	14	-32.323	-33.260	-32.776	-32.677	-32.976	-32.86
LE 019	38	-32.604	-33.110	-32.763	-32.650	-33.423	-32.99
LE 027	54	-32.165	-33.707	-32.114	-32.981	-33.456	-33.19
LE 037	74	-35.858	-33.689	-34.464	-33.451	-33.755	-33.70
LE 047	94	-39.369	-36.139	-40.102	-36.418	-37.585	-37.05
LE 057	114	-43.442	-41.823	-42.796	-40.453	-39.537	-41.04
LE 067	134	-44.018	-43.204	-44.167	-42.646	-41.692	-43.09
LE 077	154	-44.042	-41.710	-44.498	-41.000	-40.123	-41.81
LE 087	174	-42.579	-39.451	-42.201	-38.601	-38.182	-39.44
LE 097	194	-43.065	-37.400	-40.353	-36.688	-37.033	-37.60
LE 108	216		-34.668	-37.845	-34.316	-34.658	-34.71
LE 117	234		-34.621	-37.177	-33.947	-35.050	-34.53
LE 127	254		-34.119		-34.434	-35.316	-34.53
LE 137	274		-36.428	-38.310	-35.675	-35.132	-35.88

Table B.10: Core LZ1029 Long chain Fatty Acid $\delta^{13}C$ values (‰)

Sample ID	Sample depth (cm)	C24	C25	C26	C27	C28	C29	C30	MWA C24-C28 even
LE 007	14	-33.184	-34.395	-33.818	-34.237	-34.048	-35.582	-35.151	-33.72
LE 019	38	-33.044	-34.400	-33.689	-34.184	-33.897	-34.187	-34.228	-33.58
LE 027	54	-32.911	-34.136	-33.515	-33.682	-33.431	-34.121	-34.131	-33.36
LE 037	74	-33.617	-34.749	-34.167	-33.792	-33.778	-33.699	-34.387	-33.90
LE 047	94	-36.287	-36.740	-36.600	-34.850	-35.419	-32.589	-33.361	-36.12
LE 057	114	-38.686	-39.497	-39.462	-37.157	-36.921	-32.372	-32.215	-38.50
LE 067	134	-38.968	-40.485	-39.803	-38.621	-37.483	-33.403	-32.603	-38.94
LE 077	154	-38.093	-39.821	-37.937	-36.729	-37.053	-32.631	-32.408	-37.71
LE 087	174	-36.922	-36.479	-36.357	-34.853	-32.880	-34.794	-32.636	-35.34
LE 097	194	-35.791	-35.631	-35.479	-34.293	-34.261	-33.277	-32.413	-35.14
LE 108	216	-34.092	-34.913	-34.229	-34.137	-33.976	-33.576	-34.211	-34.10
LE 117	234	-34.399	-34.834	-34.604	-34.732	-33.870	-33.571	-34.875	-34.28
LE 127	254	-35.368	-34.743	-34.412	-34.228	-34.381	-33.494	-33.718	-34.60
LE 137	274	-34.666	-35.609	-34.680	-34.723	-34.114	-32.796	-33.701	-34.48

Table B.11: Core LZ1029 Normal alcohol $\delta^{13}C$ values (‰)

Sample ID	Sample depth (cm)	C21	C22	C23	C24	C25	C26	C27	C28	MWA C22 & C24	MWA C26 & C28
LE 007	14	-31.107	-28.273		-28.723		-33.450		-32.945	-28.49	-33.16
LE 019	38	-27.780	-28.419		-28.471		-33.595		-33.161	-28.46	-33.36
LE 027	54	-27.683	-28.522	-33.042	-27.763		-36.571		-33.814	-27.84	-34.86
LE 037	74	-27.646	-28.050	-32.144	-32.421		-32.532	-32.500	-32.986	-31.03	-32.78
LE 047	94	-27.859		-35.239	-28.131	-32.692	-37.680	-34.163	-35.994	-28.13	-36.83
LE 057	114	-42.166	-43.501	-35.590	-38.267	-36.783	-37.287	-36.942	-41.698	-40.49	-39.67
LE 067	134	-34.196	-46.095	-38.888	-43.815	-38.858	-36.300	-37.156	-36.191	-45.20	-36.25
LE 077	154		-44.276	-35.780	-41.085	-38.002	-35.458	-36.239	-34.984	-41.99	-35.12
LE 087	174								-43.458		-43.46
LE 097	194	-27.655	-28.124		-28.655					-28.51	
LE 108	216	-29.008	-29.568		-29.186					-29.22	
LE 117	234	-31.423	-31.224		-29.847					-30.01	
LE 127	254	-29.711	-30.314		-30.008					-30.06	
LE 137	274	-29.442	-29.651		-29.254		-32.442		-32.557	-29.30	-32.50

Table B.12: Core LZ1029 Other alcohol $\delta^{13}C$ values (‰)

Sample ID	Sample depth (cm)	Hydroxyarchaeol? (Compound I)	Diplopterol	Hydroxyarchaeol (Compound II)
LE 007	14			
LE 019	38			
LE 027	54			
LE 037	74	-37.378	-88.082	
LE 047	94	-29.384		-32.285
LE 057	114	-33.271	-91.862	-32.125
LE 067	134	-33.275	-93.455	-33.122
LE 077	154	-31.984	-96.328	-33.207
LE 087	174	-34.476		-34.156
LE 097	194	-31.815		-31.725
LE 108	216			
LE 117	234			
LE 127	254			
LE 137	274			

Table B.13: Core LZ1029 $\delta^{15}N$ values (‰)

Sample	Sample Depth (cm)	Bulk $\delta^{15}N$ (‰)	Bulk $\delta^{15}N$ 3pt. Running mean (‰)
LE7-07	14	2.6860646	
LE15-07	30	2.8832268	2.630506867
LE16-07	32	2.3222292	2.530231933
LE17-07	34	2.3852398	2.333747267
LE19-07	38	2.2937728	2.370334067
LE27-07	54	2.4319896	2.386481944
LE29-07	58	2.433683433	2.506405344
LE30-07	60	2.653543	2.548751178
LE31-07	62	2.5590271	2.619666333
LE37-07	74	2.6464289	2.733491933
LE47-07	94	2.9950198	2.638637267
LE52-07	104	2.2744631	2.391676367
LE53-07	106	1.9055462	2.0386815
LE54-07	108	1.9360352	2.1016921
LE57-07	114	2.4634949	2.027840967
LE67-07	134	1.6839928	1.8882691
LE69-07	138	1.5173196	1.706012633
LE70-07	140	1.9167255	1.933663833
LE71-07	142	2.3669464	2.748736433
LE77-07	154	3.9625374	3.6149628
LE87-07	174	4.5154046	4.3365358
LE97-07	194	4.5316654	4.242189283
LE104-07	208	3.67949785	3.982694017
LE105-07	210	3.7369188	3.688305783
LE106-07	212	3.6485007	3.736580033
LE108-07	216	3.8243206	3.5001209
LE117-07	234	3.0275414	3.3740997
LE127-07	254	3.2704371	3.2216547
LE137-07	274	3.3669856	

Table B.14: Core PG1351 $\delta^{15}N$ values (‰)

Sediment depth (cm)	Bulk $\delta^{15}N$	$\delta^{15}N$ **5pt Running mean** (‰)	$\delta^{15}N$ **3pt Running mean** (‰)
67.0	-0.0978		
73.0	-2.4849		-0.6665
77.0	0.5833	0.1297	0.0690
89.0	2.1085	0.4077	1.0770
125.0	0.5393	0.9265	1.3134
129.0	1.2925	1.5617	0.6469
137.0	0.1088	1.7716	1.7203
155.0	3.7595	2.3777	2.3420
185.0	3.1578	2.5792	3.4958
203.0	3.5700	2.9933	3.0091
219.0	2.2997	2.7038	2.6831
227.0	2.1797	2.4452	2.2637
287.0	2.3118	1.3473	2.1189
297.0	1.8651	1.6531	0.7524
299.0	-1.9197	1.5146	1.2579
347.0	3.8284	1.7690	1.1320
355.0	1.4874	2.2746	2.9665
407.0	3.5837	3.2503	3.1548
415.0	4.3932	2.9872	3.6452
437.0	2.9587	3.1899	3.2883
445.0	2.5129	3.0661	2.6575
451.0	2.5008	2.4634	2.6595
480.0	2.9647	2.6866	2.2818
482.0	1.3800	2.8990	2.8064
492.0	4.0745	2.9720	3.0099
496.0	3.5752	3.0652	3.5051
504.0	2.8657	3.6007	3.2905
506.0	3.4307	3.3416	3.4512
510.0	4.0573	3.3390	3.4224
528.0	2.7791	3.5078	3.4661
540.0	3.5621	3.3589	3.3504
550.0	3.7099	3.1369	3.3194
566.0	2.6861	2.9492	3.1144
586.0	2.9473	2.8103	2.4913
590.0	1.8407	2.3823	2.5518
614.0	2.8674	2.1608	2.0928
630.0	1.5703	2.1504	2.0054

(Continued on next page)

Table B.14, continued

Sediment depth (cm)	Bulk $\delta^{15}N$	$\delta^{15}N$ **5pt Running mean** (‰)	$\delta^{15}N$ **3pt Running mean** (‰)
638.0	1.5784	2.4025	2.0146
644.0	2.8950	2.2762	2.5249
658.0	3.1014	2.4261	2.7441
668.0	2.2360	2.6525	2.5524
702.0	2.3198	2.2806	2.4220
708.0	2.7101	2.0611	2.0218
714.0	1.0356	2.1960	1.9166
720.0	2.0040	2.2238	1.9834
742.0	2.9107	2.4484	2.4577
750.0	2.4584	3.1005	3.0675
772.0	3.8335	3.5022	3.5293
790.0	4.2959	3.5702	4.0472
800.0	4.0123	3.8701	3.8531
828.0	3.2511	3.8743	3.7403
844.0	3.9575	3.7011	3.6878
860.0	3.8548	3.5415	3.7473
876.0	3.4297	3.5738	3.4997
913.0	3.2145	3.1903	3.3523
929.0	3.4127	3.0163	2.8890
961.0	2.0397	3.0810	2.8124
995.0	2.9849	3.1420	2.9259
1025.0	3.7532	3.2479	3.4192
1057.0	3.5194	3.7137	3.7383
1116.0	3.9422	3.8481	3.9436
1126.0	4.3691	3.7926	3.9893
1136.0	3.6566	3.7302	3.8338
1146.0	3.4756	3.8014	3.4466
1164.0	3.2075	1.7683	3.6605
1176.0	4.2984	0.8822	0.5697
1190.0	-5.7966	-0.0090	-0.7574
1206.0	-0.7741		-2.5170
1216.0	-0.9802		

B.3 Additional Figures

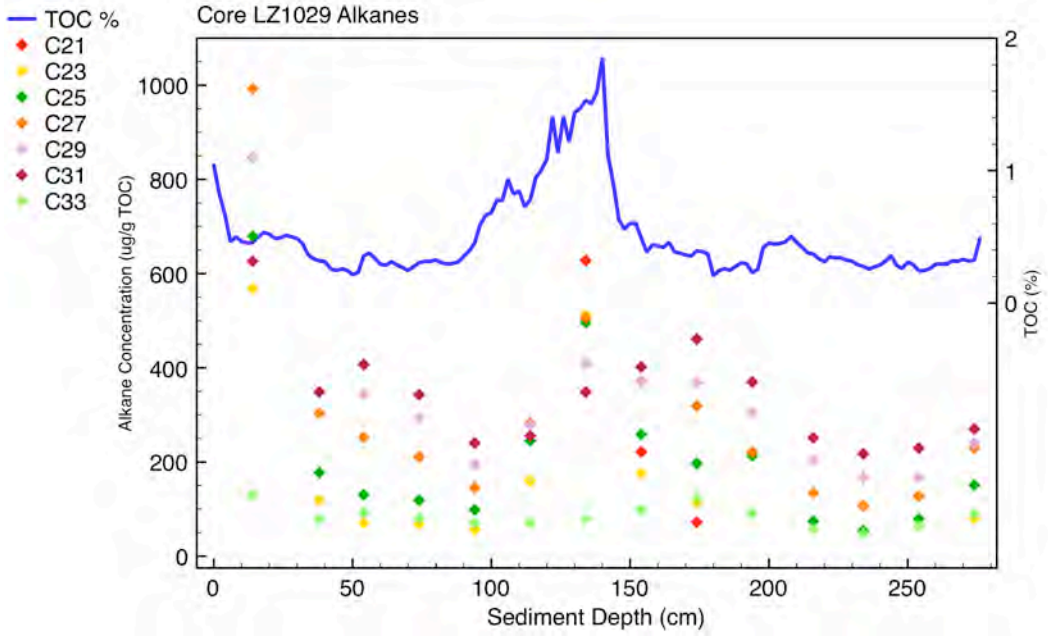

Figure B.1: Core LZ1029 Alkane absolute concentrations

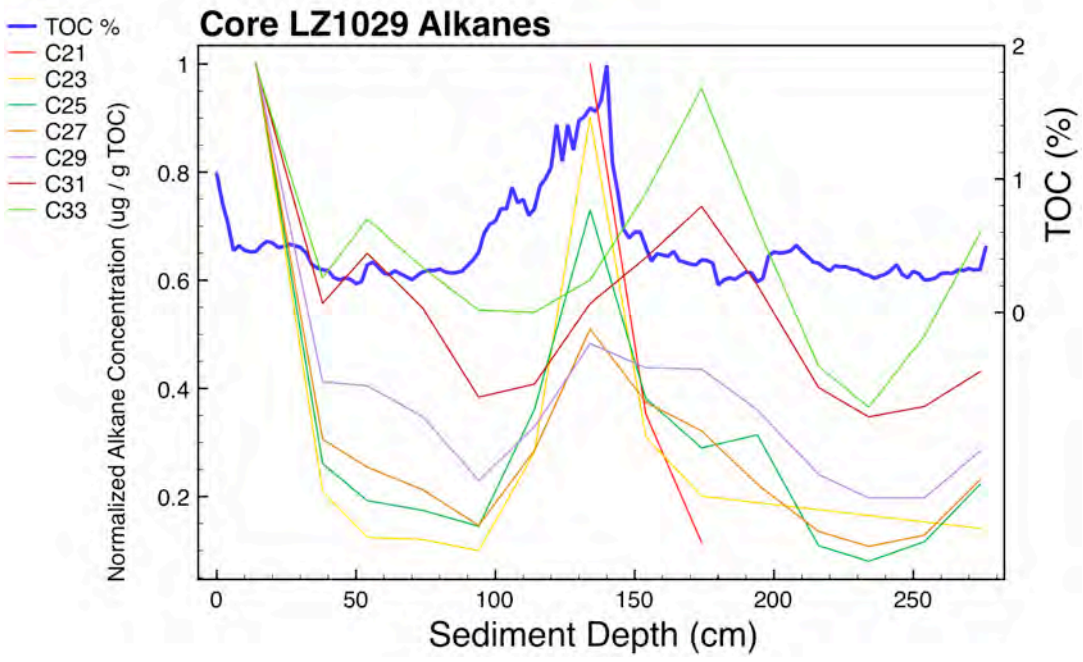

Figure B.2: Core LZ1029 Alkane relative concentrations

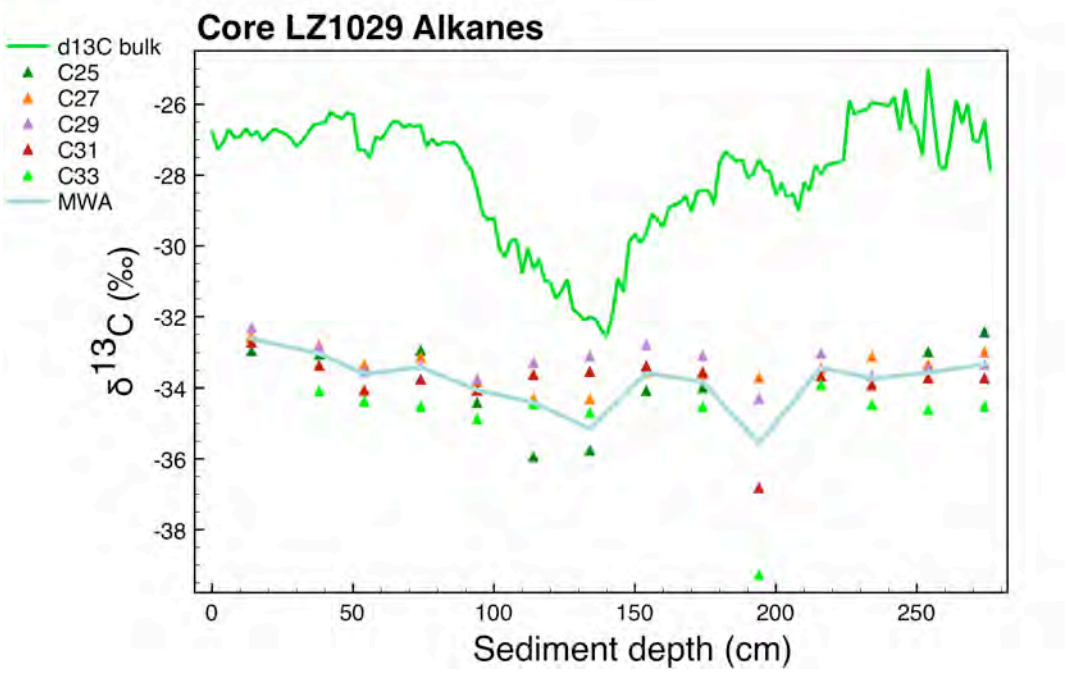

Figure B.3: Core LZ1029 Alkane $\delta^{13}C$ values

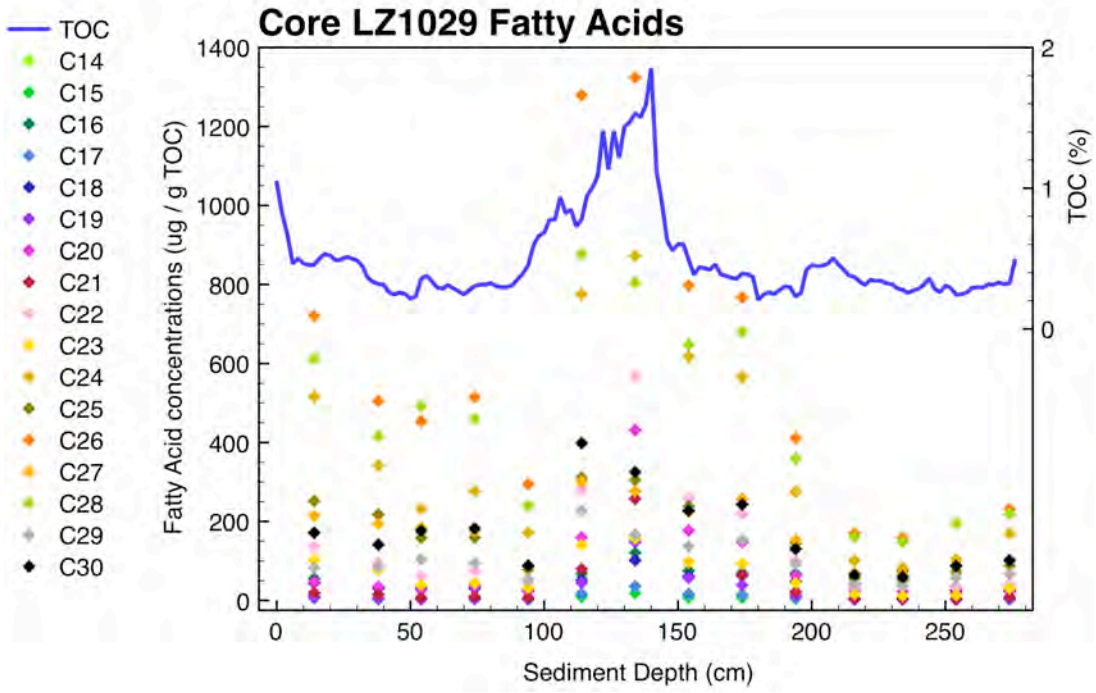

Figure B.4: Core LZ1029 Fatty acid absolute concentrations

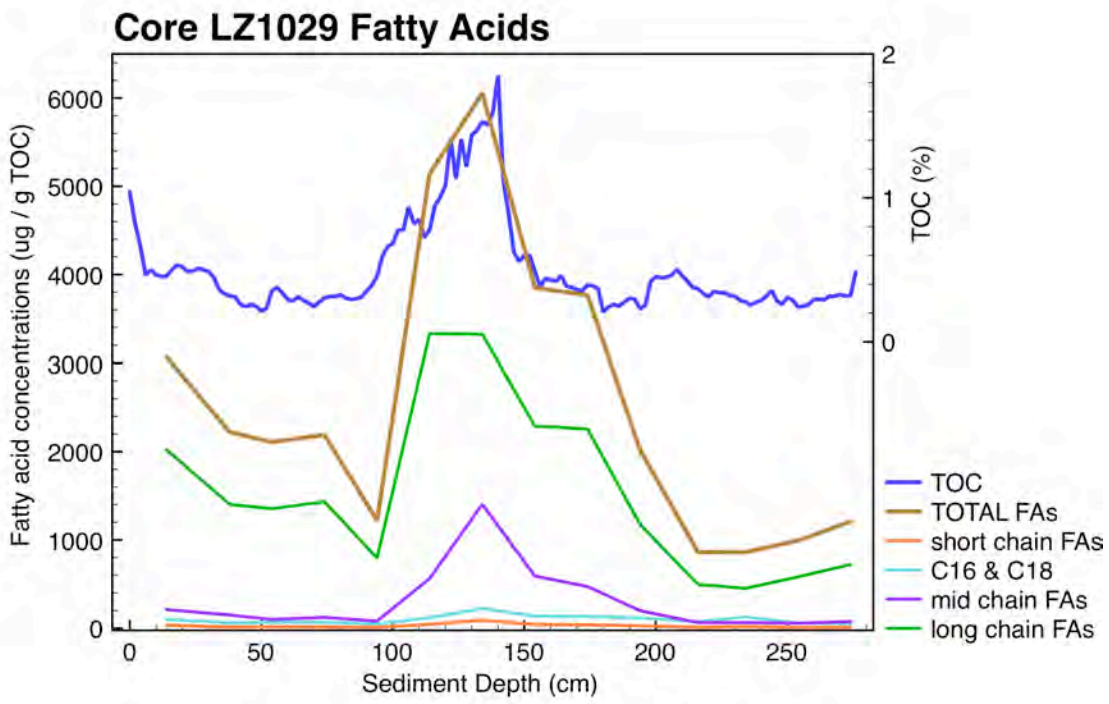

Figure B.6: Core LZ1029 Fatty acid concentrations in chain length groups

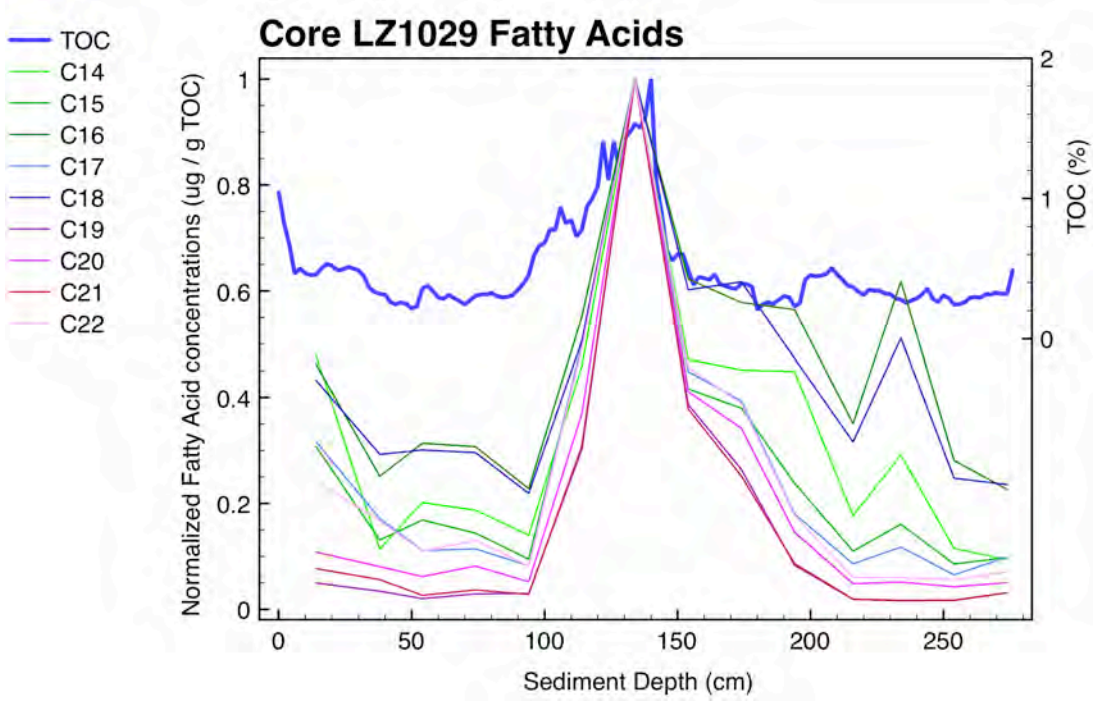

Figure B.7: Core LZ1029 Fatty acid relative concentrations (short mid chain)

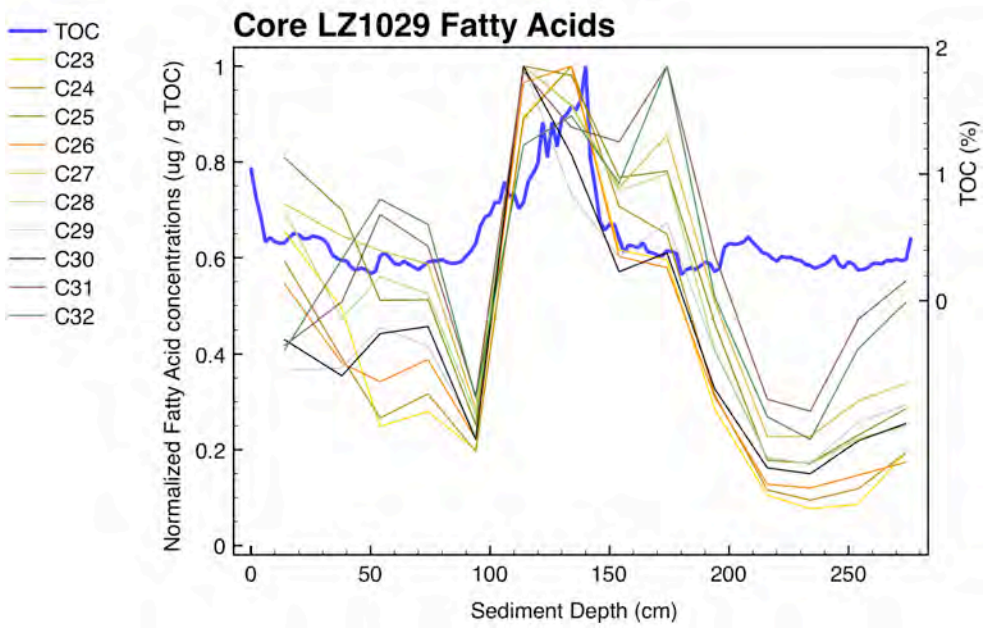

Figure B.8: Core LZ1029 Fatty acid relative concentrations (long chain)

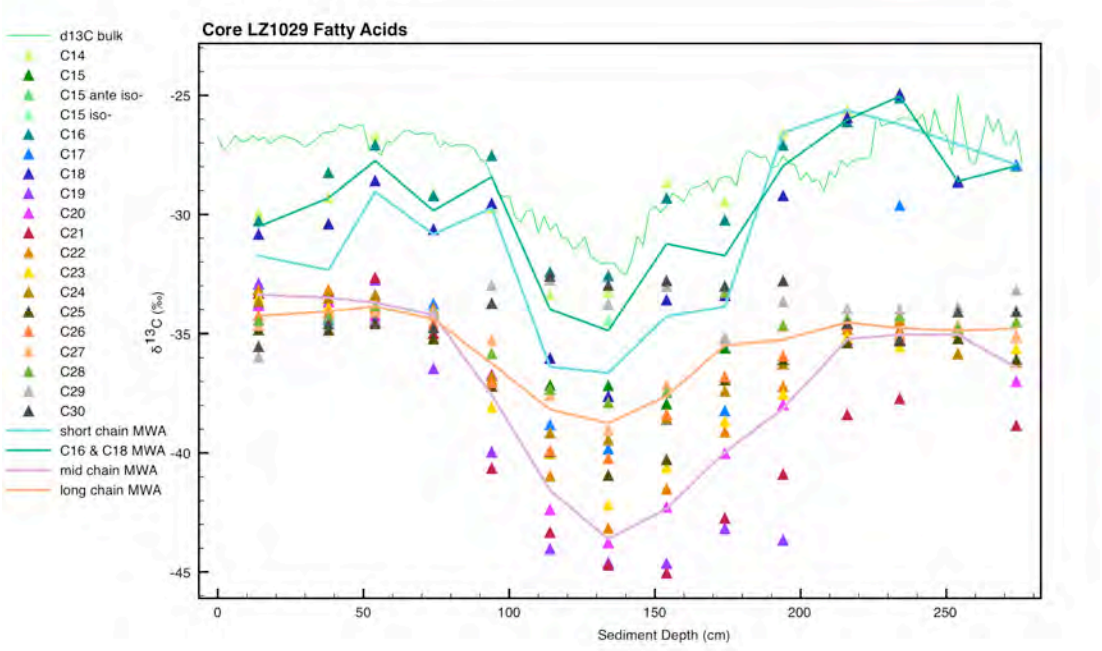

Figure B.9: Core LZ1029 Fatty acid $\delta^{13}C$ values

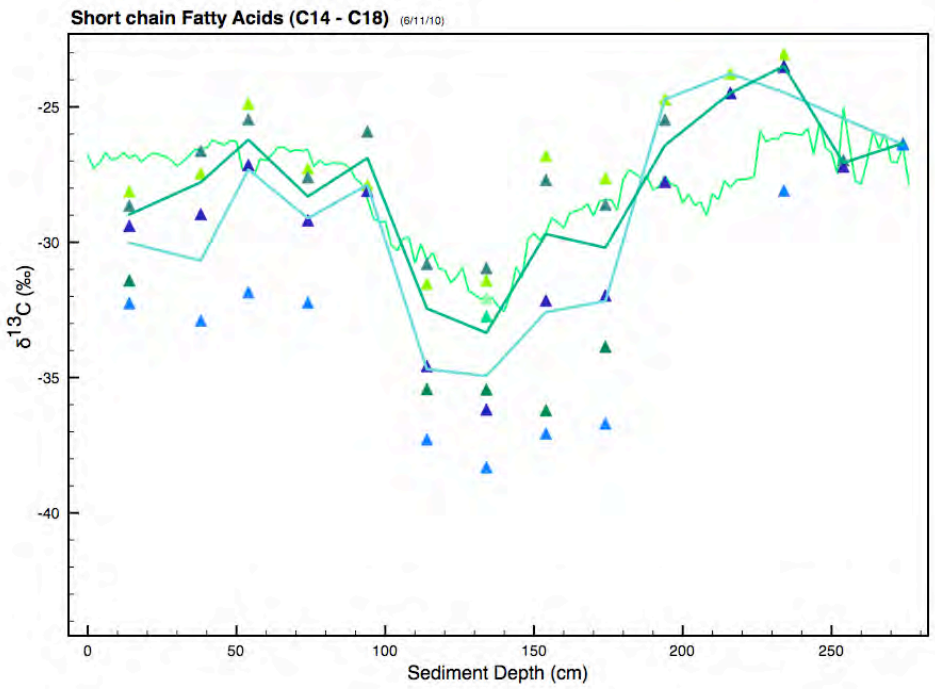

Figure B.10: Core LZ1029 Fatty acid $\delta^{13}C$ values (short chain)

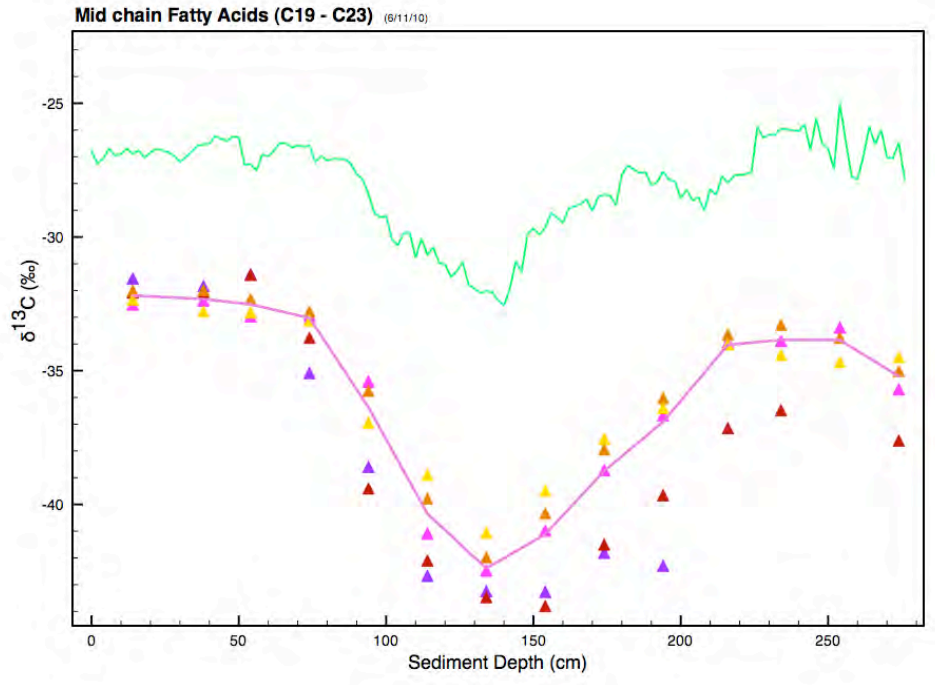

Figure B.11: Core LZ1029 Fatty acid $\delta^{13}C$ values (mid chain)

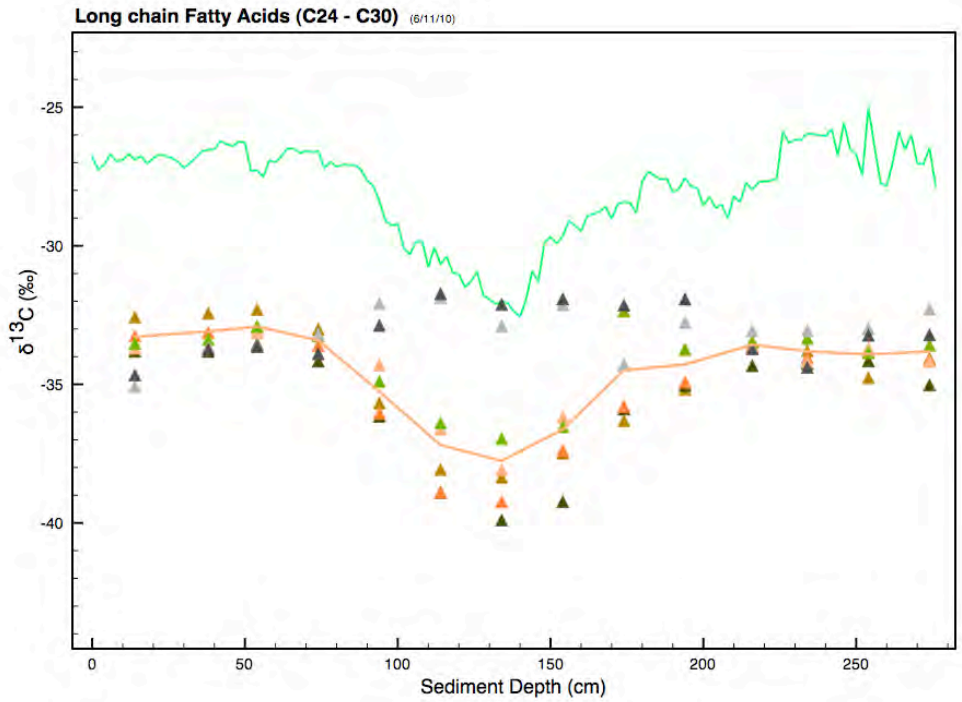

Figure B.12: Core LZ1029 Fatty acid $\delta^{13}C$ values (long chain)

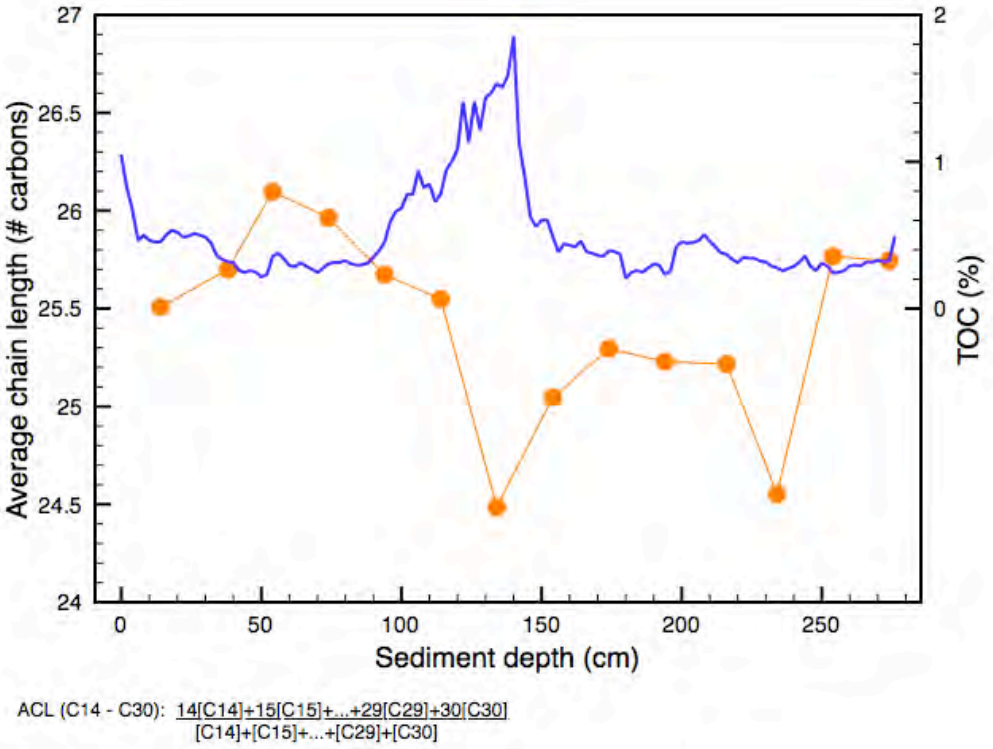

Figure B.13: Core LZ1029 Fatty acid average chain length compared with TOC

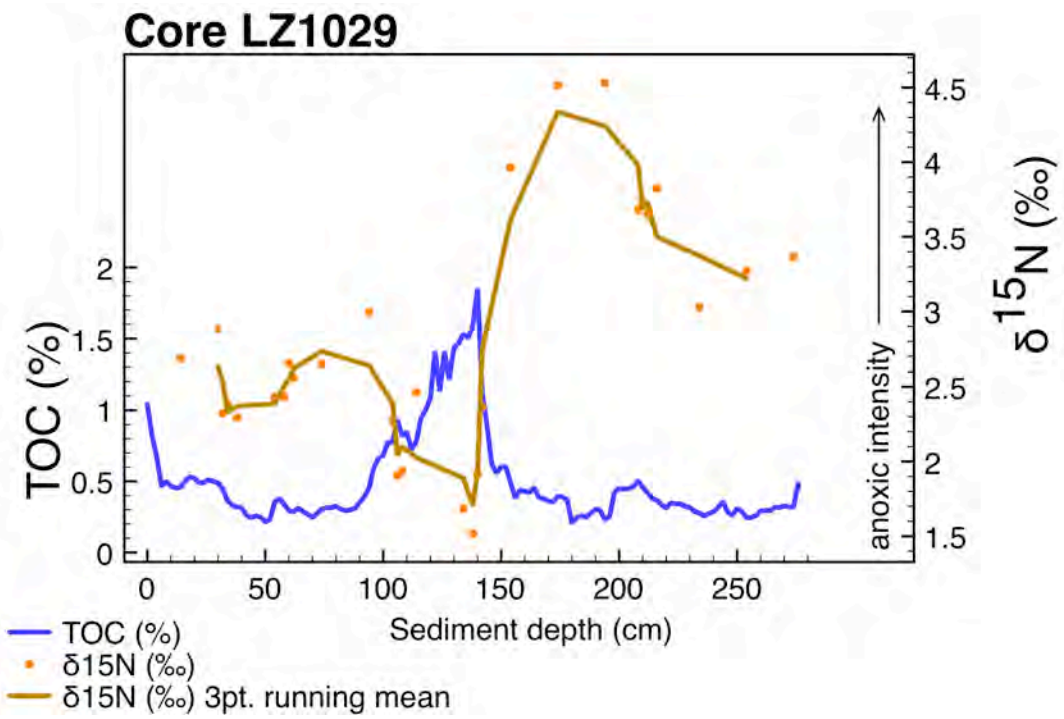

Figure B.14: Core LZ1029 $\delta^{15}N$ compared with TOC

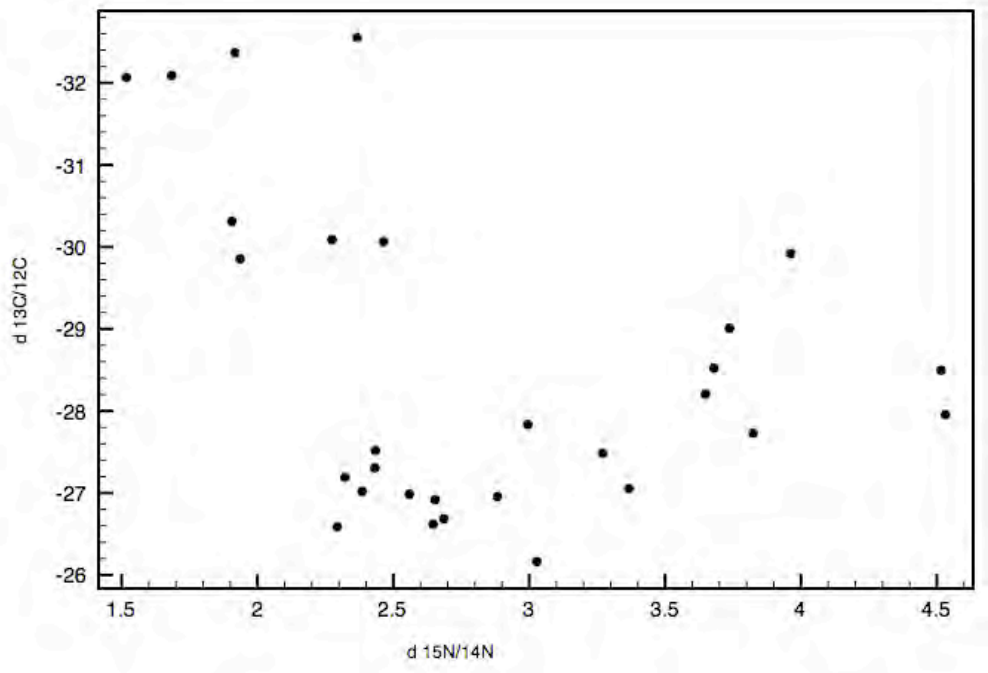

Figure B.15: Core LZ1029 bulk $\delta^{13}C$ vs. bulk $\delta^{15}N$ ($R^2 = 0.13$)

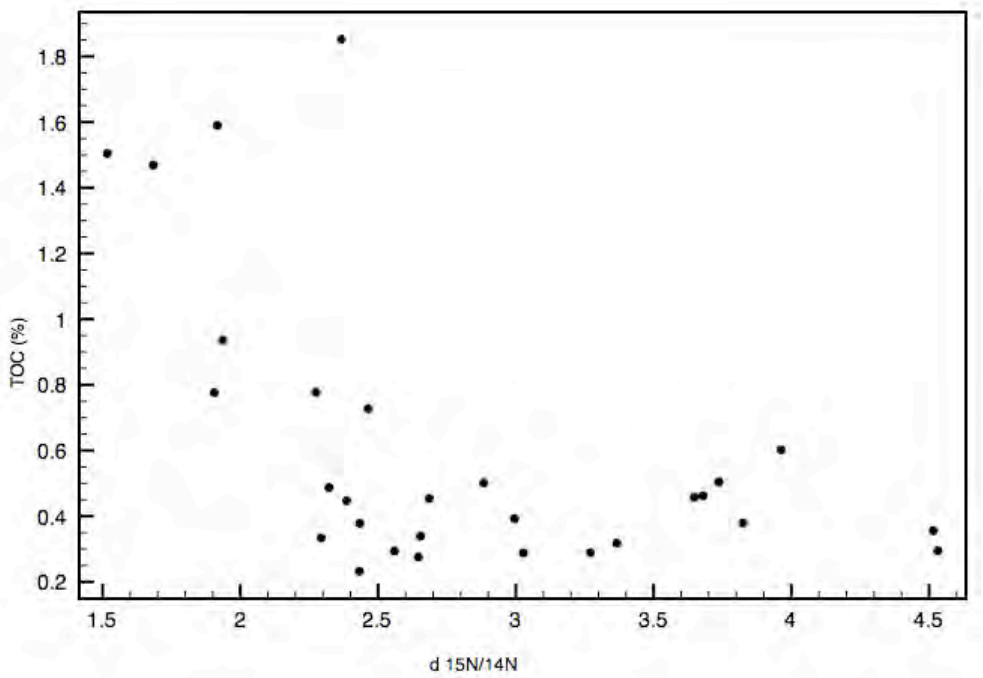

Figure B.16: Core LZ1029 TOC vs. bulk $\delta^{15}N$ ($R^2 = 0.30$)

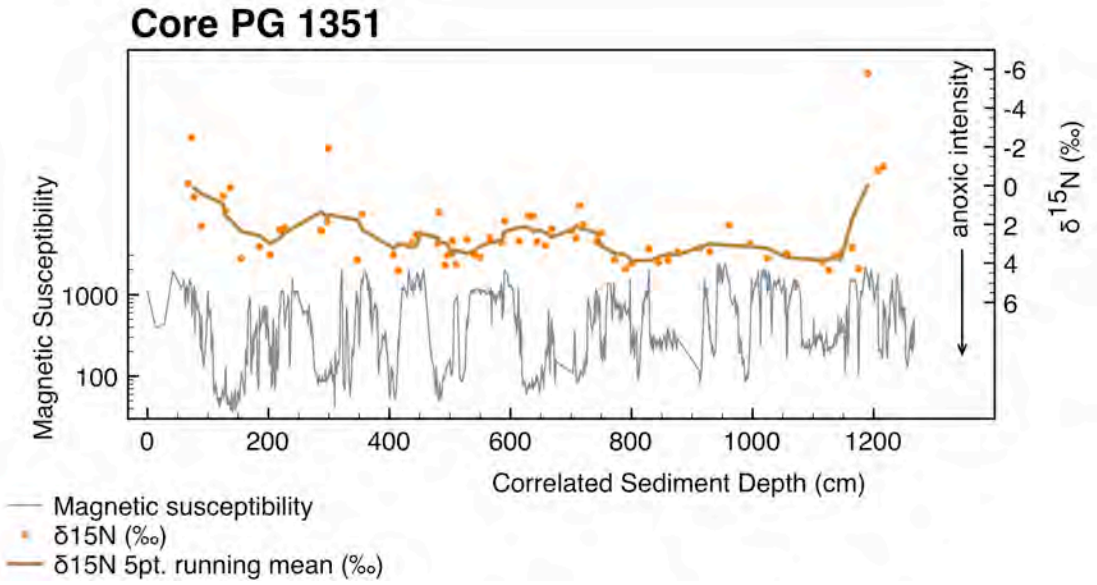

Figure B.17: Core PG1351 $\delta^{15}N$ compared with magnetic susceptibility

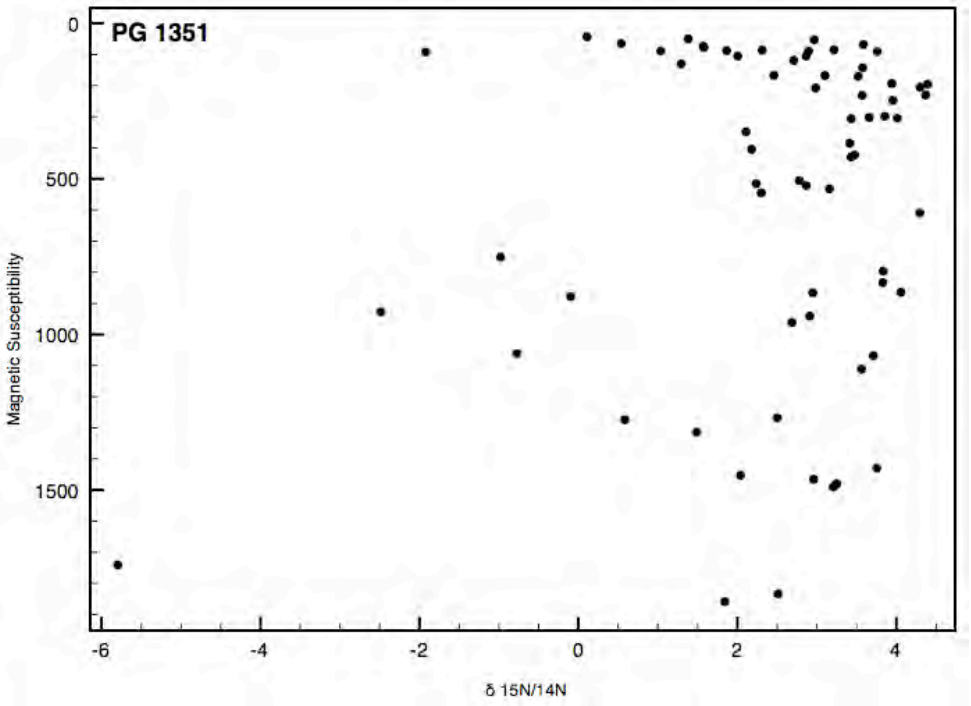

Figure B.18: Core PG1351 magnetic susceptibility vs. bulk $\delta^{15}N$ ($R^2 = 0.045$)

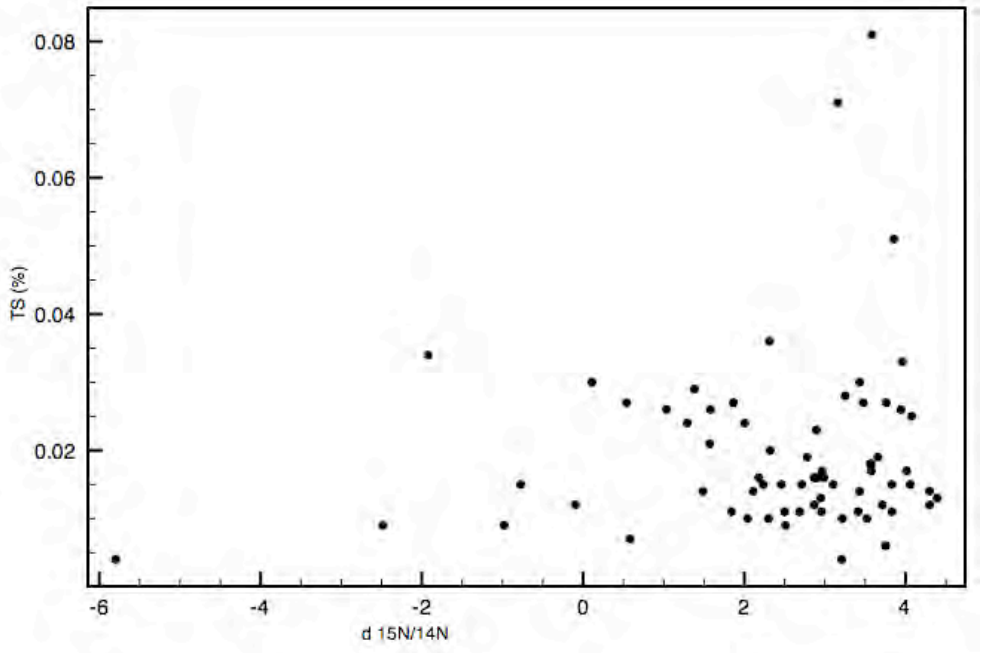

Figure B.19: Core PG1351 total sulfur vs. bulk $\delta^{15}N$ ($R^2 = 0.018$)

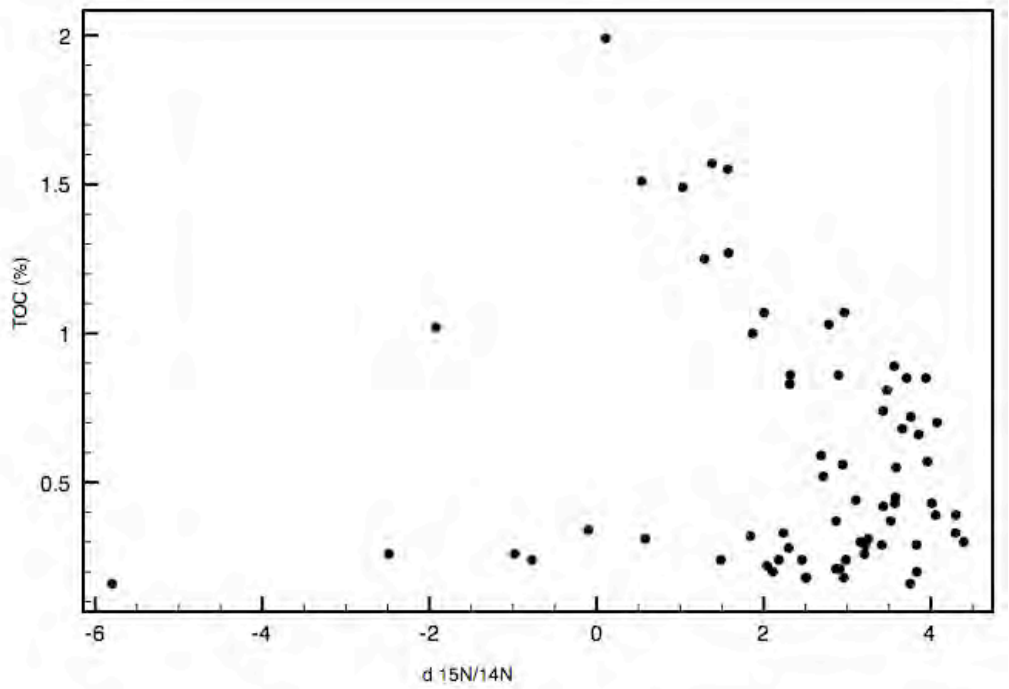

Figure B.20: Core PG1351 TOC vs. bulk $\delta^{15}N$ ($R^2 = 0.016$)

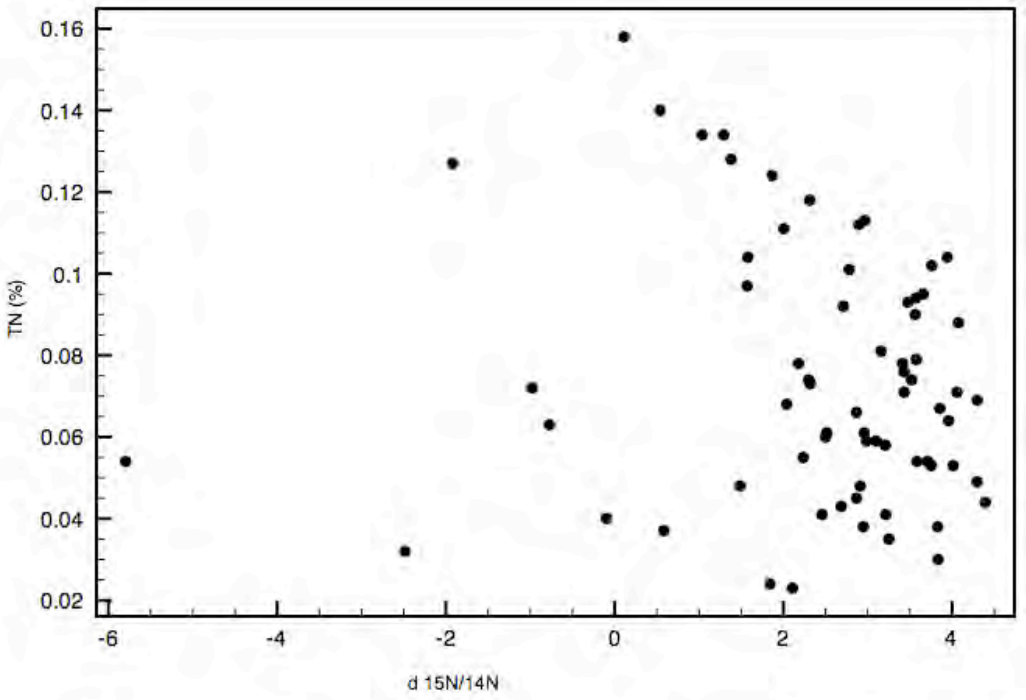

Figure B.21: Core PG1351 total nitrogen vs. bulk $\delta^{15}N$ ($R^2 = 0.016$)

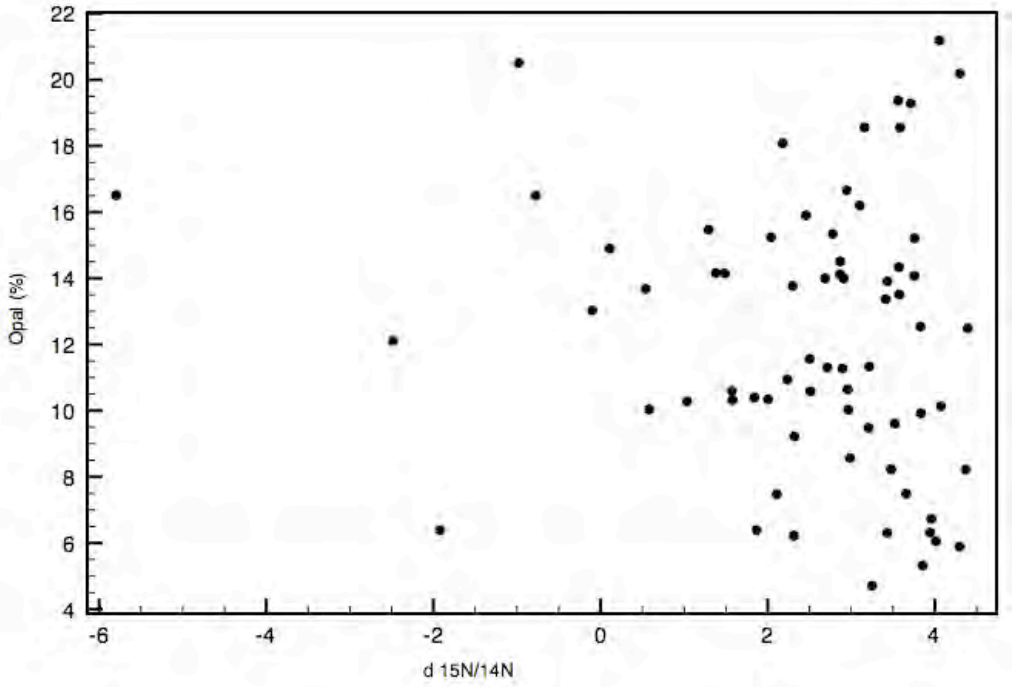

Figure B.22: Core PG1351 opal vs. bulk $\delta^{15}N$ ($R^2 = 0.019$)

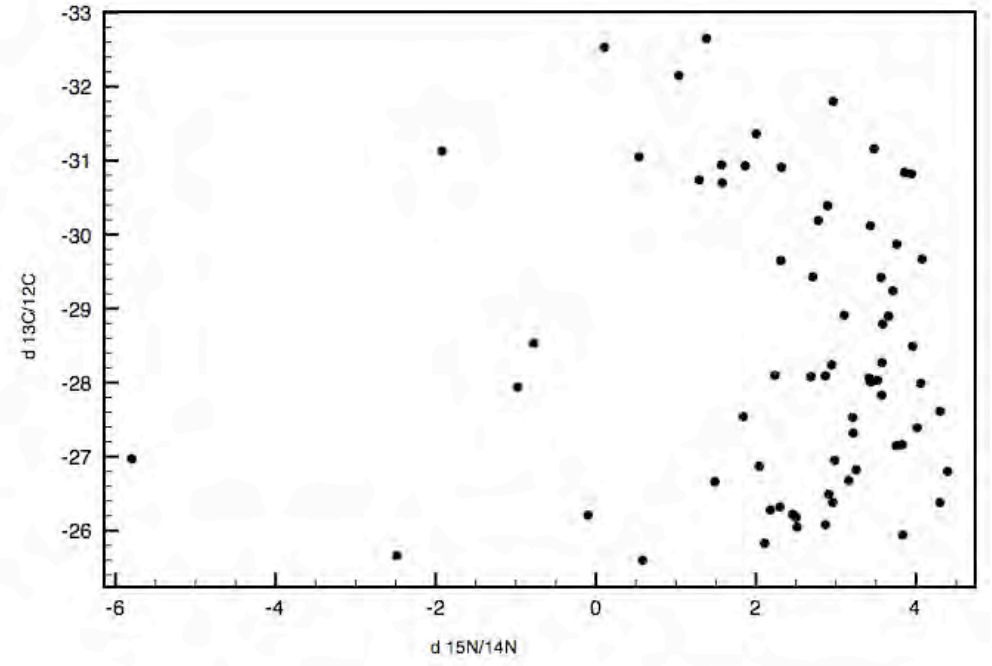

Figure B.23: Core PG1351 bulk $\delta^{13}C$ vs. bulk $\delta^{15}N$ ($R^2 = 0.002$)

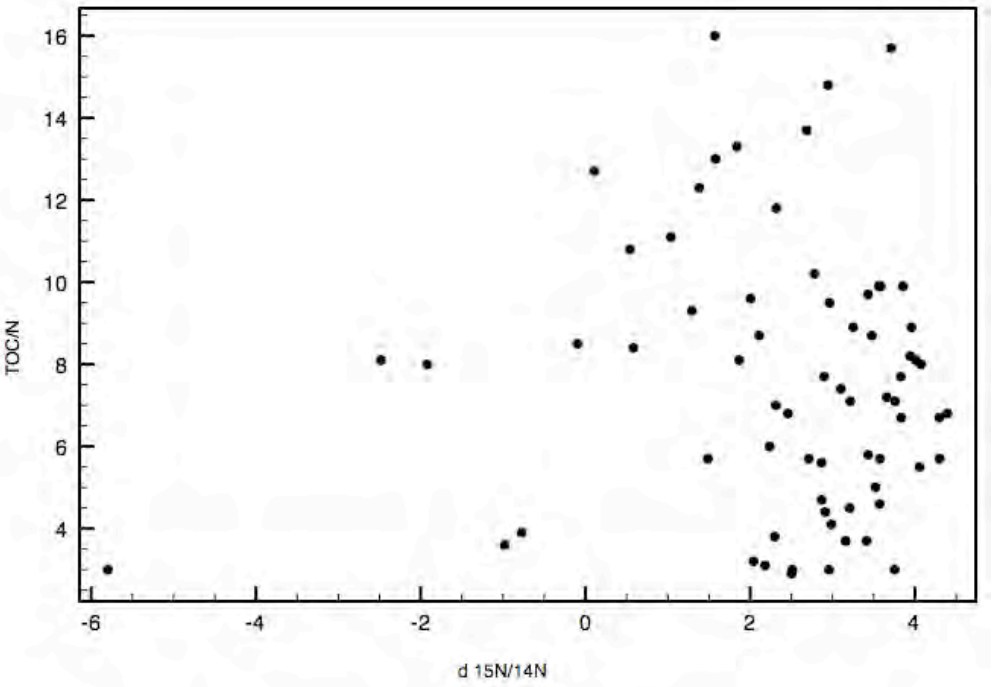

Figure B.24: Core PG1351 C/N vs. bulk $\delta^{15}N$ (R^2 = 9E-6)

APPENDIX C

REPRESENTATIVE MASS SPECTRA OF IDENTIFIED COMPOUNDS

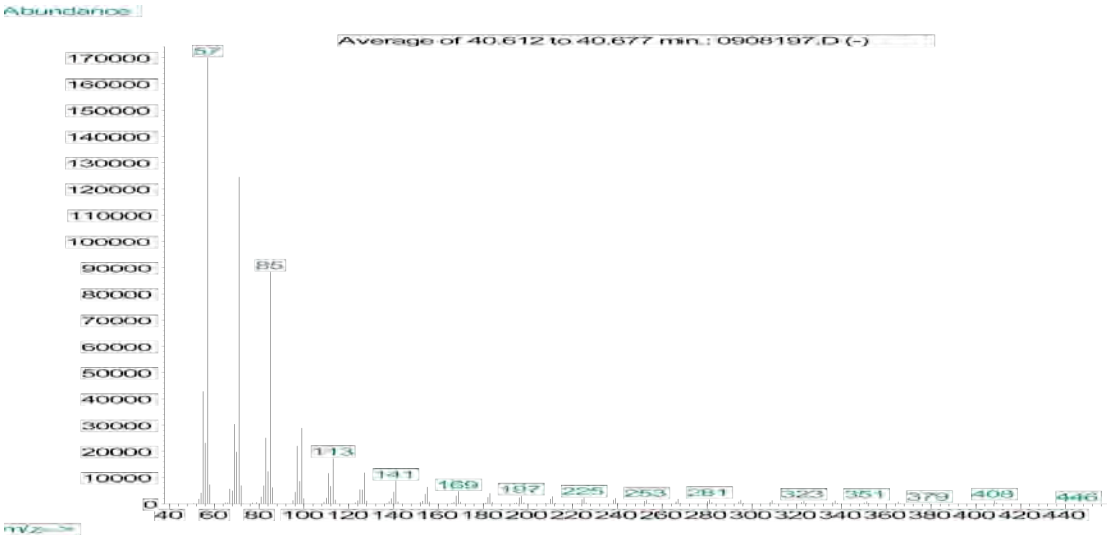

Figure C.1: C_{29} Alkane mass spectra. m/z = 408 molecular ion (M), m/z = 57, 71, 85 (typical alkane ion fragments).

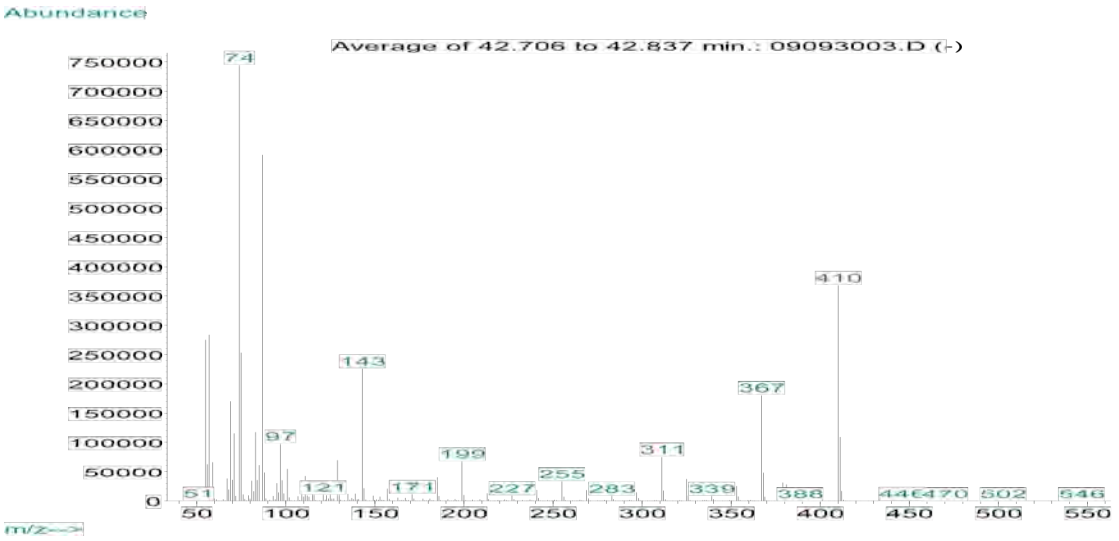

Figure C.2: C_{26} FAME mass spectra. m/z = 410, (M) m/z = 55, 74, 87 (typical fatty acid ion fragments).

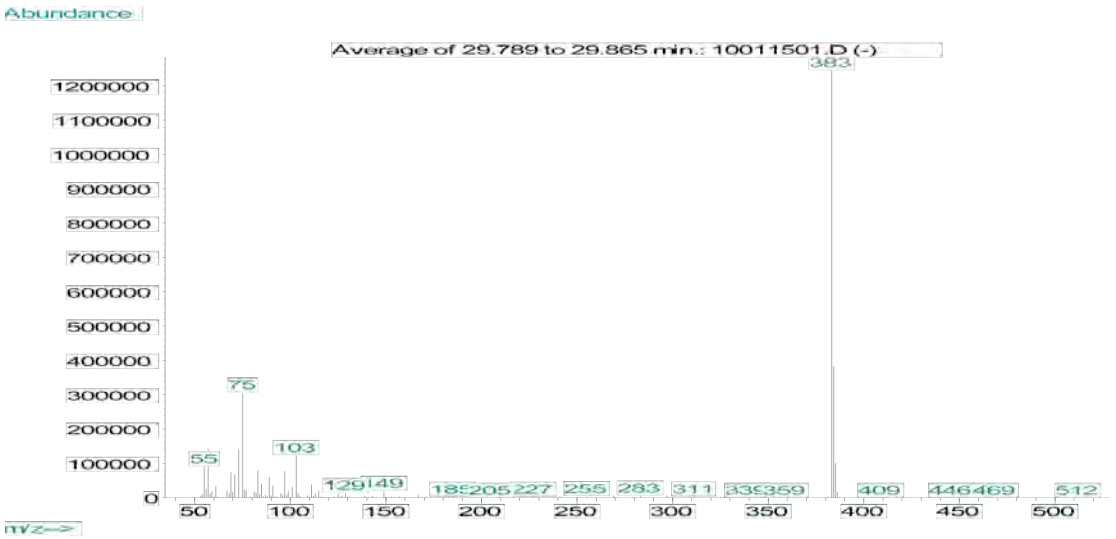

Figure C.3: C_{22} alcohol mass spectra. m/z = 383 (M-15, CH_3 fragment), m/z = 57, 75 (typical alcohol ion fragments).

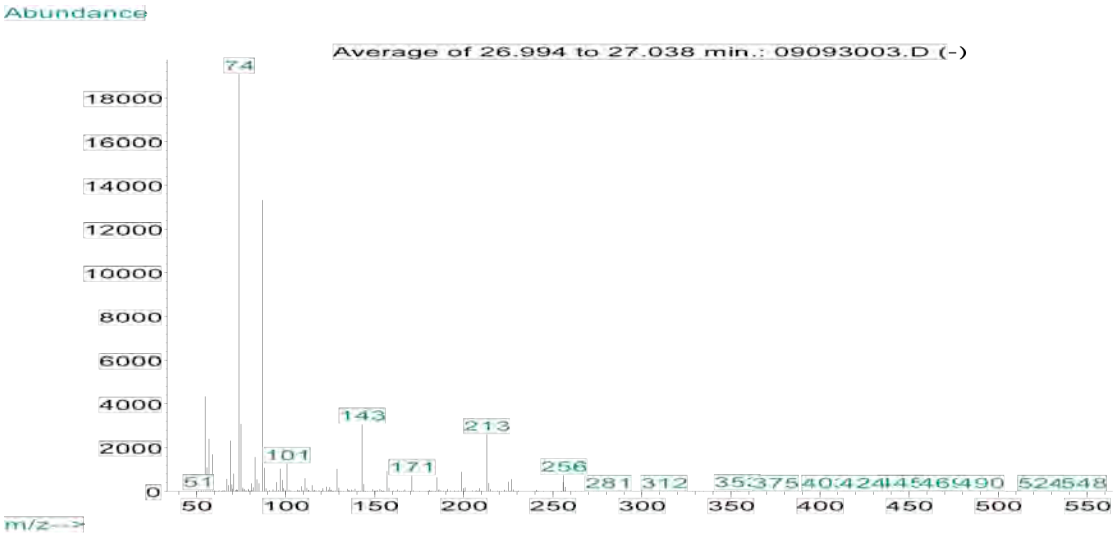

Figure C.4: C_{15} anteiso-fatty acid mass spectra. m/z = 256 (M C_{15} fatty acid), m/z = 55, 74, 87 (typical fatty acid ion fragments).

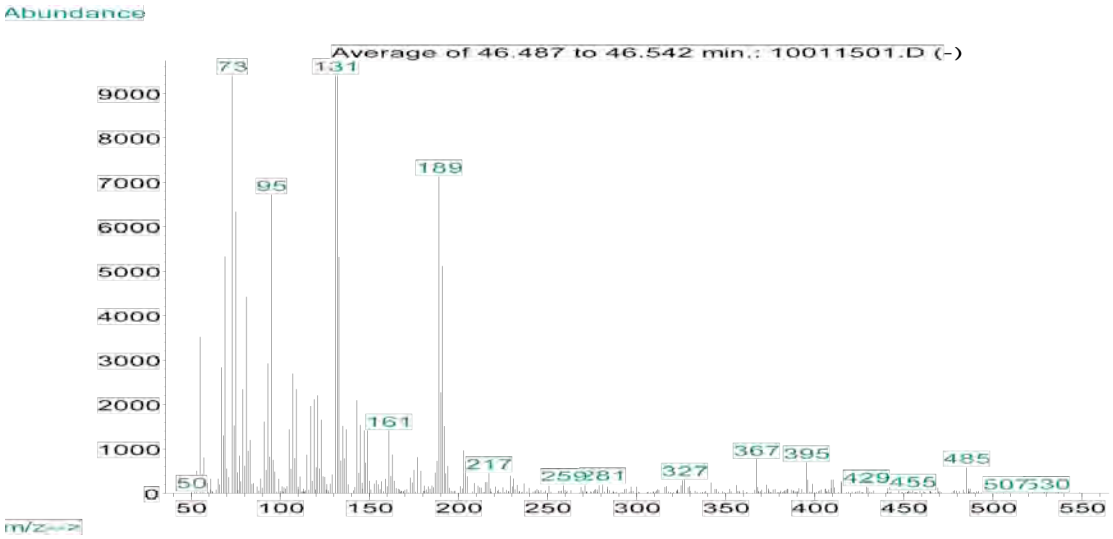

Figure C.5: Diplopterol mass spectra. m/z = 395 (M-105), m/z = 410 (M-90, OTMS + H), M-15 m/z = 485 (M-15), also (in approx. order of abundance) m/z = 131, 73, 95, 189, 367, 191.

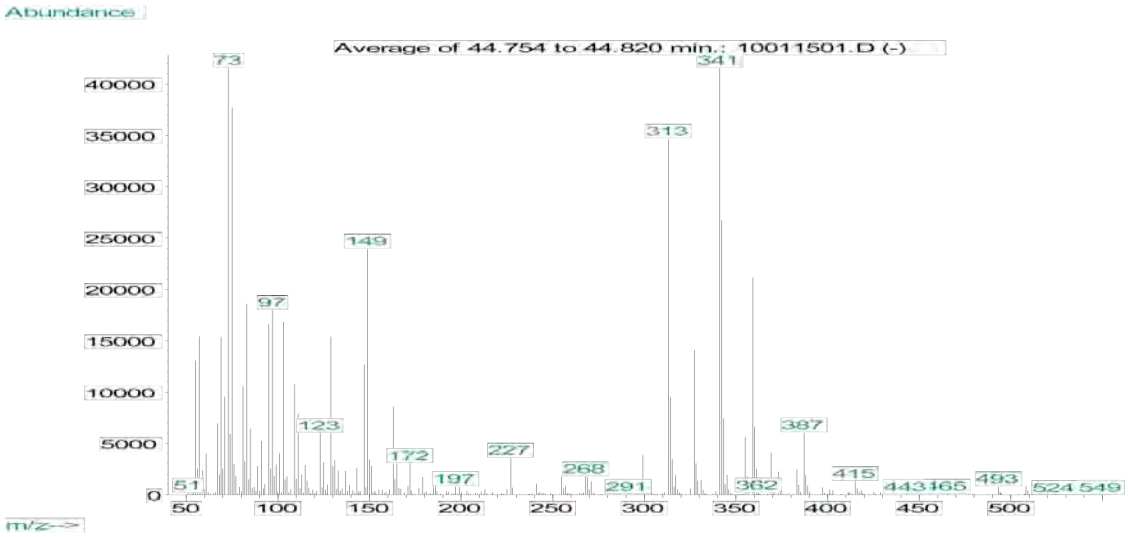

Figure C.6: Hydroxyarchaeol (Compound I) mass spectra. Typical hydroxyarchaeol m/z = 341.

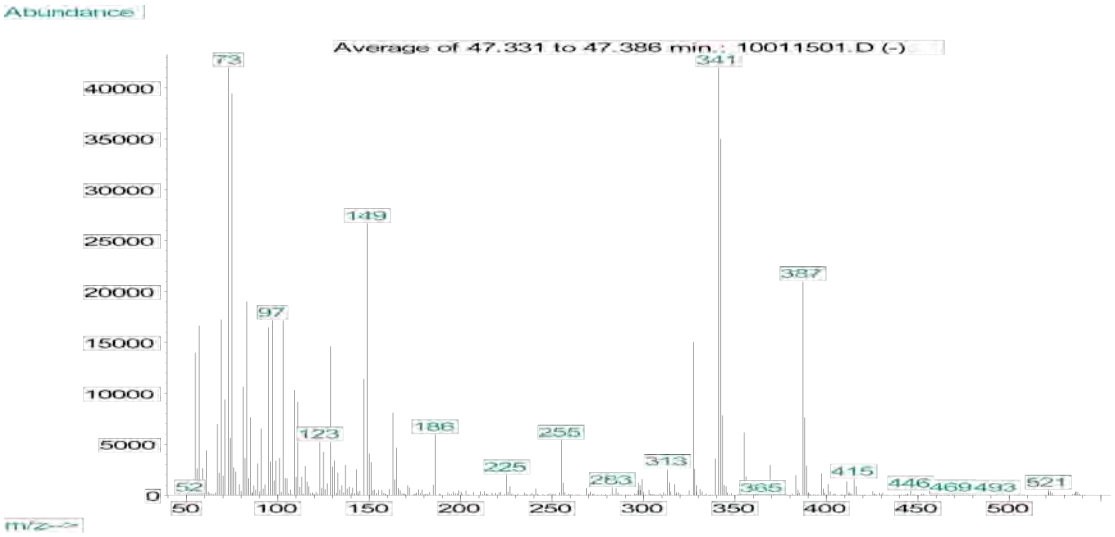

Figure C.7: sn-2-hydroxyarchaeol (Compound II) mass spectra. Typical hydroxyarchaeol m/z = 341, also m/z = 143, 57, 131, 103, 205, 278, 367, but not in accurate relative abundance, according to published mass spectra. Tentative ID.

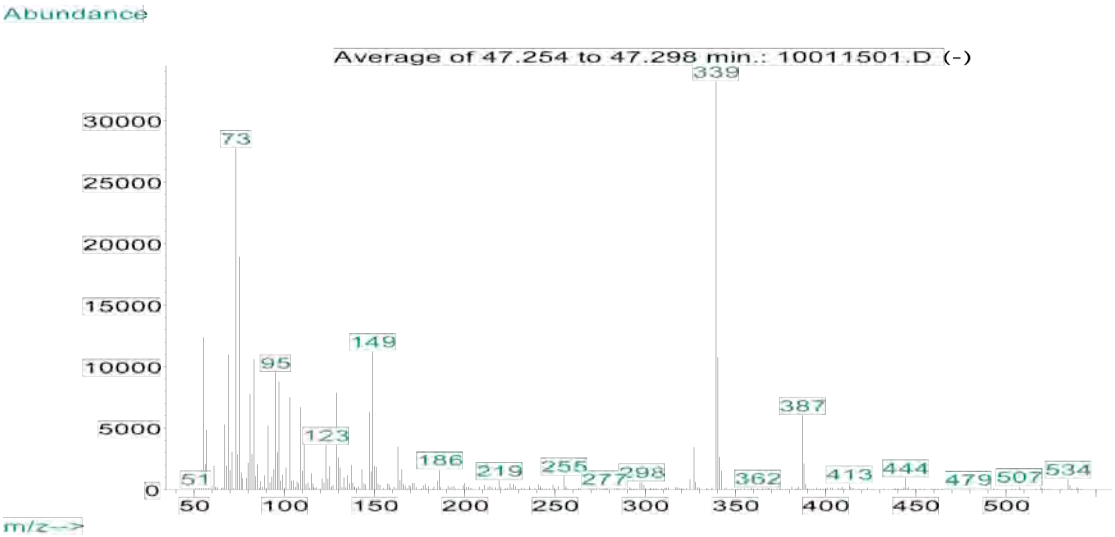

Figure C.8: sn-3-hydroxyarchaeol (tentative) mass spectra. Similar ion fragments to sn-2-hydroxyarchaeol (m/z = 73, 123, 149, 186, 255, 387). Does not contain m/z = 341 in large abundance, like other hydroxyarchaeols. Tentative ID.

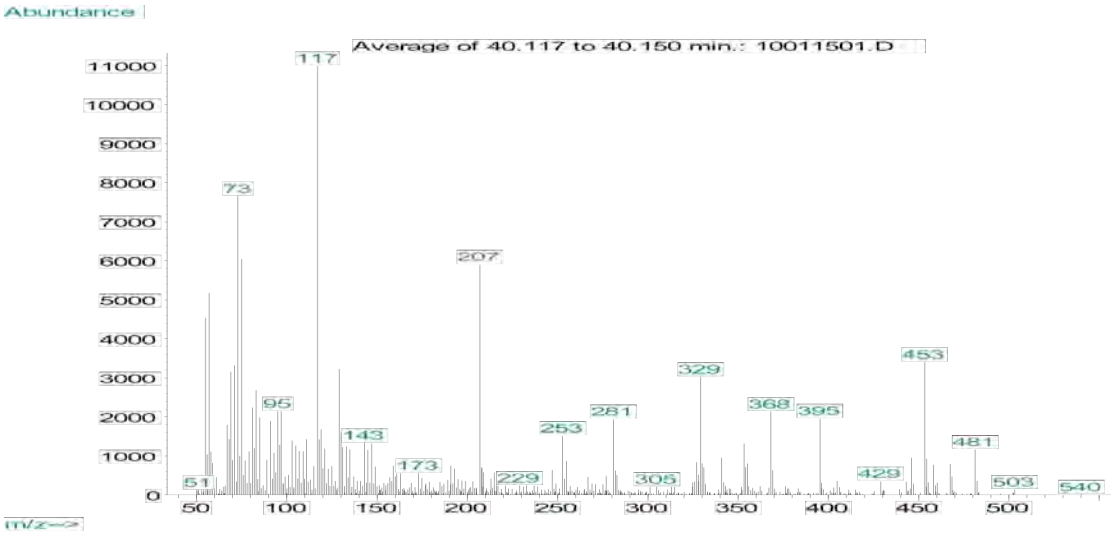

Figure C.9: Cholesterol mass spectra. m/z 458 (M), 443 (M-15), 368 (M-90), 329 (M-129).

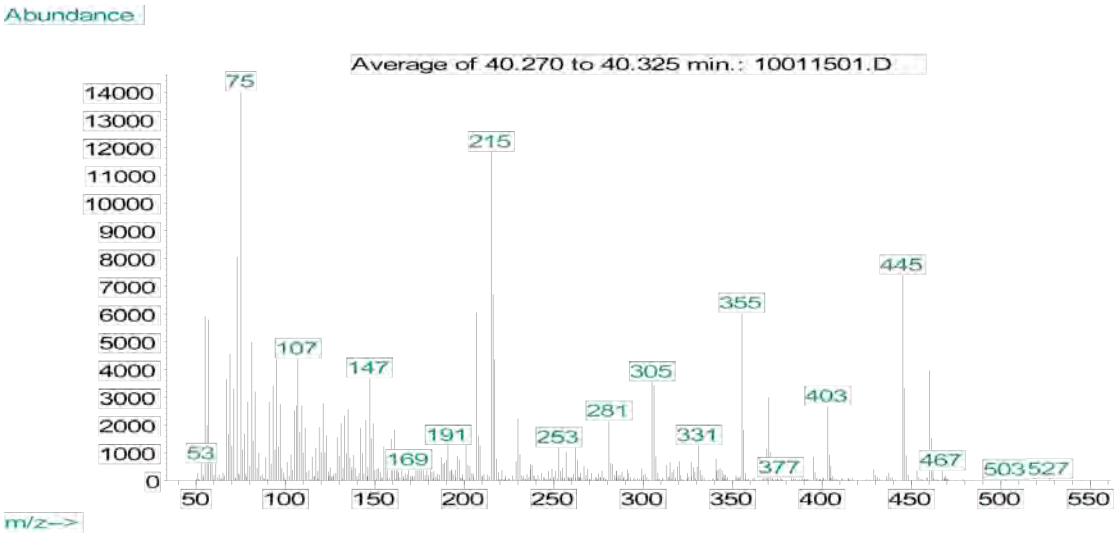

Figure C.10: Cholestanol mass spectra. m/z 460 (M), 445 (M-15), 370 (M-90), 355 (M-105), 215.

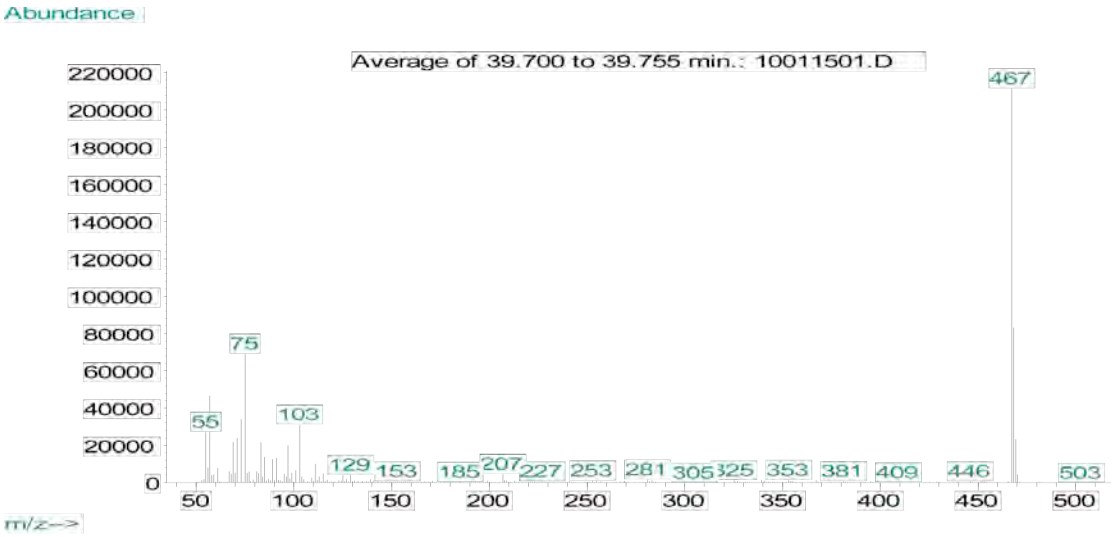

Figure C.11: Campesterol (tentative) mass spectra. m/z 467 (M-15).

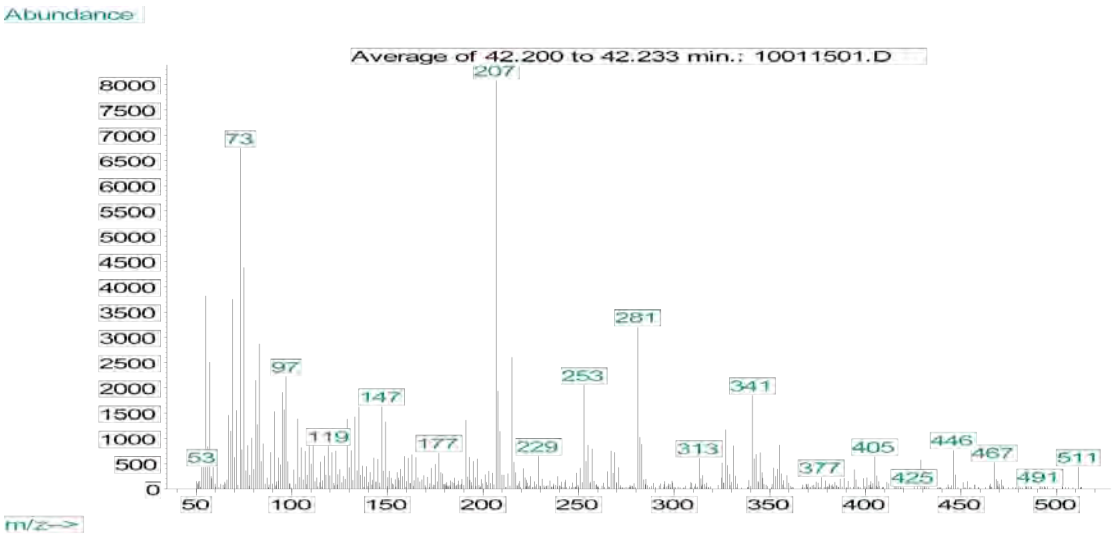

Figure C.12: Stigmasterol mass spectra. m/z 484 (M), 469 (M-15), 394(M-90), 355 (M-129), 255.

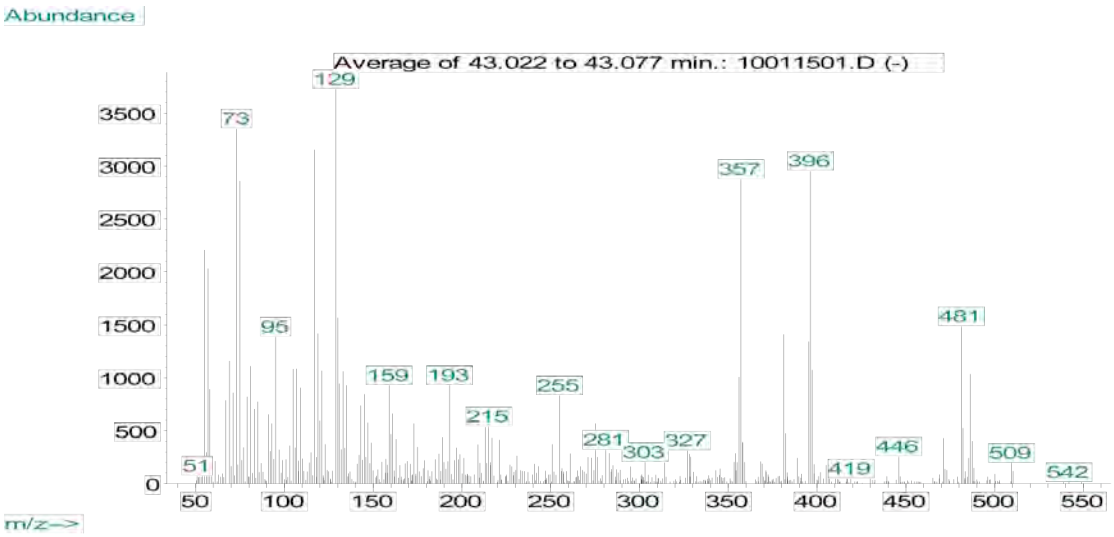

Figure C.13: β-sitosterol mass spectra. m/z 486 (M), 471 (M-15, 396 (M-90), 381 (M-105), 357 (M-129).

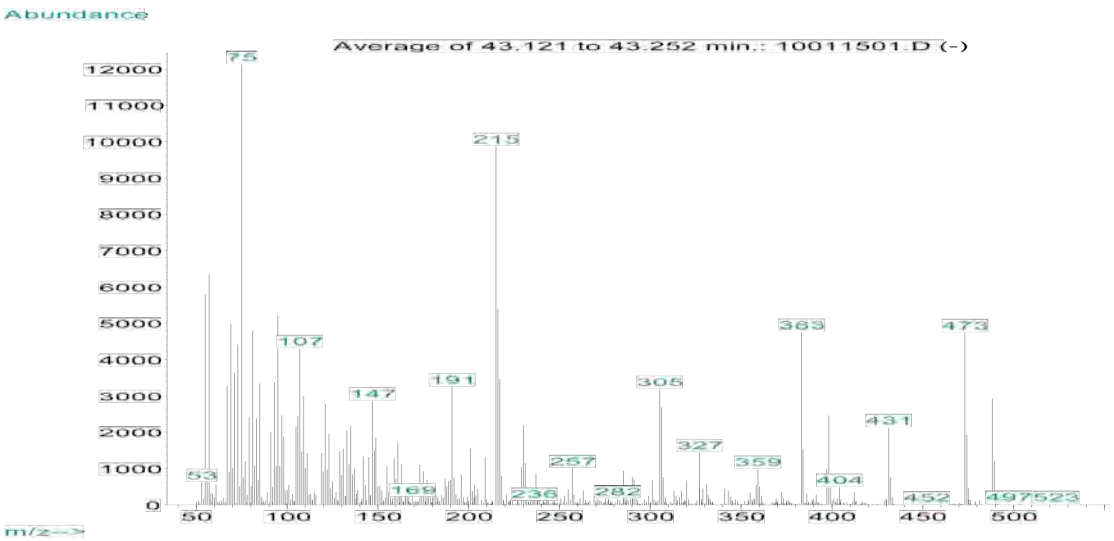

Figure C.14: Stigmastanol mass spectra. m/z 488 (M), 473 (M-15), 398 (M-90), 383 (M-105), 215, 305.

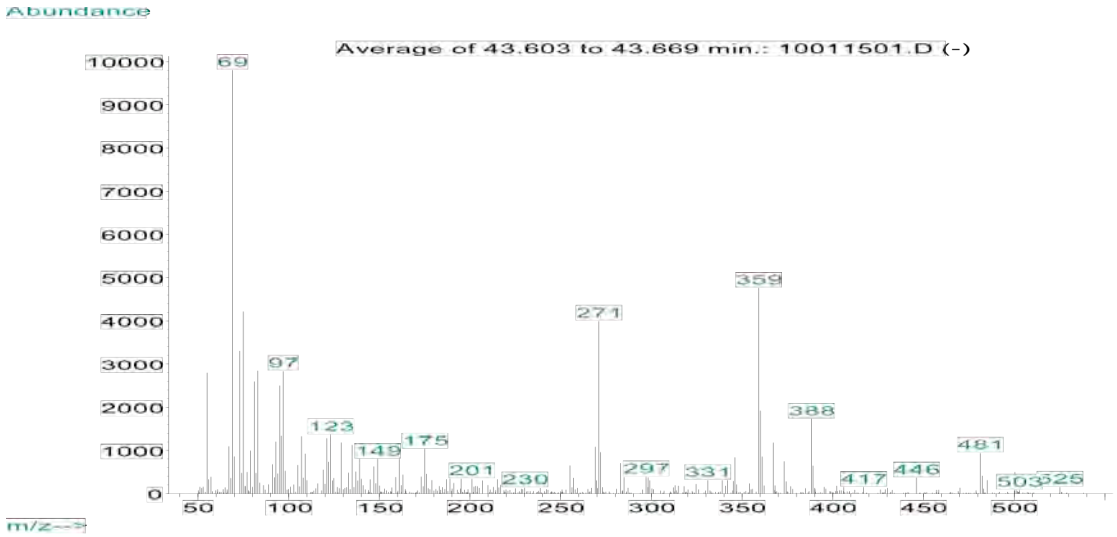

Figure C.15: Dinosterol mass spectra. m/z (in order of published relative abundance) 271, 269, 359, 283, 388, 298, 367, 229, 339, 361, 373.

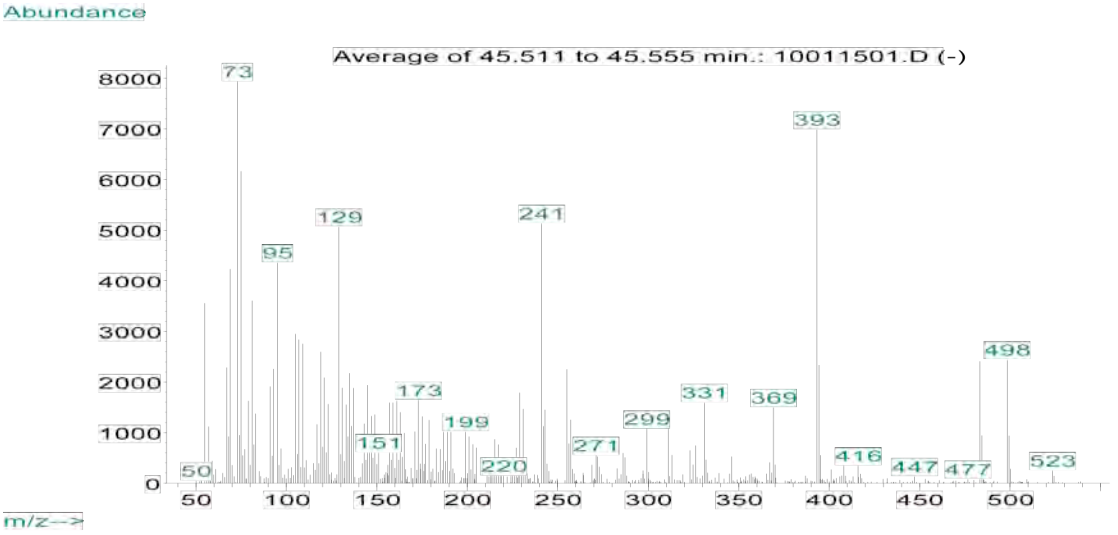

Figure C.16: Isoarborinal mass spectra. m/z 498, 483, 393, 241, 129, 95, 73.

REFERENCES

Altabet, M.A., Francois, R., Murray, D.W., Prell, W.L., 1995. Climate-related variations in denitrification in the Arabian Sea from sediment $^{15}N/^{14}N$ ratios. *Nature* 373, 506-508.

Altabet, M.A., Pilskaln, C., Thunell, R., Pride, C., Sigman, D., Chavez, F., Francois, R., 1999. The nitrogen isotope biogeochemistry of sinking particles from the margin of the Eastern North Pacific. *Deep-Sea Research I* 46, 655-679.

Asikainen, C.A, Francus, P., Brigham-Grette, J., 2007. Sedimentology, clay mineralogy and grain-size as indicators of 65 ka of climate change from El'gygytgyn Crater Lake, Northeastern Siberia. *Journal of Paleolimnology* 37, 105-122. DOI 10.1007/s10933-006-9026-5.

Birgel, D., Peckmann, J., 2008. Aerobic methanotrophy at ancient marine methane seeps: A synthesis. *Organic Geochemistry* 39, 1659-1667.

Bobbie, R., White, D.C., 1980. Characterization of benthic microbial community structure by high-resolution gas chromatography of fatty acid methyl esters. *Applied and Environmental Microbiology*, 39, 1212-1222.

Bouloubassi, I., Nabais, E., Pancost, R.D., Lorre, A., Taphanel, M., 2009. First biomarker evidence for methane oxidation at cold seeps in the Southeast Atlantic (REGAB pockmark). *Deep-Sea Research II* 56, 2239-2247.

Bechtel, A., Schubert, C.J., 2009. A biogeochemical study of sediments from the eutrophic Lake Lugano and the oligotrophic Lake Brienz, Switzerland. *Organic Geochemistry* 40, 1100-1114.

Brigham-Grette, J., Lozhkin, A.V., Anderson, P.M., Glushkova, O.Y., 2004. Paleoenvironmental conditions in Western Beringia before and during the last glacial maximum. In: Madsen, D.B. (ed) *Entering America: Northeast Asia and Beringia before the last glacial maximum*. Univ. of Utah Press, 29-61.

Brigham-Grette, J., Melles, M., Minyuk, P., Scientific Party, 2007. Overview and significance of a 250 ka paleoclimate record from El'gygytgyn Crater Lake, NE Russia. *Journal of Paleolimnology* 37, 1-16. DOI 10.1007/s10933-006-9023-8.

Canfield, D.E., 1994. Factors influencing organic carbon preservation in marine sediments. *Chemical Geology* 114, 315-329.

Cloern, J.E., Canuel, E.A., Harris, D., 2002. Stable carbon and nitrogen isotope composition of aquatic and terrestrial plants of the San Francisco Bay estuarine system. *Limnology and Oceanography* 47, 713-729.

Cherapanova, M.V., Snyder, J.A., Brigham-Grette, J., 2007. Diatom stratigraphy of the last 250 ka at Lake El'gygytgyn, northeast Siberia. *Journal of Paleolimnology* 37, 155-162. DOI 10.1007/s10933-006-9023-8.

Elvert, M., Seuss, E., 1999. Anaerobic methane oxidation associated with marine gas hydrates: superlight C-isotopes from saturated and unsaturated C_{20} and C_{25} irregular isoprenoids. *Naturwissenschaften* 86, 295-300.

Elvert, M., Suess, E., Greinert, J., Whiticar, M.J., 2000. Archaea mediating anaerobic methane oxidation in deep-sea sediments at cold seeps of the eastern Aleutian subduction zone. *Organic Geochemistry* 31, 1175-1187.

Elvert, M., Niemann, H., 2008. Occurrence of unusual steroids and hopanoids derived from aerobic methanotrophs at an active marine mud volcano. *Organic Geochemistry* 39, 167-177.

Ficken, K.J., Street-Perrott, F.A., Perrott, R.A., Swain, D.L., Olago, D.O., Eglinton, G., 1998. Glacial/interglacial variations in carbon cycling revealed by molecular and isotope stratigraphy of Lake Nkunga, Mt. Kenya, East Africa. *Organic Geochemistry* 29, 1701-1719.

Filippi, M.L., Talbot, M.R., 2004. The palaeolimnology of northern Lake Malawi over the last 25 ka based upon the elemental and stable isotopic composition of sedimentary organic matter. *Quaternary Science Reviews* 24, 1303-1328.

Forman, S., Pierson, J., Gomez, J., Brigham-Grette, J., Nowaczyk, N.R., Melles, M., 2007. Luminescence geochronology for sediments from Lake El'gygytgyn northwest Siberia, Russia: constraining the timing of paleoenvironmental events for the past 200 ka. *Journal of Paleolimnology* 37, 77-88. DOI 10.1007/s10933-006-9023-8.

Fulco, A., 1983. Fatty acid metabolism in bacteria. *Progress in Lipid Research* 27, 133-160.

Gaye, B., Fahl, K., Kodina, L.A., Lahajnar, N., Nagel, B., Unger, D., Gebhardt, A.C., 2007. Particulate matter fluxes in the southern and central Kara Sea compared to sediments: Bulk fluxes, amino acids, stable carbon and nitrogen isotopes, sterols and fatty acids. *Continental Shelf Research* 27, 2570-2594.

Gebhardt, A.C., Niessen, F., Kopsch, C., 2006. Central ring structure identified in one of the world's best-preserved impact craters. *Geology* 34, 145-148.

Gill, F.L., Dewhurst, R.J., Dungait, J.A.J., Evershed, R.P., Ives, L., Li, C., Pancost, R.D., Sullivan, M., Bera, S., Bull, I.D., 2010. *Organic Geochemistry* 41, 467-472.

Hanisch, S., Ariztegui, D., Puttmann, W., 2003. The biomarker record of Lake Albano, central Italy - implications for Holocene aquatic system response to environmental change. *Organic Geochemistry* 34, 1223-1235.

Hartnett, H.E., Keil, R.G., Hedges, J.I., Devol, A.H., 1998. Influence of oxygen exposure time on organic carbon preservation in continental margin sediments. *Nature* 391, 573-575.

Hartnett, H.E., Devol, A.H., 2003. Role of a strong oxygen-deficient zone in the preservation and degradation of organic matter: A carbon budget for the continental margins of northweast Mexico and Washington State. *Geochimica et Cosmochimica Acta* 67, 247-264.

Henderson, W., Reed, W.E., Steel, G., 1972. The origin and incorporation of organic molecules in sediments as elucidated by studies of the sedimentary sequence from a residual Pleistocene lake. In: von Gaertner, H.R., Wehner, H. (Eds.), *Advances in Organic Geochemistry* 1971. Pergamon Press, Oxford, 335-352.

Hinrichs, K.U., Hayes, J.M., Sylva, S.P., Brewer, P.G., DeLong, E.F., 1999. Methane-consuming archaebacteria in marine sediments. *Nature*, 398, 802-805.

Hinrichs, K.U., Summons, R.E., Orphan, V., Sylva, S.P, Hayes, J.M, 2000a. Molecular and isotopic analysis of anaeorobic methane-oxidizing communities in marine sediments. *Organic Geochemistry*, 31, 1685-1701.

Hinrichs, K.U., Pancost, R.D., Summons, R.E., Sprott, G.D., Sylva, S.P., Sinninghe Damste, J.S., Hayes, J.M., 2000b. Mass Spectra of *sn*-2-hydroxyarchaeol, a polar lipid biomarker for anaerobic methanotrophy. *Geochemistry, Geophysics, Geosystems*, 1, Technical Brief 2000GC000042.

Hinrichs, K.U., 2001. A molecular recorder of methane hydrate destabilization. *Gechemistry, Geophysics, Geosystems*, 2, Research Letter 2000GC000118.

Hinrichs, K.U., Boetius, A., 2002. The Anaerobic Oxidation of Methane: New Insights in Microbial Ecology and Biogeochemistry. From: Wefer, G, D Billett, D Hebbeln, BB Jorgensen, M Schluter, T Van Weering (eds), Ocean Margin Systems. Springer-Verlag Berlin Heidelberg, 457-477.

Hinrichs, K.U., Hmelo, L.R., Sylva, S.P., 2003. Molecular fossil record of elevated methane levels in Late Pleistocene coastal waters. *Science*, 299, 1214-1217.

Hoehler, T.M, Alperin, M.J., Albert, D.B, Martens, C.S., 1994. Field and laboratory studies of methane oxidation in an anoxic marine sediment: Evidence for a methanogen-sulfate reducer consortium. *Global Biogeochemical Cycles*, 8, 451-463.

Huang, W.Y., Meinschein, W.G., 1976. Sterols as source indicators of organic materials in sediments. *Geochimica et Cosmochimica Acta*, 40, 323-330.

Johnson, C.M., Skulan, J.L., Beard, B.L., Sun, H., Nealson, K.H., Braterman, P.S., 2002. Isotopic fractionation between Fe(III) and Fe(II) in aqueous solutions. *Earth and Planetary Science Letters*, 195, 141-153.

Juschus, O., Preusser, F., Melles, M., Radtke, U., 2007. Applying SAR-IRSL methodology for dating fine-grained sediments from Lake El'gygytgyn, north-eastern Siberia. *Quaternary Geochronology*, 2, 187-194.

Juschus, O., Melles, M., Gebhardt, A.C., Neissen, F., 2009. Late Quaternary mass movement events in Lake El'gygytgyn, North-eastern Siberia. *Sedimentology*, 56, 2155-2174. DOI: 10.1111/j.1365-3091.2009.01074.x

Kaneda, T. 1991. Iso- and Anteiso-Fatty Acids in Bacteria: Biosynthesis, Function, and Taxonomic Significance. *Microbiological Reviews*, 55, 288-302.

Kaufman, D.S., Schneider, D.P., McKay, N.P., Ammann, C.M., Bradley, R.S., Briffa, K.R, Miller, G.H., Otto-Bliesner, B.L., Overpeck, J.T., Vinther, B.M., Arctic Lakes 2k Project Members, 2009. Recent warming reverses long-term Arctic cooling. *Science*, 325, 1236-1239.

Killops, S., Killops, V., 2005. *Introduction to Organic Chemistry*, second edition. Blackwell Publishing, Malden, MA, 393 pp.

Koga, Y., Nishihara, M., Morii, H., Akagawa-Matsushita, M., 1993. Ether polar lipids of methanogenic bacteria: Structures, comparative aspects, and biosyntheses. *Microbiological Reviews*, 57, 164-182.

Koga, Y., Morii, H., Akagawa-Matsuhita, M., Ohga, M., 1998. Correlation of polar lipid composition with 16S rRNA phylogeny in methanogens: Further analysis of lipid component parts. *Bioscience, Biotechnology, Biogeochemistry*, 62, 230-236.

Koga, Y., Morii, H., 2005. Recent advances in structural research on ether lipids from archaea including comparative and physiological aspects. *Bioscience, Biotechnology, Biochemistry*, 69, 2019-2034.

Kokorowski, H.D., Anderson, P.M., Sletten, R.S., Lozhkin, A.V., Brown, T.A., 2008. Late glacial and early Holocene climatic changes based on a multiproxy lacustrine sediment record from Northeast Siberia. *Arctic, Antarctic, and Alpine Research,* 40, 497-505.

Logan, G.A., Eglinton, G., 1994. Biogeochemistry of the Miocene lacustrine deposit, at Clarkia, northern Idaho, U.S.A. *Organic Geochemistry*, 21, 857-870.

Lozhkin, A.V., Anderson, P.M., Matrosova, T.V., Minyuk, P.S., 2007a. The pollen record from El'gygytgyn Lake: implications for vegetation and climate histories of northern Chukotka since the late middle Pleistocene. *Journal of Paleolimnology*, 37, 135-155.

Lozhkin, A.V., Anderson, P.M., Matrosova, T.V., Minyuk, P.S., Brigham-Grette, J., Melles, M., 2007b. Continuous record of environmental changes in Chukotka during the last 350 thousand years. *Russian Journal of Pacific Geology*, 1, 550-555.

Majocka, C.S., 2007. Evaluating the possible links between heavy mineral etching, anoxia, magnetic susceptibility and sediment geochemistry: El'gygygytgyn Crater Lake, northeastern Siberia. Thesis. Department of Geosciences. University of Massachusetts Amherst. 140 pp.

Melles, M., Minyuk, P., Brigham-Grette, J., Juschus, O., 2005. The expedition El'gygytgyn Lake 2003 (Siberian Arctic). *Reports on Polar and Marine Research,* 509, 139.

Melles, M., Brigham-Grette, J., Glushkova, O.Y., Minyuk, P., Nowaczyk, N., Hubberten, H.W., 2007. Sedimentary geochemistry of a pilot core from Lake El'gygytgyn - a sensitive record of climate variability in the East Siberian Arctic during the past three climate cycles. *Journal of Paleolimnology*, 37, 89-104. DOI 10.1007/s10933-006-9023-8

Meyers, P.A., 1994. Preservation of elemental and isotopic source identification of sedimentary organic matter. *Chemical Geology*, 114, 289-302.

Meyers, P.A. 1998. Organic geochemical proxies of paleoceanographic, paleolimnologic, and paleoclimatic processes. *Organic Geochemistry*, 27, 213-250.

Meyers, P.A., Eadie, B.J., 1993. Sources degradation and recycling of organic matter associated with sinking particles in Lake Michigan. *Organic Geochemistry*, 20, 47-56.

Meyers, P.A., Ishiwatari. R., 1993. Lacustrine organic geochemistry - an overview of indicators of organic matter sources and diagenesis in lake sediments. *Organic Geochemistry*, 20, 867-900.

Meyers, P.A., R. Ishiwatari. 1995. Organic matter accumulation records in lake sediments. *Physics and Chemistry of Lakes* (Second Edition). Lerman, A., D.M. Imboden, J.R. Gat (eds.). Springer-Verlag Berlin Heidelberg New York, 334 pp.

Minyuk, P., Brigham-Grette, J., Melles M., Brokhodoev, Y., Glushkova, O.Y., 2007. Inorganic geochemistry of El'gygytgyn Lake sediments (northeastern Russia) as an indicator of paleoclimatic change for the last 250 kyr. *Journal of Paleolimnology*, 37, 123-133. DOI 10.1007/s10933-006-9023-8.

Nolan, M., Liston, G., Prokein, P., Brigham-Grette J., Sharpton, V., Huntzinger, R., 2003. Analysis of Lake Ice dynamics and morphology on Lake El'gygytgyn, Siberia, using SAR and Landsat. *Journal of Geophysical Resources,* 108, 8162-8174. DOI 10.1029/2001JD000934.

Nowaczyk, N.R., Minyuk, P., Melles, M., Brigham-Grette, J., Glushkova, O., Nolan, M., Lozhkin, A.V., Stetsenko, T.V., Andersen, P.M., Forman, S.L., 2002. Magnetostratigraphic results from impact crater Lake El'gygytgyn, northeastern Siberia: a 300 kyr long high-resolution terrestrial paleoclimatic record from the Arctic. *Geophysical Journal International*, 150, 109-126.

Nowaczyk, N.R., Melles, M., Minyuk, P., 2007. A revised age model for core PG1351 from Lake El'gygytgyn, Chukotka, based on magnetic susceptibility variations correlated to northern hemisphere insolation variations. *Journal of Paleolimnology*, 37 65-76. DOI 10.1007/s10933-006-9023-8.

Ouellette,N. 2003. *Lipid biomarkers and paloevegetation determinations for the last 30,000 years at Elikchan Lake, Northeast Siberia.* Honors Thesis. Department of Geology. Bates College.

Pancost , R.D., Sinninghe Damste, J.S., DeLint, S., Van Der Maarel, M.J.E.C., Gottschal, J.C., The MEDINAUT Shipboard Scientific Party, 2000. Biomarker evidence for widespread anaerobic methane oxidation in Mediterranean sediments by a consortium of methanogenic archaea and bacteria. *Applied and Environmental Microbiology*, 66, 1126-1132.

Pancost, R.D., Hopmans, E.C., Sinninghe Damste, J.S., The MEDINAUT Shipboard Scientific Party, 2001. Archaeal lipids in Mediterranean Cold Seeps: Molecular proxies for anaerobic methane oxidation. *Geochimica et Cosmochimica Acta*, 65, 1611-1627.

Pancost, R.D., Sinninghe Damste, J.S., 2003. Carbon isotopic compositions of prokaryotic lipids as tracers of carbon cycling in diverse settings. *Chemical Geology*, 195, 29-58.

Pancost, R.D., Steart, D.S., Handley, L., Collinson, M.E., Hooker, J.J., Scott, A.C., Grassineau, N.V., Glasspool, I.J., 2007. Increased terrestrial methane cycling at the Paleocene-Eocene thermal maximum. *Nature*, 449, 332-335. DOI 10.1038/nature06012.

Pang, P.C., Nriagu, J.O., 1976. Distribution and isotope composition of nitrogen in Bay of Quinte (Lake Ontario) sediments. *Chemical Geology*, 18, 93-105.

Pang, P.C., Nriagu, J.O., 1977. Isotopic variations of the nitrogen in Lake Superior. *Geochimica et Cosmochimica Acta*, 41, 811-814.

Pientz, R., Douglas, M.S.V., Smol. J.P., 2004. *Long term Environmental Change in Arctic and Antarctic Lakes*. Springer, Dordrecht, The Netherlands, 562 pp.

Piretti, M.V., Pagliuca, G., Boni, L., Pistocchi, R., Diamante, M., Gazzotti, T., 1997. Investigation of 4-methyl sterols from cultured dinoflagellate algal strains. *Journal of Phycology*, 33, 61-67.

Rajendran, N., Suwa, Y., Urushigawa, Y., 1993. Distribution of phospholipid ester-linked fatty acid biomarkers for bacteria in the sediment of Ise Bay, Japan. *Marine Chemistry*, 42, 39-56.

Rodgers, 2005. *Stable carbon isotope analysis of lake core sediments and lipid biomarkers as a proxy for Late Pleistovcene carbon cycling at Elikchan Lake, NE Sibera.* Honors Thesis. Department of Geology. Bates College

Routh, J., Meyers, P.A., Hjorth, T., Baskaran, M., Hallberg, R., 2007. Sedimentary geochemical record of recent environmental changes around Lake Middle Marviken, Sweden. *Journal of Paleolimnology*, 37, 529-545.

Schlesinger, W.H. 1997. *Biogeochemistry, An Analysis of Global Change*, second edition. Academic Press, San Diego, 588 pp.

Schouten, S., Van Der Maarel, M.J.E.C, Huber, R., Sinninghe Damste, J.S., 1997. 2,6,10,15,19-Pentamethylicosenes in *Methanolobus bombayensis*, a marine methanogenic archaeon, and in *Methanosarcina mazei*. *Organic Geochemistry*, 26, 409-414.

Schouten, S., Klein Breteler, W.C.M., Blokker, P., Schogt, N., Rijpstra, W.I., Grice, K., Baas, M., Sinninghe Damste, J.S., 1998. Biosynthetic effects on the stable carbon isotopic compositions of algal lipids: Implications for deciphering the carbon isotopic biomarker record. *Geochimica et Cosmochimica Acta*, 62, 1397-1406.

Schouten, S., Rijpstra, W.I.C., Kok, M., Hopmans, E.C., Summons, R.E., Volkman, J.K., Sinninghe Damste. J.S., 2001. Molecular organic tracers of biogeochemical processes in a saline meromictic lake (Ace Lake). *Geochimica et Cosmochimica Acta*, 65, 1629-1640.

Stadnitskaia, A., Bouloubassi, I., Elvert, M., Hinrichs, K.-U., Sinninghe Damste, J.S., 2008. Extended hydroxyarchaeol, a novel lipid biomarker for anaerobic methanotrophy in cold seepage habitats. *Organic Geochemistry*, 39, 1007-1014.

Summons, R.E., Franzmann, P.D. Nichols, P.D., 1998. Carbon isotopic fractionation associated with methylotrophic methanogenesis. *Organic Geochemistry*, 28, No. 7-8, 465-475.

Talbot, M.R., 2001. Nitrogen Isotopes in Paleolimnology. *Tracking Environmental Change Using Lake Sediments, Volume 2: Physical and Geochemical Methods*. Last, W.M., J.P. Smol (eds.). Kluwer Academic Publishers, Dordrecht, The Netherlands, 504 pp.

Teixidor, P., Grimalt, J.O., 1992. Gas chromatographic determination of isoprenoid alkylglycerol diethers in archaebacterial cultures and environmental samples. *Journal of Chromatography*, 607, 253-259.

Van Mooy, B.A.S., Keil, R.G., Devol, A.H., 2002. Impact of suboxia on sinking particulate organic carbon: Enhanced carbon flux and preferential degradation of amino acids via denitrification. *Geochimica et Cosmochimica Acta*, 66, 457-465.

Vincent, W.F., Laybourn-Parry, J. (eds.), 2008. *Polar Lakes and Rivers, Limnology of Arctic and Antarctic Aquatic Ecosystems*. Oxford University Press, Oxford, 327 pp.

Vitousek, P.M., Howarth, R.W., 1991. Nitrogen limitation on land and in the sea: How can it occur? *Biogeochemistry*, 13, 87-115.

Volkman, J.K., Johns, R.B., Gillian, T., Perry, G.J., 1980. Microbial lipids of an intertidal sediment – I. Fatty acids and hydrocarbons. *Geochimica et Cosmochimica Acta*, 44, 1133-1143.

Volkman, J.K., 1986. A review of sterol markers for marine and terrigenous organic matter. *Organic Geochemistry*, 9, 83-99.

Volkman, J.K., Barrett, S.M., Blackburn, S.I., Mansour, M.P., Sikes, E.L., Gelin, F., 1998. Microalgal biomarkers: A review of recent research developments. *Organic Geochemistry*, 29, 1163-1179.

Werne, J.P., Baas, M., Sinninghe Damste, J.S., 2002. Molecular isotopic tracing of carbon flow and trophic relationships in a methane-supported benthic microbial community. *Limnology and Oceanography*, 47,1694-1701.

Whiticar, M.J. 1999. Carbon and hydrogen isotope systematics of bacterial formation and oxidation of methane. *Chemical Geology*, 161, 291-314.

Wolfe, B.B., Edwards, T.W.D., Aravena, R., 1999. Changes in carbon and nitrogen cycling during tree-line retreat recorded in the isotopic content of lacustrine organic matter, western Taimyr Peninsula, Russia. *The Holocene*, 9, 215-222.

Zech, M., Zech, R., Glaser, B., 2007. A 240,000-year stable carbon and nitrogen isotope record from a loess-like palaeosol sequence in the Tumara Valley, Northeast Siberia. *Chemical Geology*, 242, 307-318.